ELECTRONIC STATES IN DISORDERED SYSTEMS

Thesis submitted to the
University of Roorkee
for the award of the degree of
Doctor of Philosophy
in
Physics

By
MUKUNDA PRASAD DAS

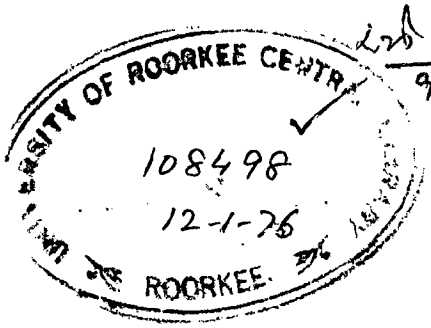

DEPARTMENT OF PHYSICS
UNIVERSITY OF ROORKEE
ROORKEE (INDIA)
March 1975

C E R T I F I C A T E

Certified that the thesis entitled 'ELECTRONIC STATES IN DISORDERED SYSTEMS' which is being submitted by Mr. Mukunda Prasad Das in fulfilment for the award of the degree of Doctor of Philosophy in Physics of the University of Roorkee is a record of his own work carried out by him under my supervision and guidance. The matter embodied in this thesis has not been submitted for the award of any other degree.

This is further to certify that he has worked for a period equivalent to 24 months full time research for preparing his thesis for Ph.D. Degree at this university.

S.K. Joshi

(S.K.Joshi)

Dated March 17 '75

Professor and Head of the
Department of Physics,
University of Roorkee,
Roorkee, 247667, India.

ACKNOWLEDGEMENTS

I wish to express my sincere gratitude to Professor Sri Krishna Joshi for his valuable guidance throughout this investigation. I have enjoyed lavishly his kindness, and constant encouragements. It was a great experience to be associated with him.

I am thankful to Dr. Madan M Pant and Dr. Radhey Shyam Tripathi for many useful discussions at several stages of the work. Thanks are also due to all the members of the Physics Department for their cooperation.

I express my gratefulness to the authorities of Indian Institute of Technology, Kanpur and Tata Institute of Fundamental Research, Bombay for making me available of their comput-er facilities.

Financial supports from Council of Scientific and Industrial Research, New Delhi, State Council of Scientific and Industrial Research, Lucknow and National Bureau of Standards, Washington(U.S.A.) are gratefully acknowledged.

Mukunda P. Das

(Mukunda P.Das)

S Y N O P S I S

The work reported in this thesis is some of the author's attempts to understand the behaviour of electrons in disordered systems. The subject dealt here is a part of the extensively growing field of noncrystalline or aperiodic systems, in which enough stimuli have been created to understand the phenomena of disorder in the recent years. Because of the great progress in the experimental techniques, yielding reliable (experimental) results in the disordered materials like metallic binary alloys, impure semiconductors, liquid metals and glasses around 1960, theoretical attempts were made to understand better, the problem of elementary excitations in disordered systems. One of the landmarks is the Anderson's classic paper "On the absence of diffusion in certain random lattice" and this was followed by discussions due to Mott, Ziman, Thouless and others regarding the nature of the wave functions of electrons in systems having random potentials. The usual tools of band theory, were not applicable to such systems where translational symmetry is incomplete or absent. Due to the impetus gained by rapid advancements of computer technology, refinement and ingenuity of experimental methods, many sophisticated techniques like Green function approach are developed to solve the problem of electrons in disordered systems.

In order to have a systematic understanding in this complex area of investigation, a brief discussion of various experimental methods will be provided and certain typical results will be presented.

The simplest of all disordered materials is the random binary alloy, which is a cellulary disordered system and the study of these will constitute the main body of the thesis. Starting with empirical rules a brief resume will be given on the phenomenological developments of the theory of binary alloys for example; rigid band model, virtual crystal approximation, minimum polarity model, virtual bound state model(Friedal-Anderson model) and Stern's charging model. After discussing the multiple scattering theory of electrons in disordered systems the Green function approach will be presented in two different forms, one of which is the coherent potential method which will be extensively discussed pointing out its strength and weaknesses.

A formalism for a system of extended potentials of muffin tin varieties will be used to solve the self-consistent coherent potential equation and finally results for spectral functions will be obtained for some real brass alloys like α-CuZn and α-CuGe and bronze alloys like α-CuAl. These calculations will be compared with available optical and photoemission data.

A systematic treatment of a tight binding approximation will be presented for random binary alloys in which

hopping integrals are also random unlike the single site cell localised CPA. This model will be used to discuss the electron transport in disordered binary alloys.

The rest of the thesis will be connected with the structurally disordered systems like liquid metals and amorphous solids. We shall discuss the nature of the electronic states in such systems by borrowing the techniques used earlier and shall present the results of our calculation on the electron density of states of liquid metals, Al and Be employing a simple approximate method known as Pseudo-atom model.

Finally a summary of the work will be provided with suggestions for improving theoretical methods.

FIGURE CAPTIONS

Fig.1. Phase diagrams of binary alloys
(a) CuZn, (b) CuGe, (c) CuAl

Fig.2. Density of states of a model binary alloy, calculated by various methods (Ref.58)(a) Virtual crystal approx., (b) Average t-matrix approx. and (c) Coherent-Potential approx; (d-f) are the comparision of ATA and CPA density of states for varying δ (Ref.56).

Fig.3. V-diagram (ref.65) for a model binary alloy $A_x B_{1-x}$ where x = 0.1.

Fig.4. A cluster involving nearest neighbours.

Fig.5. A block diagram for calculating self-consistently the spectral functions $\rho(\varepsilon,\bar{k})$ for a binary alloy.

Fig.6. Tan $\eta_1(\varepsilon)$, phase shifts as a function of energy ε for (a) copper; with Chodorow potential and (b) Aluminium; with Heine-Segall Potential.

Fig.7. Band structure of (a) Cu with Chodorow potential and (b) Al with Heine-Segall potential.

Fig.8. Comparison of band structure of Cu and $Cu_{0.7}Zn_{0.3}$ with VCA

Fig.9. Complex band structure of α-$Cu_{0.7}Zn_{0.3}$ along Γ - X symmetry direction.

Fig.10. Spectral functions $\rho(E,\bar{k})$ for CuZn for Δ_1 states for 20, 20 and 10 at % of zinc in (a), (b) and (c) respectively.

hopping integrals are also random unlike the single site cell localised CPA. This model will be used to discuss the electron transport in disordered binary alloys.

The rest of the thesis will be connected with the structurally disordered systems like liquid metals and amorphous solids. We shall discuss the nature of the electronic states in such systems by borrowing the techniques used earlier and shall present the results of our calculation on the electron density of states of liquid metals, Al and Be employing a simple approximate method known as Pseudo-atom model.

Finally a summary of the work will be provided with suggestions for improving theoretical methods.

FIGURE CAPTIONS

Fig.1. Phase diagrams of binary alloys
(a) CuZn, (b) CuGe, (c) CuAl

Fig.2. Density of states of a model binary alloy, calculated by various methods (Ref.58) (a) Virtual crystal approx., (b) Average t-matrix approx. and (c) Coherent-Potential approx; (d-f) are the comparision of ATA and CPA density of states for varying δ (Ref.56).

Fig.3. V-diagram (ref.65) for a model binary alloy $A_x B_{1-x}$ where x = 0.1.

Fig.4. A cluster involving nearest neighbours.

Fig.5. A block diagram for calculating self-consistently the spectral functions $\rho(\varepsilon, \bar{k})$ for a binary alloy.

Fig.6. Tan $\eta_l(\varepsilon)$, phase shifts as a function of energy ε for (a) copper; with Chodorow potential and (b) Aluminium; with Heine-Segall Potential.

Fig.7. Band structure of (a) Cu with Chodorow potential and (b) Al with Heine-Segall potential.

Fig.8. Comparison of band structure of Cu and $Cu_{0.7}Zn_{0.3}$ with VCA

Fig.9. Complex band structure of α-$Cu_{0.7}Zn_{0.3}$ along Γ - X symmetry direction.

Fig.10. Spectral functions $\rho(E, \bar{k})$ for CuZn for Δ_1 states for 20, 20 and 10 at % of zinc in (a), (b) and (c) respectively.

C O N T E N T S

CHAPTER-I

PHYSICS OF THE DISORDERED STATES

1. INTRODUCTION

The study of 'Electrons in Disordered Systems' has become a very flourishing and challenging field of research in the physics of noncrystalline materials. An ideal crystal in its ground state possesses perfect periodicity. For understanding the physics of condensed matter the ideal concept of Bloch electron has been used, while the real materials possess many kinds of imperfections. Any departure from the ideal ordered situation gives rise to a state of 'disorder'(1).

We shall mainly distinguish the following two types of disorder in the condensed matter considering its geometrical structure.

(i) Cellular disorder: materials which possess lattice structure, for example, substitutional alloys.

(ii) Positional disorder : the position of atoms or molecules in such materials are not isomorphic with the sites of a lattice, for example, liquids, liquid metals and amorphous solids.

Elementary excitations like phonons bring about dynamical disorder while magnons lead to magnetic disorder. Plasmons in metals and excitons in insulators represent the type of electronic disorder. In certain materials at elevated

temperatures there exists a very high degree of disorder. A ferromagnetic material above its Curie temperature has no magnetic long range order(LRO) while a short range order (SRO) may persist upto certain temperature. An alloy above its ordering temperature does not exhibit LRO but SRO may be present. Above the melting point a material has long range positional disorder. However, we shall be primarily interested in the electronic structure of disordered materials falling into the cellular and positional categories.

Looking back to the history of research on the electronic structure of the materials one finds that there have been continual development and refinement of Bloch formulation of energy band theory(2) paralleled to some extent by the evolution of the electron orbital scheme(3) of Mulliken for the atoms and molecules used in the solid state calculations. Both these schemes rely on the Hartree Fock methods of calculating the approximate wavefunctions and energies of the electronic systems employing a static lattice model justified within the Born-Oppenheimer approximation.The past two decades have been remarkedly fruitful for the energy band calculations based essentially on the independent electron model. The power and limitations of the one electron band theory are reasonably well-understood in terms of its relationship to the many body theory for electrons in crystals. With the new advancement of the band structural schemes and development of computer technology considerable progress has been made in carrying

out and interpreting the band structure of many solids. The progress in the experimental studies of band structure has become very rapid and dramatic in the last decade. In addition to the refinement of traditional experimental techniques new methods have been invented to probe the topology of the Fermi surface(4).

In contrast to the satisfactory understanding of the electronic states in crystals gained through experiments and theory during the past decades, our knowledge about the disordered materials is relatively meagre. The lack of translational symmetry does not permit us to use any of the methods developed in the conventional band theory for study of disordered systems. Most of the studies were either for unrealistically simple models or were based on phenomenological models. Besides there were no direct experiments available to study electronic spectra. The conventional powerful methods like de Haas van Alphen (dHvA) effect and cyclotron resonance can only be used when the electrons have long mean free paths. This requirement can not be met in disordered systems.

2. EXPERIMENTS

The commonly used experimental methods to obtain information on the electronic structure of solids can be classified into the following categories:

(i) Spectroscopic Probes:

(A) Optical and Photo-electron emission,
(B) Soft X-rays,

(C) Positron annihilation,
(D) Ion neutralization method,
(E) Kohn anomaly studies.

(ii) Thermal and Magnetic measurements:

(A) Electronic specific heat,
(B) Magnetic susceptibility.

(iii) Conduction Phenomena:

(A) Anomalous skin effect,
(B) Ultrasonic attenuation,
(C) Magnetoresistance,
(D) ac and dc electrical resistivity,
(E) Cyclotron resonance etc.

We shall briefly describe some of the techniques which are capable of yielding reliable information on the band structure and Fermi surfaces of metallic alloys.

(A) OPTICAL(OPT) AND PHOTO ELECTRON EMISSION SPECTROSCOPY (PES)(5)

The optical and photo-electron spectra have very intimate relations with the band structure. In fact, optical measurements have proved to be powerful tools for probing the electronic properties of materials. One of the pioneering works with regards to the pure metals was due to Ehrenreich and Phillips(6), who interpreted the optical spectra of noble metals in terms of the critical points associated with band structure. The quantity $\varepsilon_2(\omega)$, the energy dependent dielectric constant is calculated from the joint density of states derived from band structure. The transition rate and the optical constants can be

deduced from $\varepsilon_2(\omega)$. Conversely, the observed optical absorption spectra can be related to $\varepsilon_2(\omega)$. Subtracting out the Drude term, which is due to intraband transitions, the remaining part of the spectrum is attributed to direct (inter-band) transitions, where the momentum conservation is regarded as a valid selection rule. The photo-electron emission experiments give the electron distribution curves (EDC)(7). This is essentially the quantity representing the density of states of the valence-band distorted by many body effects and surface barrier. Spicer and collaborators(8) believe that the photoemission EDC is due to the nondirect transitions, in which momentum conservation is either through phonons or is non-important. When an electron leaves a state from the valence band it leaves a hole localised on one atom for a time comparable with the excitation time. This is believed to happen for small overlap of states between neighbouring atoms, like the d-wavefunctions in transition metals. This, in other words, deals with a manybody excitation involving electron relaxation around the hole(9). However, no complete theoretical treatment is available although people have started thinking that the photoemission process involves interaction of many particles and many holes(10).

Besides photoemission recently piezo-optical(11), optical modulation(12) and polar reflection Farady effect(13) experiments have been carried out to understand the band structure of the materials. On disordered alloys and

amorphous solids, a bulk of experimental data from optical and photoemission experiments are available.

B. SOFT X-RAY SPECTRA (SXS)(14)

Soft X-ray spectra are obtained, when fast electrons falling on a metal surface eject electrons from the ion core states of the atoms emitting X-rays when electrons from the conduction band fall into these core state vacancies. Since the core level has a well-defined energy, the emitted quantum has the energy equal to the difference of conduction and core state energies.The spectrum therefore provides information about the occupied part of the conduction bands. There are many complications in the interpretation of SXS . This is essentially due to the life-time of the quasi-particles for the states far from the Fermi surface, that produces the energy broadening of the low lying states and smears out any expected structure in this region.

Isochromat spectroscopy(15) is a newly developed technique. In the SXS, one needs the correction for the life-time broadening of the participating core level. The Isochromat spectroscopy is free from this feature. Fast moving electrons of well-specified energy (variable) are shot at the sample and the intensity of the outcoming radiation is analysed by using a fixed frequency X-ray monochromator. This kind of experiment probes the unoccupied energy levels.

There are large amount of SXS experimental data available for ordered and disordered alloys(16), but their quantitative interpretation is not satisfactory. Recently there are some experiments on X-ray photoemission(17) with a very moderate energy resolution.

C. ION NEUTRALIZATION SPECTRA(INS)(18)

To derive information about the density of states in solids Hagstrum has developed this technique, known as Ion neutralization spectroscopy. When a slow (5eV) rare gas ion approaches a metal surface, one of the electrons from the conduction band may tunnel out through the surface to neutralize it, giving up its excess energy to a second electron which is raised to a state above the Fermi level. If the second electron is moving towards the surface with sufficient energy it may escape from the metal and be collected outside. This process is similar as in PES as far as the emergent electron is concerned, but the experiment is difficult to carry out. Besides the interpretation of results is subject to number of assumptions like the energy spectrum of the emergent electrons yields the self-convolution of a certain quantity, that is related to the density of states. Although their precise relationship is extremely complicated, one gets the peaks in the INS for d-electron systems reasonably close in width and position to those expected from other experiments like SXS.

D. NEUTRON SCATTERING AND KOHN ANOMALY(19)

The inelastic scattering of slow neutrons has been used to map the phonon spectrum in great detail. The shape of Fermi surfaces, in principle is reflected in the phonon spectrum, showing small kinks, known as Kohn anomalies. Physically, if we think the solid as a lattice of bare ions, immersed in a sea of conduction electrons, a phonon corresponds to a periodic displacement of the bare ion that produces a periodic electric field which is then largely screened out by the conduction electrons. Their screening ability changes abruptly at certain values of the wavevectors and since screening determines the effective forces between the ions, the dispersion curve exhibits a corresponding kink at those values of the wavevectors.

E. POSITRON ANNIHILATION (POS)(20) and
MÖSSBAUER SPECTROSCOPY(MÖS)(21)

The angular correlation of γ-rays in the experiment of positron annihilation offers information on the momentum distribution of the conduction electrons. When a positron enters into a solid it loses its energy rapidly due to collisions till it is left with its residual thermal energy. Consequently it is annihilated by an electron and the total momentum of the emergent γ-rays is essentially that of the electron. The momentum distribution of the electrons is inferred from the angular intensity distribution and hence the shape of the Fermi surface (22).

A transition between an excited and the ground state of a nucleus is very sharp when the entire crystal takes up the recoil momentum. This is known as Mössbauer effect or recoilless emission of γ-rays. In case of substitutional alloys the information about the charge transfer of s-electrons of the constituents are obtained from the Mössbauer Isomer shift measurements(23). The isomer shift is due to the fact that nucleus has different nuclear charge radii in the excited and ground states. It depends on the s-electron probability density at the nucleus from which the charge transfer is found out.

In a similar manner NMR Knight shift measurements(24) provide us information about the conduction electron density at the nucleus. The specific heat and magnetic susceptibility measurements(25), also yield information about the density of states at the Fermi level.

3. NATURE OF ELECTRONIC STATES IN DISORDERED MATERIALS

It has been pointed out earlier that in the physics of Bloch electrons in crystalline materials, the conduction electrons (or quasi-particles) are itinerant giving rise to extended states possessing infinite life-times. Because of imperfections in the lattice, the quasi-particles get scattered and have only a finite life-time in an eigenstate of the perfect crystal. If we introduce a single impurity atom into a perfect crystal, the Bloch waves propagating throughout the crystal, after being incident onto the impurity, get scattered. The wave functions and

the density of states become somewhat distorted from its original unperturbed state(26). In the case when the scattering potential is very strong, discrete localised eigenstates are obtained which occur below or above the continuous band depending on the attractive or repulsive nature of scattering potential. Further, on increasing the number of impurity atoms, with a random distribution (keeping the impurity concentration still low), we may get extended states with finite phase coherence because of random impurity scattering along with the quasi-continuum localised states. Such features are believed to be more prominent on increasing disorder(27).

(i) PERCOLATION THEORY

From studies using classical percolation approach(28) it has been found that in a disordered medium, where the potentials are randomly distributed, there are finite allowed regions of localised states and allowed channels of extended states. The propagation of electrons from one space point to another depends on the height of the potential barrier between these neighbouring points which make bonds. Chemically the bond is an overlap of electron wavefunctions. When a bond is closed with certain probability, the electron tries to propagate in the medium. A similar situation has also been considered for site percolation(29). So, when a medium is characterised by a random distribution of potentials with certain probability, then the migration of an electron is possible only when it has an energy greater than a critical

energy corresponding to the critical percolation threshold. The latter is dependent on the lattice structure. There are some computer experiments on two-dimensional lattices(27) to show how one can localise a particle in a region with a potential greater than its energy. An extensive literature is available on the percolation problem(30) regarding its analytical approach, numerical results and important consequences. But if one replaces the classical particle by a quantum mechanical one in the same random medium, then the additional process involved will be the tunnelling. Localised electrons from an isolated region will tunnel into another having same energy resulting in delocalisation of states.

(ii) PROBABILITY AND ENSEMBLE-AVERAGE

Before discussing quantum mechanically the nature of electronic states, the notion of probability distribution should be discussed. As we can not have the complete information on the structural details of a physical system possessing certain degree of randomness, we seek to know the most probable configuration or configurations for any particular material. From any experiment one gets certain quantities pertinent to the macroscopic behaviour of the system, these are sharply distributed around the ensemble-averaged value. So the knowledge of the probability distribution for certain configuration of the system is necessary to obtain information about the processes, those have observable relevance. There are two ways of calculating the ensemble-average (a) from

the knowledge of the probability distribution and (b) a technique to calculate directly the ensemble-average like a mean field method.

(iii) ANDERSON MODEL

The class of problems in disordered structures falls in the category (a) is typically the'Anderson model'. Physically let us look into the situation where there is a random assembly of atoms, each possessing a single s-type atomic orbital. An electron is left into such a medium. Let the distribution of energy levels of various atoms or the random potential due to them follow a certain type of probability distribution. At a certain instant of time if one knows the probability amplitude of the electron orbital and observes at that space point how the amplitude behaves with lapse of time, then the information about the (single particle) states can be derived. In atomic systems an electron with the nucleus forms the bound state. In periodic solids, the valence electrons form extended states by modulation of periodic potentials. In both these cases states are stationary with infinite life-time. In the disordered medium the states are intermediate between these two extreme limits. Unlike infinite phase coherence in Bloch states, electrons in disordered medium have finite phase coherence.

Anderson(31) studied the problem of localisation, as to how a localised state will be obtained due to randomness. Since the localised states have important bearing on the

transport phenomena(32) it is necessary to obtain the range of localisation. Anderson's paper is famous for being very complicated and obscure but recently considerable simplification has been achieved by a number of workers such as Ziman, Thouless, Anderson, Kikuchi, Economou and Cohen and many others(33).

The logical structure of the simple Anderson model based on a simple tight-binding Hamiltonian is given by

$$H = \sum_{\alpha} \varepsilon_{\alpha} |\alpha\rangle\langle\alpha| + \sum_{\substack{\alpha,\beta \\ \alpha\neq\beta}} |\alpha\rangle\, t_{\alpha\beta}\langle\beta| \ , \qquad \ldots (1.1)$$

where, ε_{α} is a random independent variable i.e. the eigenvalue of an electron belonging to the atom at the αth site. ε_{α} obeys a common distribution function, $t_{\alpha\beta}$ is the tight binding or hopping integral and is in the present context a positive constant t for α,β being nearest neighbours but zero otherwise. $|\alpha\rangle$ denotes a Wannier state, centered at site α.

In the absence of the tight binding integral the eigen state of the system is nonpropagating, but switching the former on, the state will start propagating to the nearest neighbour site and consequently over the whole system. Stronger the $t_{\alpha\beta}$, easier is the propagation. Besides the eigen energies of the atomic species should be close to each other to permit propagation easily. In the perfect crystal the eigen energies are same all over, as a result of which propagating states are obtained without any scattering. In the present context the strength of the tight binding

integral and the spread of the eigenenergies will decide whether the electron states will propagate in the crystal or be localised; i.e. a critical ratio of t and W(the width of probability distribution of the eigen energies) exists, below which all the states become localised. This has been studied within suitable mathematical framework by introducing the response function (or the Green function) and examining the analytical behaviour of it in the complex energy plane.

Briefly the relation between the Anderson arguments and Green function is shown below. We define the retarded Green function following Zubarev(34):

$$G_{\beta\alpha}(t) = -i\,\theta(t)\,\langle 0|a_\beta(t)a_\alpha^+(o)|0\rangle \quad \ldots (1.2)$$

where $a_\alpha(t)(a_\alpha^+(t))$ is the annihilation(creation) operator in the Heisenberg representation,

$$a_\alpha(t) = \exp(iHt)\; a_\alpha(o)\; \exp(-iHt), \quad \ldots (1.3)$$

$|0\rangle$ is the vacuum state and $\theta(t)$ is the Heaviside step function,

$$\theta(t) = 1 \qquad \text{for} \quad t \geqslant 0$$
$$= 0 \qquad \text{otherwise} .$$

The equation of motion of $G_{\alpha\beta}(t)$ with Hamiltonian(1.1) is

$$i\,\frac{\partial}{\partial t}\,G_{\beta\alpha}(t) = \delta_{\beta\alpha}\delta(t) + \varepsilon_\beta G_{\beta\alpha}(t) + \sum_{\gamma \neq \beta} t_{\beta\gamma}\, G_{\gamma\alpha}(t) \quad \ldots (1.4)$$

The probability amplitude $A_\alpha(t)$ for the state $|\alpha\rangle$ satisfies

the kinetic equation

$$i\frac{\partial}{\partial t} A_\beta(t) = \varepsilon_\beta A_\beta(t) + \sum_{\gamma \neq \beta} t_{\beta\gamma} A_\gamma(t) \qquad \ldots (1.5)$$

with the boundary condition $A_\beta(t) = 0$ for $t = 0$ and $\beta \neq \alpha$, so $A_\beta(t)$ is identified as $G_{\beta\alpha}(t)$ for $t > 0$. Now introducing the Fourier transform

$$G_{\beta\alpha}(t) = \frac{1}{2\pi} \int G_{\beta\alpha}(E) \exp(-iEt)\, dE \qquad \ldots (1.6)$$

we write

$$(E-\varepsilon_\beta) G_{\beta\alpha}(E) = \delta_{\alpha\beta} + \sum_{\gamma \neq \beta} t_{\beta\gamma} G_{\gamma\alpha}(E) \qquad \ldots (1.7)$$

The behaviour of $A_\beta(t)$ after a long time is obtained from the analytic properties of $G_{\beta\alpha}(E)$. When $G_{\alpha\alpha}(E)$ possesses a pole on the real energy axis of the complex energy plane the amplitude of the perturbed state remains stationary as $t \to \infty$ and hence it is a strictly localised state. The situation when $G_{\alpha\alpha}(E)$ acquires a branch cut corresponds to extended states. For the sake of convenience the one particle Greenfunction derived from the resolvent operator $(E-H)^{-1}$ that satisfies the same equation (1.7) will be used hereafter. For real E the Green function is written as

$$G_{\alpha\alpha}(E-i\eta) = \frac{1}{E-\varepsilon_\alpha - i\eta - \Sigma_\alpha^t(E-i\eta)} \qquad \ldots (1.8)$$

with η as a positive infinitesimal and Σ_α^t is the socalled total self-energy, arising out of scattering due to random

elements in an infinite series. The conditions of localisability for a given value of E should hold

$$\lim_{\eta \to 0^+} \mathrm{Im}\ \Sigma_\alpha^t(E-i\eta) = 0 , \qquad \ldots (1.9a)$$

with probability unity, and

$$E-\varepsilon_\alpha - \lim_{\eta \to 0^+} \mathrm{Re}\ \Sigma_\alpha^t (E-i\eta) = 0 \qquad \ldots (1.9b)$$

when the random elements $\{\varepsilon_\alpha\}$ fall inside the width of the probability distribution. Essentially the complicacy of the analysis of this model lies in the convergence of the series for Σ_α^t .

$$\Sigma_\alpha^t = \sum_{\gamma \neq \alpha} t_{\alpha\gamma} \frac{1}{E-\varepsilon_\gamma} t_{\gamma\alpha} + \sum_{\substack{\gamma \neq \alpha \\ \delta \neq \alpha}} t_{\alpha\gamma} \frac{1}{E-\varepsilon_\gamma} t_{\gamma\delta} \frac{1}{E-\varepsilon_\delta} t_{\delta\alpha} + \ldots\ldots \qquad \ldots (1.10)$$

For convenience the series is summed diagrammatically using the method of self-avoiding walks by which a site is not visited more than once. Finally the series (1.10) is rewritten

$$\Sigma_\alpha = \sum_{\gamma \neq \alpha} t_{\alpha\gamma} \frac{1}{E-\varepsilon_\gamma - \Sigma_\gamma^\alpha} t_{\gamma\alpha} + \sum_{\substack{\gamma \neq \alpha \\ \delta \neq \gamma, \alpha}} t_{\alpha\gamma} \frac{1}{E-\varepsilon_\gamma - \Sigma_\gamma^\alpha} \times t_{\gamma\delta} \frac{1}{E-\varepsilon_\delta - \Sigma_\delta^{\alpha,\gamma}} t_{\delta\alpha} + \ldots\ldots \qquad \ldots (1.11)$$

with $\Sigma_\gamma^\alpha = \sum_{\delta \neq \gamma \neq \alpha} t_{\gamma\delta} \frac{1}{E-\varepsilon_\delta - \Sigma_\delta^{\alpha,\gamma}} t_{\delta\gamma}$ and so on.

This hierarchy of (1.11) is known as renormalised perturbation

series (RPS). A similar analytical derivation has been obtained by Fujita and Hori(35) in a continued fraction series.

Using a strong statistical dependence of the quantities in various terms of RPS, Economou and Cohen wrote a function

$$L(E) = \lim_{M \to \infty} \left[\sum t_{\alpha\gamma_1} \frac{1}{E-\varepsilon_{\gamma_1} - \Sigma^{\alpha}_{\gamma_1}} t_{\gamma_1\gamma_2} \ldots t_{\gamma_M\alpha} \right]^{1/M} \quad \ldots (1.12)$$

(where all subscripts are distinct) whose properties are

for $L(E) > 1$ - Eigen states corresponding to E are all extended

< 1 - Either no eigen state at E or Eigen states are localised.

and $= 1$ - the corresponding E separates localised from extended states known as mobility edge.

These results were derived when the RPS is convergent according to a probabilistic analysis. The result(1.12) is further approximated by removing the restricted summation with a factor K^M, when K is the connectivity of the lattice given by 2/3 of the number of nearest neighbours. Further the product of quantities, $1 / (E-\varepsilon_{\gamma} - \Sigma^{\alpha}_{\gamma})$ etc. are approximated by $g(E, H_{eff.})$, a function of an effective Hamiltonian so that for the Hamiltonian (1.1) with constant nearest neighbour hopping, t :

$$L(E) \simeq Zt\,|g(E, H_{eff})| \quad \ldots (1.13)$$

This form of the function has been used in showing the localised states in the density of states out of effective

Hamiltonian by Economou and collaborators (33) which is inconsistent in the effective Hamiltonian theory.

As it has been pointed out earlier, the localisation is not to be seen in a particular space point (like examining the diagonal Green function), one has to find out a domain to determine the size of the localised states. There are many analytical attempts in this direction by Anderson and many others(36).

4. MODELS ON DISORDERED BINARY ALLOYS

The theories of binary alloys have initially relied heavily on simplified models. We shall discuss mainly binary disordered alloys of substitutional type A_xB_{1-x}. The first question arises on the structural stability of the alloy, if the element B is miscible in A through a wide range of concentration - a problem often considered by metallurgists in terms of certain empirical rules. The commonest of all are the socalled Hume Ruthery rules, that put restrictive conditions on the formation of structurally stable solid solution (37), (a) Atomic size, (b) Difference of electronegativity and (c) Electron per atom ratio.

It is difficult to form solid solutions if the diameters of A and B type of atoms differ by more than 15%.. Typically for brass alloys like CuZn, with their atomic radii 2.55 A° and 2.66 A° respectively, the sizes are favourable for zinc to go into copper as a solid solution upto 38 at %. of Zn in contrast to Cd(with atomic radius 2.97 A°) is soluble in Cu to about 1.7 at %. . Secondly, even if the atomic sizes are in favourable ratio,

the solid solutions will not be formed if A and B elements have a tendency to form a stable compound in definite proportion. If A is strongly electronegative and B is strongly electro-positive like III-V or II-VI compounds, it is very likely that instead of solid solutions compounds, such as AB or A_2B etc. will be precipitated out of the solution. For example, the atomic diameter ratio (1.09) is favourable for Sb in Mg but the solubility of Sb in Mg is small because of electro-negativity difference. Thirdly in alloys different constituent valancies (the ratio of electrons per atom) are sometimes used to find the structural changes in the phase diagram. We shall illustrate this below by considering some Cu based alloys.

(i) PHASE DIAGRAM OF ALLOYS (38)

In Fig.1 we show the phase diagrams of copper-based binary alloys with zinc, germanium and aluminum as the second element. The first two are known as brass alloys and CuAl is known as bronze alloy. When zinc is added to copper, the primary solution of zinc in copper is formed with the same fcc structure as pure copper. This is known as α-phase of brass which goes upto 38%. (atom)of zinc. Between the limits of 38 to 46%. of zinc a two-phase region occurs corresponding to α-β phases while from 46-49%. the alloy becomes a secondary solid solution changing its structure i.e. b.c.c. in β-phase. The β-phase undergoes an order disorder phase transition at a temperature of

about 540°C below which one gets an ordered β' phase with Cs-Cl structure. At higher zinc concentrations we get cubic γ-phase hexagonal ϵ-phase with an axial ratio ~ 1.56 and a hexagonal η-phase with axial ratio ~1.8. The η phase like α-phase is a primary solid solution of Cu in zinc while β, γ and ε are all phases of secondary solid solutions.

In Fig.1(b) and (c) we show the phase diagrams of CuGe and CuAl.

(ii) Phenomenological Models

A. Rigid band model (RBM)(39)

In this simple model one assumes the shape of the density of states $\rho(E)$ does not change on alloying, but the concentration of the electron 'n' in the conduction band changes. The Fermilevel on alloying is obtained from the simple relation

$$n = \int_{-\infty}^{E_F} \rho(E)\, dE \qquad \ldots (1.14)$$

RBM has been sometimes used to correlate the electron concentration with structural stability. On alloying one pours the valence electrons of the constituent element into a single nearly free electron band. Once the filled states reach the zone boundary it is costly to add further electrons which can only be accommodated in states above the energy gap which occurs at the zone

boundary or states at the corners of the zone both of which are of high energy. On further adding electrons a structural transformation takes place so that the new phase contains a large number of states before it makes contact with zone boundary. The stability of alloys like α-brasses ($^{e}/_{a}$ limit of CuZn being 1.36) which undergoes a transformation from f.c.c. to b.c.c. was interpreted in the above said manner. However, it is now felt(40) that there is in general no special stability associated with Fermi sphere to touch Brillouin zone boundary. There are other factors like presence of SRO and charge transfer which influence the structural stability. The rigid band model is inadequate in many cases to explain measurements of magnetic susceptibility, specific heat, soft x-ray emission and photo-emission of transition metal alloys like Ni-Cu(41).

Several authors(42) attempted to go beyond RBM of Cu based alloys arguing that density of states at the Fermi level could be improved by impurity scattering in order to fit the increase of linear term of the specific heat coefficient with impurity concentration.

B. Virtual Crystal Approximation (VCA)(43)

The potential for an AB alloy in the band theory is written as superposition of atomic potentials of the constituents in the following manner,

$$V(\bar{r}) = \sum_{\alpha} \left[\frac{1}{2} (1+c(\bar{R}_{\alpha})) v^{A}(\bar{r}-\bar{R}_{\alpha}) + \frac{1}{2}(1-c(\bar{R}_{\alpha})) v^{B}(\bar{r}-\bar{R}_{\alpha}) \right] \quad \ldots (1.15)$$

structure. The key feature of this model is the dependence of the gap between the conduction band and the next higher energy band. The energy gap is estimated by relating it to the atomic s-p excitation energies of the solute and solvent atoms. The importance of the energy gap results from the dependence of the curvature of the Fermi surface on the magnitude of the gap. General trends in the band structure with positions in the periodic table can then be interpreted in terms of the s-p excitation energies and the atomic volume, which increases as one moves down or to the right of the table. For Cu based alloys a large atomic volume means a small Fermi energy while an increase in atomic number means an increase in s-p excitation in Cu alloys; both favour a small energy band gap and a spherical energy surface.

D. Minimum Polarity Model (MPM)(48)

In contrast to the RBM, the minimum polarity model is valid in the limits where the random potential in the Hamiltonian is strong. This is suitable for transition metal alloys. MPM assumes that the electronic configurations of each component in its pure state are carried over to the alloy. The RBM leads to appreciable polar character on each site, where MPM assumes charge neutrality.

This model has been applied in a heuristic way to the NiCu system yielding nice agreement with experiment.The band calculation of Ni and Cu with starting configurations $3d^9 4S$ and $3d^{10} 4S$ respectively give results in

substantial agreement with experiment. Use of these configurations in the alloys confines extra d-electrons to the Cu-sites. This is only possible in the band picture if d-states associated with Cu are below the Fermi level. Since 4s configurations are same in both components the s-bands undergo little change on alloying. Essentially this model takes care of the repulsive interaction between the d-holes.

E. Virtual Bound-state Model (VBM) (49)

The virtual bound-state model lies in between the two extremes, RBM and MPM. This is also known as Friedel-Anderson resonance model and is appropriate for transition metal impurity in noble metals. It is assumed that the electron correlation of opposite spin becomes important when they belong to the same atomic level with energy, say E_α. In the simple Hartree Fock approximation one can write the interaction $U \langle n_{d\uparrow} \rangle \langle n_{d\downarrow} \rangle$ with $\langle n_{d\sigma} \rangle$ as the average number of d-electrons with spin σ and U the strength of interaction. In the alloy if the atomic levels remain sharp on the dissolution of the transition metal into ordinary metals then the levels will be polarized with say $n_{d\uparrow}$ as much as possible. Now on introducing a spin-independent interaction between the localised d-state and s-band state linking with same spin, there will be a transition to or from the conduction band at the rate proportional to the density of state available at E_d and the square of the strength of s-d interaction. This

transition gives rise to a broadening of the d-state. The density of conduction state hence acquires a resonance peak. This state contains enough charge to screen the valence difference between impurity and host. The rest of the screening may be due to conduction electrons in the vicinity of impurity. The Fermi level in this model does not shift. This model is found satisfactory to explain the optical and photo-emission experiments on alloys upto 20 at % transition metal solutes in noble metals(50) like CuNi, CuMn, CuPd, AgPd, AgMn, AuPd, AuNi.

F. Stern's Charging Model(7)

In the crystalline periodic systems the conduction electron sees only the potential due to ion or ions in its own unit cell, that is why the periodicity requirement demands the Wigner Seitz cell to be charge neutral. This requirement is no longer valid when the periodicity is destroyed in disordered alloys. The charging which is due to the non-uniform electron distribution in disordered system has to be included in the bare ion potential in a self-consistent manner. Suppose due to the charge fluctuation the impurity cell is, say positively charged, this will produce a net long ranged Coulomb field throughout the whole solid. In dilute alloys the shielding clouds are such that they completely neutralise the positive charge of the impurity outside the screening length which is of the order of the atomic dimension. But for concentrated

alloys, this question has to be answered by a quantitative calculation. In a tight binding approximation Stern(52) has shown that there is in general a net electric charge in the cell about each constituent i.e. neutralization does not occur in concentrated alloys. The calculation of net electric charge and ion core potential has to be done in a self-consistent fashion.

5. PLAN OF THE THESIS

We shall adopt the multiple scattering approach for studying electrons in a medium of random binary alloys. In Chapter II the Green function theory is used to describe the multiple scattering. The self-consistent Green function hierarchy is decoupled within a single site approximation which is known as coherent potential approximation (CPA). The limitations of the cell-localised CPA, which is widely used in the recent days are pointed out and improvements are shown in two ways. Firstly by considering a many atom cluster instead of a single site description. Secondly we have employed a single site extended potentials of muffin tin variety. This formulation in its first iteration (which is the well known Averaged T-matrix approximation(ATA)) is used to calculate the spectral functions for some Cu based alloys in Chapter III. The results of the calculations are compared with the available experimental data on optical, photoemission, soft x-rays and positron annihilation spectroscopies. In Chapter IV a detailed treatment of a tight-

binding approximation is presented for a random binary alloy in which the hopping integrals are also random unlike the single site cell-localised CPA. In Chapter V this formulation is used to calculate the static electrical conductivity using the linear response theory of Kubo. Chapter VI is concerned with the positionally disordered systems. A canonical density matrix method is used to calculate the density of states of liquid metals like Al and Be. Chapter VII provides the summary of the thesis as to how one could improve the results presented here.

CHAPTER II

MULTIPLE SCATTERING THEORY

The recent theories of disordered systems are usually viewed within the framework of the multiple scattering theory(53). The system is looked upon as a medium in which the atoms or molecules are randomly distributed and the conduction electrons while propagating suffer from scattering due to the random part of the potentials. It has been pointed out earlier that one has to perform a configurational averaging in order to obtain a quantity of physical interest, like density of states, conductivity tensor and so on. Therefore the formulation of any theory for disordered system has to be cast in such a manner that this configurational and/or thermodynamic averaging(34) can be done very easily. Averaging wave functions in disordered medium makes no meaning but the Green function which is a natural language of discussing the elementary excitations in condensed materials offer a possibility of affecting such an averaging. It is for this reason that most of the formulations of the disordered materials make use of the Green functions in one way or other.

1. GREEN FUNCTION AND T-MATRIX

We outline the Green function theory in the independent particle picture with Hamiltonian

$$H = H_o + V \qquad \ldots (2.1)$$

where H_o is the free or unperturbed part of the Hamiltonian and V is the potential operator that scatters the electrons and is regarded here as sum of contributions from the scattering centers having potentials v_α, so that

$$V = \sum_\alpha v_\alpha \qquad \ldots (2.2)$$

1. GREEN FUNCTION

The Schrödinger equation in the coordinate representation with the single particle Hamiltonian H is written as

$$(E-H)\ \psi(\bar{r}) = 0\ , \qquad \ldots (2.3)$$

Corresponding to this one can write the Green function equation

$$(E-H)\ G(\bar{r},\bar{r}';E) = \delta(\bar{r}-\bar{r}') \qquad \ldots (2.4)$$

with suitable boundary conditions. If the energy parameter E does not coincide with the eigen value of H, then eq.(2.4) uniquely defines $G(\bar{r},\bar{r}',E)$. In general we use a complex number z in place of real E, with an infinitesimal imaginary part and define

$$G^{\pm}(z) = \underset{\eta\to o}{Lt}\ G(E\pm i\eta) \qquad \ldots (2.5)$$

when E coincides with any eigen value of H, G^+ and G^- are not identical. In the operator form the Green function

known as Green operator is formally written as

$$G(z) = (z-H)^{-1} \qquad \ldots (2.6)$$

Using the relation

$$\underset{y \to o}{\text{Lt}} \frac{1}{x \mp iy} = \frac{P}{x} \pm i\pi\delta(x)$$

we can write

$$G^{\pm}(z) = P \frac{1}{E-H} \mp i\pi\delta(E-H) \qquad \ldots (2.7)$$

where P stands for the principal value integral. So, it follows that

$$\text{Im } G^{\pm}(z) = \mp \pi \, \delta(E-H) \; . \qquad \ldots (2.8)$$

If $|\alpha\rangle$ and ε_α be the eigen functions and eigen values of H then

$$\begin{aligned} \sum_\alpha \langle\alpha|\delta(E-H)|\alpha\rangle &= \sum_\alpha \delta(E-\varepsilon_\alpha) \\ &= \mp \frac{1}{\pi} \text{Im} \sum_\alpha \langle\alpha| G^{\pm}(z) |\alpha\rangle \\ &= \mp \frac{1}{\pi} \text{Im tr } G^{\pm}(z) \qquad \ldots (2.9) \end{aligned}$$

where tr stands for the trace of the operator. Therefore, the density of states is given by

$$\rho(E) = \mp \frac{1}{\pi} \text{Im tr } G^{\pm}(E) \qquad \ldots (2.10)$$

If we introduce a complete set of states $\{|\lambda\rangle\}$ in a certain representation then we can write, the matrix element of G

$$\langle\lambda|G^{\pm}(z)|\lambda'\rangle = G^{\pm}_{\lambda\lambda'}(z) = \sum_{\alpha} \frac{\langle\lambda|\alpha\rangle\langle\alpha|\lambda'\rangle}{E-\varepsilon_{\alpha}\pm i\eta}$$

$$= \sum_{\alpha} \frac{\langle\lambda|\alpha\rangle\langle\alpha|\lambda'\rangle}{E-\varepsilon_{\alpha}} \mp i\pi \sum_{\alpha} \langle\lambda|\alpha\rangle\langle\alpha|\lambda'\rangle\, \delta(E-\varepsilon_{\alpha}) \qquad \ldots (2.11)$$

The real and imaginary part of $G_{\lambda\lambda'}(z)$ are related by the Kronig-Kramer dispersion relation and Green function is known completely if the imaginary part of it is known. The analytic behaviour of the Green function yields the following information.

When the eigen spectrum of H is discrete, at the eigen values the second term of (2.11) is a sum of δ-functions with coefficients $\langle\lambda|i\rangle\langle i|\lambda'\rangle$ equal to the residues. In such a situation $G_{\lambda\lambda'}(z)$ has discrete set of first order poles at the eigen values. In case of continuous spectrum of extended eigen states $G_{\lambda\lambda'}(z)$ possesses a cut along the real axis within the range where the spectrum is continuous. The discontinuity along the branch cut is obviously proportional to the Im $G_{\lambda\lambda'}(z)$. The third kind of eigen states which we have pointed out earlier is the localised ones. They may occur in the continuous spectrum. Instead of branch cut such singularities are closely spaced poles with nonzero residues and are socalled natural boundaries(54).

With the Hamiltonian in (2.1) the total and unperturbed Green functions are thus defined by (2.6) and

$$G_{o}(z) = \frac{1}{E - H_{o}} \qquad \ldots (2.12)$$

respectively. So we can write suppressing the boundary conditions

$$G(z) = \frac{1}{E-H_o-V}$$

$$= \frac{1}{G_o^{-1}(z) - V}$$

$$= G_o(z)+G_o(z)V\,G_o(z) + \ldots\ldots \quad \ldots (2.13a)$$

$$= G_o(z)+G_o(z)VG(z). \quad \ldots (2.13b)$$

where we have V, is the total scattering potential.

In an inhomogeneous medium which is constituted of random scatterers we can write the total wave function in terms of incident wave with Lipmann-Schwinger type of equation

$$\psi = \psi_o+G_oV\psi$$

$$= \psi_o+\sum_\alpha G_o v_\alpha \psi_\alpha \quad \ldots (2.14)$$

where $\psi_\alpha = \psi_o+\sum_\beta G_o v_\beta \psi_\beta$, $\quad \ldots (2.15)$

ψ_o being the unperturbed wavefunction, ψ_α, wave function that describes the field at the αth site and β runs over all sites. Equation (2.15) can be rewritten as

$$\psi_\alpha = (1-G_o v_\alpha)^{-1}(\psi_o+\sum_{\beta\neq\alpha} G_o v_\beta \psi_\beta) \quad \ldots (2.16)$$

$$= (1-G_o v_\alpha)^{-1}\,\psi^\alpha \quad \ldots (2.17)$$

where ψ^α is the effective incident wave function constituted of the unperturbed one and those due to scattered wave from all other sites except the αth site. Multiplying v_α on both sides we get

$$v_\alpha \Psi_\alpha = t_\alpha \Psi^\alpha \qquad \ldots (2.18)$$

where $$t_\alpha = \frac{v_\alpha}{1-G_o v_\alpha} \qquad \ldots (2.19)$$

is the single site t-matrix.

From (2.13b) we obtain

$$G(z) = G_o(z) + G_o(z)\, T(z)\, G_o(z) \qquad \ldots (2.20)$$

where
$$T(z) = V + V\, G_o(z) V + \ldots.$$
$$= V(1-G_o V)^{-1} \qquad \ldots (2.21)$$
$$= V(1+G(z)V) = V(1+G_o T) \qquad \ldots (2.22)$$

$T(Z)$ is the total t-matrix, which is directly related to the scattering cross-section. Now we shall relate the total t-matrix with the single site t-matrix using (2.22) and (2.2).

$$T(z) = \sum_\alpha v_\alpha (1+G_o T(z))$$
$$= \sum_\alpha T_\alpha(z) \qquad \ldots (2.23)$$

This expresses total t-matrix as a contribution from all individual sites. Dropping the energy argument, we write

$$T_\alpha = v_\alpha + v_\alpha G_o T_\alpha + v_\alpha G_o \sum_{\beta\neq\alpha} T_\beta \qquad \ldots (2.24)$$

which can be further written as

$$T_\alpha = t_\alpha (1+G_o \sum_{\beta\neq\alpha} T_\beta) \qquad \ldots (2.25a)$$
$$= t_\alpha + t_\alpha G_o \sum_{\beta\neq\alpha} t_\beta + t_\alpha G_o \sum_{\beta\neq\alpha} t_\beta G_o \sum_{\gamma\neq\beta} t_\gamma + \ldots. \qquad \ldots (2.25b)$$

Equation (2.25b) is the infinite series for the t-matrix that contain interference terms due to scattering of waves from all sites. Thus,

$$T = \sum_{\alpha} t_{\alpha} + \sum_{\alpha} t_{\alpha} G_{o} \sum_{\beta \neq \alpha} T_{\beta} \qquad \ldots (2.26)$$

is an exact series which will be examined in the next section.

2. COHERENT POTENTIAL APPROXIMATION (CPA) (56)

In this section we shall utilize the knowledge of multiple scattering theory to obtain workable expressions in the single site approximation and extend it to the case of a finite cluster. It has been said earlier that an ensemble average over all possible configurations of the atomic arrangements in the lattice structure is necessary to obtain any quantity of physical interest. In the present method the average will be carried out approximately so as to obtain an effective medium in which the electrons are embedded.

Going back to eq.(2.1) we find the Hamiltonian H contains a free part i.e. periodic and configuration independent and the potential part is random and configuration dependent. The periodic part is the reference part which can be suitably chosen depending on the physics of the problem, while the random part will be correspondingly defined. In the case of 'cell localised disorder', the randomness of potential does not go beyond the atomic cell of the lattice site. We write the potential as a superposition as in (2.2) and divide the Hamiltonian in the following manner.

$$\begin{aligned} H &= (H_{o}+\sigma)+(V-\sigma) \\ &\equiv H^{e}+V^{e} \end{aligned} \qquad \ldots (2.27)$$

where,

$$\sigma = \sum_{\alpha} |\alpha\rangle \sigma_{\alpha} \langle\alpha|$$

$$V = \sum_{\alpha} |\alpha\rangle v_{\alpha} \langle\alpha|$$

and $$V^{e} = \sum_{\alpha} |\alpha\rangle (v_{\alpha}-\sigma_{\alpha}) \langle\alpha|$$

$$= \sum_{\alpha} |\alpha\rangle v^{e}_{\alpha} \langle\alpha|$$

Now we have renormalised the medium in such a way that an electron will suffer scattering at various sites and at say α^{th} site will be scattered by potential v^{e}_{α} relative to the medium H^{e}. Defining the Green function G^{e} as

$$G^{e}(z) = \frac{1}{z - H^{e}} \qquad \ldots (2.28)$$

and with the t-matrix corresponding to the scattering potential v^{e}_{α}

$$T_{\alpha} = t_{\alpha}+t_{\alpha} G^{e} \sum_{\beta\neq\alpha} T_{\beta} \qquad \ldots (2.29)$$

As we have seen earlier, the iteration of (2.29) yields the standard multiple scattering series which depends on the location of all sites. We note here that the characteristic exclusions prevent the electron from scattering twice on the sequence from the same site. All the multiple scatterings with the same particle have been gathered together in t_{α}, so that we have only true sequential multiple scattering. t_{α} includes all the multiple interactions of electron with scatterers at the α site and it describes completely their interaction. Now performing the relevant configurational averaging on the t-matrix, we obtain from (2.29)

$$\langle T_\alpha \rangle = \langle t_\alpha (1 + G^e \sum_{\beta \neq \alpha} T_\beta) \rangle$$

$$= \langle t_\alpha \rangle (1 + G^e \sum_{\beta \neq \alpha} \langle T_\beta \rangle)$$

$$+ \langle (t_\alpha)\ G^e \sum_{\beta \neq \alpha} (T_\beta - \langle T_\beta \rangle) \rangle \qquad \ldots (2.30)$$

The first term describes the scattering of the effective wave on the αth site, while the second term is known as the fluctuation term. In the single site approximation (SSA), the fluctuation is completely ignored corresponding to the neglect of all statistical correlations between the αth and rest other sites.

So,

$$\langle T_\alpha \rangle = \langle t_\alpha \rangle (1 + G^e \sum_{\beta \neq \alpha} \langle T_\beta \rangle) \qquad \ldots (2.31)$$

If we now define the average of the true Green-function with a self-energy $\sum (z)$, which is unknown of the problem, then

$$\langle G \rangle = \left\langle \frac{1}{z - H_o + V} \right\rangle = \frac{1}{z - H_o - \Sigma(z)} \qquad \ldots (2.32)$$

We note that the average $(H_o + \Sigma (z))$ has the full symmetry of the lattice, $\Sigma (z)$ yields information about the scattering and also possesses the full symmetry of the lattice.

From (2.28 ~~4.2~~) $\quad G^{e^{-1}} = \left(\frac{1}{z - H_o - \sigma}\right)^{-1}$

and $\quad \langle G \rangle = \left(\frac{1}{z - H_o - \Sigma}\right)^{-1} = \left(G^{e^{-1}} - (\Sigma - \sigma)\right)^{-1}$

So $\quad \langle G \rangle = G^e + G^e (\Sigma - \sigma) \langle G \rangle \qquad \ldots (2.33)$

From (2.23) using

$$\sum_{\beta\neq\alpha} T_\beta = T - T_\alpha, \quad (2.31) \text{ is written as}$$

$$\langle T_\alpha \rangle = \langle t_\alpha \rangle \left(1 + G^e \sum_{\beta\neq\alpha} \left[\langle T \rangle - \langle T_\alpha \rangle\right]\right) \qquad \ldots (2.34)$$

or $(1+\langle t_\alpha \rangle G^e)\langle T_\alpha \rangle = \langle t_\alpha \rangle (1+G^e \langle T \rangle)$

$$= \langle t_\alpha \rangle \langle G \rangle G^{e-1} \qquad \ldots (2.35)$$

because $$\langle G \rangle = G^e + G^e \langle T \rangle G^e \qquad \ldots (2.36)$$

and $$\langle G \rangle G^{e-1} = 1 + G^e \langle T \rangle$$

Then $$\langle T \rangle = \sum_\alpha \langle T_\alpha \rangle$$

$$= \sum_\alpha \frac{1}{1+\langle t_\alpha \rangle G^e} \langle t_\alpha \rangle \langle G \rangle G^{e-1} \qquad \ldots (2.37)$$

Substituting (2.37) into (2.36) we get

$$\langle G \rangle = G^e + G^e \sum_\alpha \frac{1}{1+\langle t_\alpha \rangle G^e} \langle t_\alpha \rangle \langle G \rangle \qquad \ldots (2.38)$$

Comparing this with (2.33) we obtain

$$\bar{\Sigma} - \sigma = \sum_\alpha \frac{\langle t_\alpha \rangle}{1+\langle t_\alpha \rangle G^e} \qquad \ldots (2.39)$$

Equation (2.39) is written in the form

$$\sum_\alpha |\alpha\rangle \bar{\Sigma}(z) \langle\alpha| = \sum_\alpha |\alpha\rangle \sigma(z) \langle\alpha| + \sum_\alpha |\alpha\rangle \frac{\langle t \rangle}{1+\langle t \rangle F(z)} \langle\alpha|$$

where $$\langle t_\alpha \rangle = |\alpha\rangle \langle t \rangle \langle\alpha| \qquad \ldots (2.40)$$

and $$F(z) = \langle\alpha| G^e(z) |\alpha\rangle \ . \qquad \ldots (2.41)$$

$\langle t \rangle$ will be same for all sites, so no index is put with it and in (2.40) $\underline{\Sigma}(z)$, $\sigma(z)$, $F(z)$ and $\langle t \rangle$ are all numbers. So we get

$$\underline{\Sigma}(z) = \sigma(z) + \frac{\langle t \rangle}{1+\langle t \rangle F(z)} \qquad \ldots (2.42)$$

The equation (2.42) can be solved in two ways.

(i) Non-self consistent solution (ATA)

With a suitable choice of $\sigma(z)$, $\langle t \rangle$ and $F(z)$ are calculated. This method is otherwise known as 'Averaged T-matrix approximation(ATA)'(57) and a detailed discussion is provided by Schwartz et al.(58). If we consider the single band Hamiltonian of (2.1) and use an interpolation

$$F(z) = F^{o}(z-\sigma(z))$$

with $$F^{o}(z) = \langle \alpha | \frac{1}{z-H_o} | \alpha \rangle$$

and we shall get $\underline{\Sigma}(z)$ from $\langle t \rangle$ which is given by

$$\langle t_\alpha \rangle = x \langle t_\alpha^A \rangle + y \langle t_\alpha^B \rangle$$

$$= x \frac{(\varepsilon^A - \sigma)}{1-(\varepsilon^A-\sigma)F} + y \frac{(\varepsilon^B-\sigma)}{1-(\varepsilon^B-\sigma)F}$$

and we choose $\sigma = \bar{\varepsilon} = x\varepsilon^A + y\varepsilon^B$

then $$\underline{\Sigma}(z) = \bar{\varepsilon} + \frac{xy\delta^2 F^{o}(z-\bar{\varepsilon})}{1+2\bar{\varepsilon}F^{o}(z-\bar{\varepsilon})} \qquad \ldots (2.43)$$

where $\delta = \frac{\varepsilon^A - \varepsilon^B}{W}$, W being the band width.

(ii) Self-consistent solution(CPA)

For the requirement $\langle G \rangle = G^e$, $\Sigma(z)$ will be equal to

$$\sigma(z) , \text{ when } \langle t \rangle = 0 \qquad \ldots (2.44)$$

This equation(2.44) is same for all sites due to the periodicity in the averaged system. This method is known as single site Coherent Potential Approximation (CPA)(55,56).

The physical basis of the approximation is viewed in the following manner. The true disordered Hamiltonian, for example (2.1) is replaced by an effective periodic Hamiltonian which in general has complex eigenvalues corresponding to the damping of the states. The self-energy $\Sigma(z)$ which is an unknown of the problem is so determined that the effective wave does not get scattered from any site. The effective wave contains the incident wave and contribution from all sites to the scattered waves, except that coming from the site in question. In the self-consistent procedure we consider the waves propagating in the medium such that it can not be scattered on the average by an atom situated at the αth site. Thus, it follows from the self-consistent solution of the usual multiple scattering problem, in which generally $\langle T \rangle = 0$ is the requirement for the situation when the effective medium is equivalent to the true averaged medium. In the single site version the properties of all sites but one are averaged over and that one is treated exactly. Effects due to the local surrounding are averaged over in this

approximation.

In the nonself-consistent procedure we calculated $\langle t \rangle$ for a choice of effective medium and here we shall find out the medium from (2.44). Because

$\langle G(z) \rangle = G^e(z)$, we shall write (2.44) as

$$x \frac{v_\alpha^A}{1-v_\alpha^A F(z)} + y \frac{v_\alpha^B}{1-v_\alpha^B F(z)} = 0 \qquad \ldots (2.45)$$

where $v_\alpha^{A(B)} = \varepsilon^{A(B)} - \Sigma(z)$.

After some simplification we shall obtain

$$\Sigma(z) = \bar{\varepsilon} - (\varepsilon^A - \Sigma(z))\ F(z)(\varepsilon^B - \Sigma(z)) \qquad \ldots (2.46)$$

which can also be cast into the form

$$\Sigma(z) = \bar{\varepsilon} + \frac{xy\delta^2 F(z)}{1+(\bar{\varepsilon}+\Sigma)F(z)} \qquad \ldots (2.47)$$

Equation (2.46) and (2.47) are two alternate forms of CPA equation derived by Soven(55) and Velický et al.(56) respectively.

Here we note that the Green function method discussed by Yonezawa and Matsubara(59), Das and Joshi(60) and Leath(61) is an equivalent scheme of the CPA. Besides similar schemes have been employed by Taylor and others(62) for phonons, and Onodera and Toyozawa(63) for Frenkel excitons and Roth(64) for spin waves. Thus, CPA has become a working tool for

understanding the behaviour of elementary excitations in disordered systems. This method correctly interpolates to the limits of virtual crystal, dilute alloy and split band situations.

Using the semi-circular model for the density of states of the host, the density of states for A_xB_{1-x} random alloy is shown in Fig.2. $x = 0.15$ and varying δ in both CPA and ATA scheme. In both approximations for increasing δ, we get the distortion of the band at its upper edge and finally at a certain δ the band splits off. Now we shall briefly discuss the well-known results from CPA using the so-called V-diagram(65) as shown in Fig.3 for the same model alloy with $x = 0.1$. The hatched portion shows the density of states for various values of δ. The exact bounds and CPA bounds are demarcated for the density of states. One finds for small δ, there is a common band. A dip appears in the upper region of the band on increasing δ and for large δ the impurity band splits off. Here it is interesting to note that the density of states of the alloy cuts off sharply, without showing any band edge tailing effect. The majority band (or B sub-band) approaches the exact limits of the spectrum and is very much like that of the pure B crystal with not much damping of the states. The minority band is restricted to lie well inside the exact-spectral bounds and the electronic states are strongly damped. For large δ the two sub-bands are essentially independent.

With this cell-localised, CPA model in which the self-energy of the electron is momentum independent there are some calculations for the alloy system NiCu(66) in which the pure density of states of Ni is used from experimental PES data. The same scheme of interpolating the density of states from pure A band structure density is used by Stocks et al.,(67), Leoni et al. and Hasegawa et al.(68) for noble transition metal alloys of CuPd, AgPd and CuNi through a range of concentrations.

The main drawback of such calculations is that the calculated density of states does not possess host-impurity symmetry(59) i.e. the density of states of NiCu calculated from Ni as host is not same as that of Cu-host alloy. Besides, such calculations share the following objection of the single site cell-localised (CPA) theory in which the self-energy is $\bar{k}$-independent.

We have discussed earlier that while calculating the random potential in a disordered system, one should consider the screening of electrons. CPA discussed above is a localised perturbation model which has been shown(69) to violate the screening requirement and the potential in this scheme can not be made self-consistent via Friedel sum rule. Therefore, this particular model can not have much applicability so far as real systems are concerned. Lasseter and Soven(69a) on the other hand have calculated the potential for a single impurity through a self-consistent procedure by utilizing Friedel sum rule.

The calculated changes in the density of states are not sufficient to account for the measured changes in the linear term of the specific heat.

In view of the above limitations of single site CPA it is natural to attempt at improving this approximation. In the recent past many workers have worked out many possible extensions of CPA by including the off-diagonal randomness in the transfer integral and/or by considering the effect of cluster due to pairs, triplets etc. The straight forward extension of single site CPA to clusters is carried out in the next section.

3. CLUSTER MODEL OF ALLOYS

As discussed above the CPA is a single site theory and all the higher order effects are averaged to provide an uniform environment to a single site scatterer; the theory neglects the effect of clusters of atoms in the alloy. The cluster-effects are known to show explicit structures in the energy spectrum. In a model tight binding Hamiltonian in which diagonal disorder is only taken it becomes equivalent to the assumption that the density of states of pure metal of each constituent is the same except for the shift of the energy level. This restriction is removed when one considers the off-diagonal disorder.

Gyrot-Lackmann and Ducastelle (70) have developed a self-consistent pair theory. This theory in the dilute limit is exact to x^2 and it has included the scattering

from all possible pairs with various separations, but it has neglected the presence of random off-diagonal element (RODE) in the tight binding integral. In a similar manner Schwartz and Ehrenreich(71) have calculated the multiple scattering series for a pair by performing the repeated scattering. One can very easily calculate the correction of various orders to the T-matrix from a pair. The nonvanishing correction from it comes in the fourth order which is calculated as

$$\langle \Delta T_\alpha^{(4)} \rangle_{pair} = x^2(1-x)^2 \Delta_\alpha G^e \sum_{\beta \neq \alpha} \Delta_\beta G^e \Delta_\alpha G^e \Delta_\beta, \quad \ldots(2.48)$$

$$\Delta_\alpha = t_\alpha^A - t_\alpha^B, \quad t_\alpha^A = \langle t_\alpha \rangle + (1-x)\,\Delta_\alpha$$

with $$t_\alpha^B = \langle t_\alpha \rangle - x\,\Delta_\alpha \text{ and}$$

$$\langle t_\alpha \rangle = x\,t_\alpha^A + (1-x)t_\alpha^B ,$$

where t_α^A and t_α^B are single-site t-matrices of site α for A and B type of atoms respectively. This theory also shares the same drawback as does that of CyrotLackmann and Ducastelle and such theories can not be unambiguously self-consistent when nonlocal coherent potentials are introduced. Here we note that there are some attempts to include RODE in these theories, which can be derived from a general theory of clusters of tight binding character as discussed below.

A large number of experiments have shown the effect

of local environment on the electronic properties of disordered alloys and it is well known that interatomic forces in general favour some kind of local order(72). Therefore, along with the atom that scatters an electron one should include its neighbours so as to describe the response of an electron to a cluster of atoms. The approach presented here is mainly based on the cluster theory of Freed and Cohen(73) and local disorder theory of Butler and Kohn(74). Freed and Cohen have derived the multiple scattering hierarchy considering a fixed set of scatterers, forming a cluster. Because they describe clusters of finite size, the resulting equation do not preserve the requirement of translational periodicity of the average system, which they overcome by introducing an alternate equation of motion known as extended coherent potential cluster method (ECPn). The cluster Green Function carries with it a weight factor which is the probability distribution function of atoms of a given cluster in an ensemble of all possible configurations. If we periodically repeat such clusters, then after proper averaging we shall obtain a continuous spectrum. Here we shall assume the principle of locality, in which the asymptotic theorem for the operators, having a finite range is valid (74). Let us consider now the same tight binding Hamiltonian (1.1) in which $t_{\alpha\beta}$ is not translationally invariant. It can have any one of the following values t^{AA}, t^{BB}, t^{AB} and t^{BA}.

Taking the same spirit as in single site CPA, we can choose an effective Hamiltonian

$$H^e = \sum_{\alpha,\beta} |\alpha\rangle \sum_{\alpha-\beta} \langle\beta| \qquad \ldots (2.49)$$

for all values of α and β

or $$H^e = \sum_{\alpha} |\alpha\rangle \sum_{o} \langle\alpha| + \sum_{\substack{\alpha,\beta \\ \alpha\neq\beta}} |\alpha\rangle \sum_{\alpha-\beta} \langle\beta| \qquad \ldots (2.50)$$

Here the diagonal element of H^e will be $\sum_o$ and off-diagonal one will be $\sum_{\alpha-\beta}$, which are unknowns of the problem. Looking to (1.1) and (250), $\sum_o$ is the renormalised atomic energy level and $\sum_{\alpha\beta}$ is the new hopping integral that is dependent on $\alpha-\beta$. Here one can note that H^e is translationally invariant. If we now describe scattering with respect to the medium H^e, then the perturbation is

$$V = H - H^e \qquad \ldots (2.51)$$

and the corresponding T-matrix is found out from

$$T = V / (1 - G^e V) \qquad \ldots (2.52)$$

with G^e defined in terms of new H^e in (2.50). For the $\langle H\rangle = H^e$ i.e. $\langle G\rangle = G^e$, we can show from both physical grounds and mathematics that

$$\langle T_{\alpha-\beta}\rangle = 0 \qquad \ldots (2.53)$$

for all values of α and β, and this is the self-consistent condition of the present theory. If $\alpha = \beta$ then (2.53) gives the self-consistent requirement of the single site CPA.

$$T_{\alpha\alpha} = V_{\alpha\alpha} + T_{\alpha\alpha} G^{e}_{\alpha\alpha} V_{\alpha\alpha} + T_{\alpha\alpha} \sum_{\beta \neq \alpha} G^{e}_{\alpha\beta} V_{\beta\alpha} + \sum_{\beta \neq \alpha} T_{\alpha\beta} G^{e}_{\beta\alpha} V_{\alpha\alpha} + \sum_{\substack{\beta\beta' \\ \beta \neq \beta' \neq \alpha}} T_{\alpha\beta} G^{e}_{\beta\beta'} V_{\beta'\alpha} \quad \ldots (2.58)$$

and

$$T_{\alpha\beta} = V_{\alpha\beta} + T_{\alpha\alpha} G^{e}_{\alpha\beta} V_{\beta\beta} + T_{\alpha\alpha} G^{e}_{\alpha\alpha} V_{\alpha\beta} + \sum_{\beta' \neq \beta \neq \alpha} T_{\alpha\beta'} G^{e}_{\beta'\alpha} V_{\alpha\beta} + \sum_{\beta' \neq \beta \neq \alpha} T_{\alpha\beta'} G^{e}_{\beta'\beta} V_{\beta\beta} \quad \ldots (2.59)$$

Eq.(2.59) is a set of Z(nearest neighbour coordination number) simultaneous equations because β runs over all nearest neighbour sites. The self-consistency condition $\langle T_{\alpha-\beta} \rangle = 0$ implies

$$\langle T_{\alpha\alpha} \rangle = 0 \quad \ldots (2.60a)$$

and

$$\langle T_{\alpha\beta} \rangle = 0 \quad \ldots (2.60b)$$

In this approximation closed form of equations for $T_{\alpha\alpha}$ and $T_{\alpha\beta}$ are obtained by defining a matrix

$$Y_{\beta\beta'} = \delta_{\beta\beta'} - X_{\beta\beta'} \quad \ldots (2.61)$$

so that

$$T_{\alpha\beta} = \left[\sum_{\beta' \neq \beta \neq \alpha} V_{\alpha\beta'} y_{\beta'\beta} + T_{\alpha\alpha} \sum_{\beta' \neq \beta \neq \alpha} X_{\alpha\beta'} y_{\beta'\beta} \right] / \Delta \quad \ldots (2.62)$$

and

$$T_{\alpha\alpha} = \frac{V_{\alpha\alpha} + \sum_{\beta \neq \alpha} \sum_{\beta' \neq \beta \neq \alpha} X_{\alpha\beta} y_{\beta\beta'} V_{\beta'\alpha} \Delta^{-1}}{1 - X_{\alpha\alpha} - \sum_{\beta \neq \alpha} \sum_{\beta' \neq \beta \neq \alpha} X_{\alpha\beta} y_{\beta\beta'} X_{\beta'\alpha} \Delta^{-1}} \quad \ldots (2.63)$$

where,

$$X_{\alpha\alpha} = G^{c}_{\alpha\alpha} V_{\alpha\alpha} + \sum_{\beta\neq\alpha} G^{e}_{\alpha\beta} V_{\beta\alpha} ,$$

$$X_{\alpha\beta} = G^{e}_{\alpha\beta} V_{\beta\beta} + G^{e}_{\alpha\alpha} V_{\alpha\beta} ,$$

$$X_{\beta\alpha} = G^{e}_{\beta\alpha} V_{\alpha\alpha} + \sum_{\beta'\neq\beta\neq\alpha} G^{e}_{\beta\beta'} V_{\beta'\alpha} ,$$

$$X_{\beta'\beta} = G^{e}_{\beta'\alpha} V_{\alpha\beta} + G^{e}_{\beta'\beta} V_{\beta\beta} ,$$

Δ is the determinant of Y and y is the cofactor of the matrix Y.

Using (2.62) and (2.63) from (2.60) one can calculate the Coherent Potentials Σ_0 and Σ_1. This general result in the case of diagonal randomness only will yield the socalled self-consistent condition for pair cluster due to CyrotLackmann and Ducastelle (70) and Nickel and Krumhansl (75). The vanishing of the T-matrix in the random case as we have seen above can also be used for a correlated system possessing a short range order. Simply for the case of a pair the equation for $T_{\alpha\beta}$ will be replaced by $\int T_{\alpha\beta} g(R) dR$ where $R = |\alpha-\beta|$, and $g(R)$ is the pair correlation function.

Once the coherent potentials Σ's are determined the density of states can be calculated from the knowledge of the medium Green function G^c. A large number of papers (75) on the cluster and off-diagonal treatment of disordered systems have appeared in the recent days. Some of them report model calculations for a cluster of atom and its nearest neighbours.

CHAPTER-III

ELECTRONS IN THE EXTENDED RANDOM POTENTIALS

We discussed in the last chapter that the cell localised potential model has several limitations for use in the calculation of the electronic structure of real disordered alloys. One of the assumptions that both the constituents in an alloy should have in their pure form identical band shapes is a severe limitation. In the band structure calculation of ordered crystals generally a system of potentials with muffin-tin form(76,77) is used, which is very convenient to handle. This kind of potential is assumed to be spherically symmetric within a certain sphere surrounding each atom while the interstitial space is having a constant (or a zero) potential. Since we consider a random alloy having a definite lattice structure it is tempting to use the conventional band structure scheme like the Green function theory, otherwise known as KKR (Korringa (78), Kohn and Rostoker(79)) method. The formulation of this problem has been very neatly carried out by Soven(80). Gyorffy(81) on the other hand, has rederived in a different way the coherent potential equation for nonoverlapping muffin tin potentials without resorting to δ-shell form.
We shall use the result of Soven's formulation along with certain approximations for our calculation and finally

show the numerical results.

Here we recall that the nonselfconsistent ATA (82-84) can become a good first approximation in an iteration scheme leading finally to the self-consistent CPA solution. We describe below the muffin-tin formalism of CPA scheme in an iterated ATA following essentially the formulation of Soven and examine its applicability.

1. MODEL POTENTIALS AND SELF-CONSISTENT EQUATIONS

The choice of model potentials for the constituent atoms in the alloy are written in the form

$$V^i(\bar{r}, \bar{r}') = \sum_L Y_L(\hat{r}) \frac{\delta(r-R)}{R^2} W_L^i(E) \frac{\delta(r'-R)}{R^2} Y_L(\hat{r}') \quad \ldots (3.1)$$

where L is a composite index for the angular momentum quantum number (l,m). $Y_L(\hat{r})$ is the real spherical harmonics of angle $\hat{r}$, $W_L(E)$ is an appropriately chosen energy dependent (model) potential amplitude, index i stands for the type of atom, R is the radius of the muffin-tin sphere. If the potential amplitude satisfy the equation

$$W_L^i(E) = R^2\left[\mathcal{L}_l^i(E) - \mathcal{K}\, j_l'(\mathcal{K}R) \,/\, j_l(\mathcal{K}R)\right] \quad \ldots (3.2)$$

then the model potential will have the same phase shifts as the true atomic potential of i. Here $\mathcal{L}_l^i(E)$ is the exact logarithmic derivative of the radial wave function of angular momentum l and energy E for ith atom, j and j' are the spherical Bessel function and its derivative and $\mathcal{K} = \sqrt{E}$.

Now with two sets of potentials $V^{(i)}$, the model potential and $\bar{V}^{(i)}$ the true muffin-tin potentials, we can compare the corresponding Green functions, $G^{(i)}$ and $\bar{G}^{(i)}$. While doing this we say that the Green function is in the exterior region of the muffin-tin well when both of its arguments lie outside of it, otherwise it is in the interior region. It can be shown that in the exterior region the Green function $\bar{G}^{(i)}$ is solely determined by the phase shift of the individual potentials. Since $V^{(i)}$ and $\bar{V}^{(i)}$ have same phase shifts, the corresponding Green functions are identical in the exterior region. But in the interior region the Green functions differ. We know that the density of states

$$\rho(E) = -\frac{1}{\pi} \operatorname{Im} \operatorname{tr} \langle G(E) \rangle$$

and now if $\rho^{(i)}(E)$ denote the part of the trace of the above equation arising from the integration over the volume within the sphere surrounding a particular type of atom i then

$$\rho^{(i)}(E) = -\frac{1}{\pi} \operatorname{Im} \int \langle G(\bar{r},\bar{r}) \rangle_{(i)} \, d\bar{r} \qquad \ldots (3.3)$$

where, $\langle \cdots \rangle_{(i)}$ is a restricted average for (i), is definitely at a particular site. In a spherically symmetric situation the angular momentum decomposition of the Green function is given by

$$G(\bar{r},\bar{r}') = \sum_{LL'} Y_L(\hat{r}) \, G_{LL'} Y_{L'}(\hat{r}') \qquad \ldots (3.4)$$

angular momentum subscripts, which arise from the fact that $\langle G \rangle$ and hence $\sum$ need only have the point group symmetry of the lattice. We can write the operator equation for T-matrix of A and B type of atoms corresponding to this medium as

$$T^i = (V^i - \sum) + (V^i - \sum) \langle G \rangle T^i \qquad .. (3.10)$$

As shown above $\langle T \rangle = 0$ from which

$x T^A + (1-x) T^B = 0$ will give the operator form of equation (2.46) as

$$\sum = U + (\sum - V^A) \langle G \rangle (\sum - V^B) \qquad .. (3.11)$$

where $U = x V^A + (1-x) V^B$ and has the same form as in (3.1). Here onwards we shall write CPA medium G for $\langle G \rangle$, because the true averaged medium is described by $\sum$. Then we have

$$G^i = G + G(V^i - \sum) G^i , \qquad .. (3.12)$$

from which (3.8) is written as

$$\rho(E) = -\frac{1}{\pi} \left\{ \mathrm{tr}\, G - N \sum_L \left[x (G_{LL})_A \frac{dW_L^A}{dE} + (1-x)(G_{LL})_B \frac{dW_L^B}{dE} \right] \right\} \qquad .. (3.13)$$

Using the δ-shell model for all the operators (3.11) is written out as a matrix equation in the angular momentum representation:

$$W_{LL'} = U_L \delta_{LL'} + \sum_{L''L'''} \left[W_{LL''} - \delta_{LL''} W_L^A \right] G_{L''L'''} \times \left[W_{L'''L'} - \delta_{L'''L'} W_{L'}^B \right] \qquad .. (3.14)$$

or $$W = U + (W-W^A)\, G(W-W^B) \qquad \ldots (3.15)$$

Now in the above coherent potential equation G occurs which is a functional of W. Since lattice periodicity is there, defining the Fourier transform

$$G(\bar{r},\bar{r}') = \frac{1}{N}\sum_{\bar{k}}' G^{\bar{k}}(\bar{r},\bar{r}') \qquad \ldots (3.16)$$

where the prime over the summation sign restricts the $\bar{k}$ vectors to lie in the first Brillouin zone. Using the Green function in the KKR form we can write in the mixed representation

$$G^{\bar{k}}(\bar{r},\bar{r}') = G_o^{\bar{k}}(\bar{r},\bar{r}') + \sum_{L,L'} G_o^{\bar{k}}(\bar{r},L)\, W_{LL'}\, G^{\bar{k}}(L',\bar{r}') \qquad \ldots (3.17a)$$

$$= G_o^{\bar{k}}(\bar{r}-\bar{r}') + \sum_{LL'} G_o^{\bar{k}}(\bar{r},L)\left[\frac{W}{1-G_o^{\bar{k}}W}\right]_{LL'} G_o^{\bar{k}}(L',\bar{r}') \qquad \ldots (3.17b)$$

where G_o is the free electron Green function, given explicitly in the coordinate representation as

$$G_o^{\bar{k}}(\bar{r},\bar{r}') = \frac{N}{\Omega}\sum_{\bar{k}_n} \frac{e^{i(\bar{k}+\bar{k}_n).(\bar{r}-\bar{r}')}}{\left[E-|\bar{k}+\bar{k}_n|^2\right]} \qquad \ldots (3.18)$$

where Ω is the volume of the crystal, $\bar{k}_n$ denote the reciprocal lattice vectors.

Again using the δ-shell form for $G^{\bar{k}}$ we can straight forwardly write the matrix equation

$$G = \frac{1}{N}\sum_{\bar{k}}' \frac{1}{(I-G_o^{\bar{k}}W)} P^{\bar{k}}, \qquad \ldots (3.19)$$

and

$$\mathrm{tr}\ G = \sum_{\bar{k}}' \left[\sum_{\bar{k}_n} \frac{1}{(E-|\bar{k}+\bar{k}_n|^2)} - \sum_{LL'} \frac{\partial G_o^{\bar{k}}{}_{L'L}}{\partial E}\left(\frac{W}{1-G_o^{\bar{k}}W}\right)_{L'L}\right] \qquad \ldots (3.20)$$

for which the relation $\int G_o^k(\bar{r},L)\ G_o^k(L',\bar{r})d\bar{r} = -N \frac{\partial G_{o\,LL'}^{\bar{k}}}{\partial E}$ has been used. It has been shown by Beeby that the poles of the first term in (3.20) for the electron energies get cancelled by the corresponding poles in the second term.

Now G_{LL}^i is calculated as

$$G_{LL}^i = \sum_{L'} \left[1-(W^i-W)G\right]^{-1}_{LL'} G_{L'L} \text{ from which the}$$

formula for the density of states can be written as

$$\rho(E) = -\frac{1}{\pi}\,\mathrm{Im} \sum_{\bar{k}}{}' \sum_{LL'} \left(\frac{\partial G_{o\,L'L}^{\bar{k}}}{\partial E}\right)\left[\frac{W}{1-G_o^k W}\right]_{LL'}$$

$$-N\,\mathrm{Im} \sum_{LL'} G_{L'L}\left[x \frac{dW_{LA}}{dE}\left\{(1-(W_A-W)G)^{-1}\right\}_{LL'}\right.$$

$$\left.+(1-x)\frac{dW_{LB}}{dE}\left\{(1-(W_B-W)G)^{-1}\right\}_{LL'}\right] \qquad \ldots (3.21)$$

The above formula is further simplified using the KKR method where the values of its argument lie inside the muffin-tin sphere so that

$$G_o^{\bar{k}}(\bar{r},\bar{r}') = \kappa \sum_{LL'} Y_L(\hat{r})\left[\delta_{LL'} j_l(\kappa r_<)\ n_l(\kappa r_>)\right.$$

$$\left.+ i^{l-l'} j_l(\kappa r)\, j_{l'}(\kappa \bar{r}')\ B_{LL'}^{\bar{k}}\right] Y_{L'}(r') \qquad \ldots (3.22)$$

where $r_>$ and $r_<$ are greater or less of $\bar{r}$ and $\bar{r}'$ and $B_{LL'}^{\bar{k}}$ is the structure constant matrix to be described later. The potential amplitude defined in eqn. (3.2) can be obtained as

$$W_{L,i} = - \left[\mathcal{K} j_l(\mathcal{K}R) \left(j_l(\mathcal{K}R)\, C_{L,i} - n_l(\mathcal{K}R) \right) \right]^{-1} \qquad .. (3.23)$$

from the elementary potential scattering, where $C_{L,i}$ are the cotangent of the phase shifts for i kind of potential. For the complex potential $\sum$, C_L will be complex, so that

$$W_L = - \left[\mathcal{K} j_l(\mathcal{K}R) \left[j_l(\mathcal{K}R) C_L - n_l(\mathcal{K}R) \right] \right]^{-1} \qquad .. (3.24)$$

Now from (3.22) we have

$$G^{\tilde{k}}_{o_{LL'}} = \mathcal{K} \left[j_l(\mathcal{K}R) n_l(\mathcal{K}R) \delta_{LL'} + i^{l-l'} j_l(\mathcal{K}R) j_{l'}(\mathcal{K}R)\, B^k_{LL'} \right] \qquad ... (3.25)$$

Using the above two equations in (3.17b) we get

$$G^k_{LL'} = \mathcal{K} j_l(\mathcal{K}R) \left[j_{l'}(\mathcal{K}R) C_L - n_{l'}(\mathcal{K}R) \right] \delta_{LL'} - \mathcal{K}\, i^{l-l'} \left[j_l(\mathcal{K}R) C_L - n_l(\mathcal{K}R) \right] \times \left(j_{l'}(\mathcal{K}R) C_{L'} - n_{l'}(\mathcal{K}R) \right) \left[C + B^k \right]^{-1}_{LL'} \qquad ... (3.26)$$

Now aumming over $\tilde{k}$ we get

$$G_{LL} = \mathcal{K} j_l (j_l C_L - n_l) - \mathcal{K} (j_l C_L - n_l)^2 g_L \qquad ... (3.27)$$

where,

$$g_L = \frac{1}{N} \sum_k{}' \left[C + B^k \right]^{-1}_{LL} \qquad ... (3.28)$$

Using (3.23) and (3.24) in the coherent potential equation (3.15) we shall obtain a system of equations

$$C_L = C_{L,av} + (C^A_L - C_L) g_L (C^B_L - C_L) \qquad ... (3.29)$$

where $C_{L,av} = xC_L^A + (1-x)C_L^B$ ... (3.30)

Here we note that eqn.(3.28) and (3.29) are coupled equations which need be self-consistently determined.

Now we go back to equation (3.21) for the density of states, Using (3.24) and (3.25) we can write

$$\left[\frac{W}{1-G_o^{\bar{k}}W}\right]_{LL'} = -i^{l-l'}(\mathcal{K}j_l j_{l'})^{-1}\left[C+B^{\bar{k}}\right]^{-1}_{LL'} \quad \ldots (3.31)$$

and $$\frac{\partial}{\partial E} G^{\bar{k}}_{o_{LL'}} = i^{l-l'}\left[\delta_{LL'}\frac{d}{dE}(\mathcal{K}j_l n_l) + B^{\bar{k}}_{LL'}\frac{d}{dE}(\mathcal{K}j_l j_l) + \mathcal{K}j_l j_l \frac{\partial}{\partial E} B^{\bar{k}}_{L'L}\right], \quad \ldots (3.32)$$

so that the first term of (3.21) is

$$\mathrm{Im}\sum_L \left\{ \sum_{\bar{k}}' \left[\frac{\partial B^{\bar{k}}}{\partial E}\left[C + B^{\bar{k}}\right]^{-1}\right]_{LL} + N g_L (\mathcal{K}j_l^2)^{-1}\left[\frac{d}{dE}(\mathcal{K}j_l n_l) - C_L \frac{d}{dE}(\mathcal{K}j_l^2)\right]\right\} \quad \ldots (3.33)$$

and similarly the second term is obtained as

$$-N\mathrm{Im}\sum_L \left\{ (1-x)(C_L^A - C_L)^{-1}\frac{dC_L^A}{dE} + x(C_L^B - C_L)^{-1}\frac{dC_L^B}{dE} + (\mathcal{K}j_l^2)^{-1} g_L\left[\frac{d}{dE}(\mathcal{K}j_l n_l) - C_L \frac{d}{dE}(\mathcal{K}j_l^2)\right]\right\} \quad \ldots (3.34)$$

Now on adding together the final expression for the spectral density of states per atom is obtained as

$$\rho(E,\bar{k}) = \frac{1}{\pi} \mathrm{Im} \sum_L \left[\left[C+B^{\bar{k}} \right]^{-1} \frac{dB^{\bar{k}}}{dE} \right]_{LL} + \mathrm{Im} \sum_L \{ (1-x)(C_L - C_L^A)^{-1} \frac{dC_L^A}{dE} + x\,(C_L - C_L^B)^{-1} \frac{dC_L^B}{dE} \} \quad \ldots (3.35)$$

In order to obtain the total density of states we have to integrate over the first Brillouin zone i.e. a summation over the rhs of (3.35) is to be carried out.

We realize that the use of the above formalism is an extremely difficult task because of the fact that in one of the coupled CPA equations (3.28), there is a summation on the first Brillouin zone, performing this summation for once only is already a difficult task because the function is highly anisotropic in $\bar{k}$. Use of standard methods like linear interpolation scheme (86) or QUAD scheme (87) in this case is practically impossible. Besides there is an extremely simple method of k-sum known as 'Mean Value Point Method' due to Balderschi(88). But this method is useful only when the function is smooth in $\bar{k}$. In view of these difficulties we shall use the ATA result for the phase shift in eq.(3.29) and then calculate the quantities as described in the block-diagram (Fig.5). Mean value point method was used to perform the $\bar{k}$-sum, and was found to be poorly convergent in view of the fact that it is not to be used for arbitrary functions (unless smooth). So, the results may not be reliable.

We found that the CPA program as detailed in Fig.5 is difficult to implement, we avoid the iterations of (3.28) and (3.29). The details of this calculation for CuAl is described below.

We have also calculated the spectral functions by assuming the potentials of the constituent atoms and the medium to be of the δ-shell form as in (3.1). The amplitude of the medium potential is obtained from CP equation(77)

$$W_L = \frac{G_L^o W_L^A W_L^B - (x W_L^A + (1-x) W_L^B)}{G_L^o \left[(1-x) W_L^A + x W_L^B \right] - 1} \qquad \ldots (3.36)$$

where $G_L^o = G_L^o(R,R)$, l^{th} angular momentum component of the free particle Green function.

Now the t-matrix has also the same δ-shell-form

$$T(\bar{r},\bar{r}') = \sum_L Y_L(\hat{r}) \frac{\delta(r-R)}{R^2} t_l(E) \frac{\delta(r'-R)}{R^2} Y_L(\hat{r}') \qquad \ldots (3.37)$$

where $t_l = \frac{W_L}{1-G_L^o W_L}$ $\qquad \ldots (3.38)$

The Fourier transform of $T(\bar{r},\bar{r}')$ is written as

$$T(\bar{k}) = 4\pi^2 N \sum_{LL'} Y_L(\hat{k})\, Y_{L'}(\hat{k}) \left\{ t_l(\kappa,k)\delta_{LL'} + \left[t(k,\kappa) \left\{ G'(1-G't(\kappa,\kappa))^{-1} \right\} t(\kappa,k) \right]_{LL'} \right\} \qquad \ldots (3.39)$$

where, $t(k,\kappa) = t_l j_l(kR)\, j_l(\kappa R)$ $\qquad \ldots (3.40)$

and $G'_{LL'} = A_{LL'} + i\kappa\delta_{LL'}$ $\qquad \ldots (3.41)$

We can find out the spectral function $\rho(E,\bar{k})$ as(57)

$$\rho(E,\bar{k}) = -\frac{1}{\pi\Omega(E-k^2)^2} \operatorname{Im} T(\bar{k}) \qquad \ldots (3.42)$$

2. DETAILS OF CALCULATIONS

The method described above has been used to calculate the spectral functions of copper based alloys like CuZn, CuGe and CuAl. Our choice of the numerical work on these systems is mainly because of the fact that the one electron spectrum of copper is well-understood and there are variety of experiments carried out on such systems. Because of the very involved nature of calculations as well as approximations the results of the calculation can at best be regarded at best approximate. Again the reliable calculations of the potentials is a difficult problem. In case of alloys, it is well known that the non-uniform site environments and the different atomic properties of the species compound the uncertainties of the alloy potentials, still we assume that the basic form of the potential does not get seriously changed. However, if one undertakes a self-consistent calculation these aspects should be considered in greater detail. We shall use the formulae (3.42) and (3.35) to compute spectral functions. While using the formula (3.42) we have calculated the medium potential amplitude (3.2) by numerically solving the differential equation for the radial part of the wave functions and finally calculated the logarithmic derivative at the muffin-tin sphere. From the knowledge of the medium potential amplitude, the t-matrix was calculated and then the spectral density of states. While using (3.35) we use the parametrized phase shift scheme to calculate cotangents of the phase shifts and then the procedure

described in the flow chart (Fig.5) was followed. In both the cases the calculation of the structure constants was carried out using the method as outlined below.

(i) CALCULATION OF STRUCTURE CONSTANTS

The derivation of the KKR method has been discussed by many authors, particularly by Ham and Segall in their review article(69). In the muffintin approximation the wave function within the muffintin sphere is written as

$$\psi_{\bar{k}}(\bar{r}) = \sum_{l=o}^{l_{max}} \sum_{m=-l}^{+l} i^{l} C_{lm}^{\bar{k}} R_l(E,\bar{r}) y_{lm}(\theta,\phi)$$

where $C_{lm}^{\bar{k}}$ are the expansion coefficients, $R_l(E,\bar{r})$ is the radial function of the equation containing the potential and $y_{lm}(\theta,\phi)$ are the real spherical harmonics. The $E(\bar{k})$ are obtained from the zeroes of the determinant

$$\| A_{lml'm'}(E,\bar{k}) + \sqrt{E}\, \delta_{ll'}\delta_{mm'} \cot\eta_l(E) \|$$

The structure dependent part is $A_{lml'm'}$, which is independent of the potential. These quantities are conveniently expressed as

$$A_{lml'm'}(E,\bar{k}) = 4\pi \sum_{LM} C_{lml'm'}^{LM} D_{LM}(E,\bar{k}),$$

where $C_{lml'm'}^{LM} = \int d\Omega\; y_{LM}(\theta,\phi)\; y_{lm}(\theta,\phi)\; y_{l'm'}(\theta,\phi)$

are known as gaunt numbers. For a given $(E,\bar{k})$ pair due to the properties of $C_{lml'm'}^{LM}$, $(2l_{max}+1)^2$ distinct structure

constants $-D_{LM}$ are evaluated since the largest L value is $2l_{max}$. $D_{LM}(\bar{k},E)$ are readily evaluated by using the expression of Ham and Segall and the efficient numerical technique of Davis (90).

(ii) CALCULATION OF POTENTIALS AND LOGARITHMIC DERIVATIVES:

The type of crystal potential which has been found to be reasonably successful in calculating the band structure of noble and transition metals is obtained from a superposition of atomic potentials on neighbouring sites. The crystal potential is represented as the sum of a Coulomb and an exchange part, both being obtained from atomic wave functions. At any lattice point, the Coulomb part is taken to be the Coulomb potential located at that site plus contributions from neighbouring sites. This is evaluated by employing Löwdin's α-function expansion technique and retaining only the spherically symmetric term as implied in the muffintin approximation. The crystal charge densities are obtained by a spherically symmetric superposition of the atomic charge densities in an analogous manner. The exchange potential is calculated from Slator's formula. The average potentials of the species of the alloy, V_A and V_B, were calculated with the method described by Pant and Joshi(46) by following the procedure similar to the Mattheiss prescription(91). With these potentials the radial equations were solved numerically by employing Numerov method. Then the logarithmic derivatives were calculated at each energy and angular

momentum on the radius of the muffin-tin sphere.

This program was used for CuZn and CuGe alloy to calculate the spectral functions employing eqn.(3.42).

(iii) CALCULATION OF PHASE SHIFTS FROM A PARAMETERIZED SCHEME

(A) Phase shifts for metals

The KKR band structure method works very well even if we restrict ourselves to using $l_{max}=2$. So essentially one needs to calculate 3 phase shifts η_0, η_1 and η_2 as functions of energy in order to solve the secular determinant. For realistic band calculations for alloys, it is quite cumbersome to construct potentials for each concentration of the solute atoms in alloys. Therefore, a parametrised scheme is useful which can fit first principal calculation of band structure of pure metals. Such a scheme is developed within the framework of KKR scheme by Cooper et al.(92).

The essential step in this procedure is to obtain the functional form of η for their energy dependence. This has been carried out by taking the leading terms in the series expansion of the Bessel and Neumann functions. Then for noble and transition metals the d-band resonance is taken in η_2. In an emperical manner the three phase shifts are specified with 10 adjustable parameters for noble and transition metals and 6 adjustable parameters for free electron like metals. These are to be adjusted in order to get best fit to the first principle band structure

calculations.

We have employed this scheme for Cu and Al in order to get the pure band structure of the metals using our KKR program. The phase shifts of copper are fitted with the Chodorow potential and that of aluminum to Heine-Segall Potential. Tan η_l's are shown in Fig.6(A,B) and the computed band structure of Cu and Al in Fig.(7A,B).

(B) Phase Shifts for Alloys

In the elementary theory of scattering the t-matrix is written as

$$t_l(E) = -\frac{1}{\sqrt{E}} e^{i\eta_l(E)} \sin\eta_l(E) = -\frac{1}{\sqrt{E}}(\cot\eta_l(E)-i)^{-1}$$

The alloy phase shifts corresponding to the ATA result is written as

$$\langle t \rangle_l = x\, t_l^A + (1-x)\, t_l^B$$
$$= -\frac{x}{\sqrt{E}}(\cot\eta_l^A(E)-i)^{-1} - \frac{(1-x)}{\sqrt{E}}(\cot\eta_l^B(E)-i)^{-1}$$

Now we can write $\langle t \rangle_l = -\frac{1}{\sqrt{E}}(\cot\bar{\eta}_l(E)-i)^{-1}$ so that

$$\cot\bar{\eta}_l(E) = i + \left[\frac{x}{\cot\eta_l^A(E)-i} + \frac{1-x}{\cot\eta_l^B(E)-i}\right]^{-1}$$

In terms of $\cot\eta_l^A$ and $\cot\eta_l^B$, we calculated the ATA phase shifts of the alloy of CuAl.

Here we note that the phase shifts for the alloy are complex for real value of energy. One could do a

complex band structure calculation with these complex phase shifts while making $\bar{k}$-real. These complex cot η_l's make the sharp dispersion of $E_{\bar{k}}$ to be blurred giving rise to anwidth. With these phase shifts we calculated $\rho(E,\bar{k})$ from eqn.(3.35).

In addition to the parameters to obtain the phase shifts an additional parameter V_o - a constant potential, is necessary to find out the muffin-tin zero of the potential. In our calculation, we choose it to be $\bar{V}_o = xV_o^A + (1-x)V_o^B$.

3. RESULTS

We have discussed earlier that the Bloch states of an electron get diffused because of the aperiodicity of the potential. So the crystal momentum-$\bar{k}$ is no more a good quantum number. That is why we have preferred to calculate the spectral function

$$\rho(E,\bar{k}) = \sum_n \delta(E-E_n) |\psi_{n\bar{k}}|^2 ,$$

where $\psi_{n\bar{k}}$ is the $\bar{k}$th Fourier component of the eigen function ψ_n with E_n as its eigen value. We have calculated the spectral functions for both 'Energy and Wave-vector searches' as is conventionally done in the KKR scheme. The peaks of the $\rho(E,\bar{k})$ are taken to be the energy(wavevectors) corresponding to the chosen wavevector (energy) of the band. The width of the $\rho(E,\bar{k})$ is supposed to be the spread of the one electron state, from which the decay time can be found out. In Fig.7a we have shown the band structure of pure copper along the principal symmetry directions $[\Gamma\Delta X]$,

$[\Gamma\Lambda L]$ and $[\Gamma\ \Sigma\ K]$ by using the phase shift parametrization scheme for the Chodorow potential of Cu. We shall see how the substitution of the second component in the α-phase change the bands.

(A) Brass alloys(CuZn(93), CuGe(94))

As mentioned earlier, there are several calculations on CuZn in its α-phase. In Fig.8 we show how the bands of copper shift when zinc is added within the virtual crystal approximation. The observations are (1) the alloy bands are found to be displaced to the lower energy, (2) the Fermi energy of the alloy has shifted to higher energy as compared to that of pure copper. The complex band structure has been calculated along the $[\Gamma\Delta X]$ direction and is shown in Fig.9. We have shown how the disorder brings the spread in the dispersion curves in Δ_2, $\Delta_{2'}$, and Δ_5-bands marked by hatched line. The solid line is drawn through the peak energies of $\rho(E,\bar{k})$ at the values of 0.0, 0.25, 0.50, 0.75 and 1.0 of the k/k_{max} in the direction of the Bz. The bands are found to be more diffused in the central part of the zone than at the centre and the zone face. The spread of the band was taken to be equal to the width of the spectral function $\rho(E,\bar{k})$. This spread is found to increase with increase in concentration of the solute atoms. For Δ_5 band the widths of the spectral functions are approximately in the ratio 4.5:6:7 for 10, 20 and 30 at %. of zinc respectively. In Fig.10 we have shown $\rho(E,\bar{k})$ for fixed value of energy against $\bar{k}$ for the Δ_1 representation

of the band for 3 concentrations of zinc. The half-width of the d-states (Δ_2, Δ_5) is about 4.5%. of the Bz dimensions while for the s-states it is about 1%. of it. From our calculations we find that Δ_1, and Λ_1 bands suffer a downward shift and this agrees with the results of Amar et al. (46). Because the calculations are very tedious, we calculated the spectral functions for a few selected symmetry points on the Bz for α-CuZn and α-CuGe.

CuZn

Biondi and Rayne(95) have measured the optical abserptivity of α-brass as a function of frequency and have obtained the absorption edge at 2.2 eV for pure copper. This edge shifts to higher energy on alloying with zinc. It has been observed that an absorption peak at 4.2 eV moves to lower energies on addition of zinc atoms. Another weak absorption maximum is found near 3.45 eV for pure copper which also moves up on alloying. These measurements have been discussed and interpreted by several authors taking energy values from the pure copper band structure. The optical absorption results are shown in Figs.11. Lettington(96) attempted to interprete these measurements on the basis of the band structure calculation for Cu due to Segall (97), Cooper et al.(98), Ehrenreich and Phillips(6), Beaglehole(99) have studied the frequency dependent $\varepsilon_2(w)$ for copper and suggested some assignments for the optical transitions. So far as the peak positions are concerned, the measurements are consistent, but the

Table 1

Approximate position of the peak → / Systems ↓	2.2 eV	3.45 eV	4.3 eV
Cu	(1) $L_{32} \rightarrow L_2$, d $\rightarrow E_F$ (b), (d) (2) Virtual excitation resonance (c)	$X_5 \rightarrow X_4$, d $\rightarrow$ p (d)	(1) $X_5 \rightarrow X_4$, d $\rightarrow$ p (b) (2) L_2, $\rightarrow L_1$ (c), (d)
CuZn	$L_{32} \rightarrow L_2$, d $\rightarrow E_F$ (a), (b)	(1) L_2, $\rightarrow L_1$ (a) (2) $X_5 \rightarrow X_4$, (d)	(1) $X_5 \rightarrow X_4$, d $\rightarrow$ p (2) L_2, $\rightarrow L_1$ (c), (d)

Table 2

Systems Transitions	Cu		CuZn(10 %)		CuZn(20 %)		CuZn(30 %)	
	Theory	Expt.	Theory	Expt.	Theory	Expt.	Theory	Expt.
$L_{32} \rightarrow L_{2'}$	1.807[a] 1.196[b] 1.481[c] 1.252[d]	2.20	1.504 1.753[d]	2.30	1.658 2.269[d]	2.42	1.712	2.58
$L_{2'} \rightarrow L_1$	5.925[a] 4.865[b] 4.661[c] 4.756[d]	4.30	3.669 4.362[d]	3.82	3.302 3.995[d]	3.335	2.935	2.90
$X_5 \rightarrow X_{4'}$	4.579[a] 3.832[b] 3.968[c] 3.860[d]	3.45	4.050 4.208[d]	4.02	4.104 6.170[d]	4.60	5.517	5.08

assignments to transitions differ. In table 1 we present the assignments due to various authors for the optical absorption peaks of pure copper and α-brass. For the edge at 2.3 eV in copper the assignment $L_{32}-L_{2'}$, by Lettington and Cooper et al. fits well with our calculations. The absorption peak at 4.3 eV also agrees with the assignment (L_2-L_1) transition by Mueller and Phillips and Gerhardt et al., but Lettington and Cooper et al. have assigned this peak to $(X_5-X_{4'})$ transition. Our calculations show that the secondary absorption peak may be due to (X_5-X_4') as proposed by Gerhardt et al. Lettington has identified this with $(L_{2'}-L_1)$ transition. A recent optical reflectivity study due to Hummel et al.(100) reveals the peak at 2.27 for 9%. Zn in Cu which may be due to $L_{32}-L_{2'}(E_F)$ transition. Besides these authors have made the reflectivity measurements over a very wide range of concentration of Zinc. Although their observation of $(L_{2'}-L_1)$ transition and the provision of edge agrees well with other measurements, the transition (X_5-X_4') is observed for pure copper at about 4.2 eV and falls to 2.84 eV for 24.8 at %. of zinc in Cu. In table2 we have displayed the concentration dependence of various transitions according to our calculations. The experimental optical absorption data of Biondi and Rayne has also been shown.

CuGe

Rayne(101) has measured the optical absorptivity of CuGe alloys with varying concentrations of Ge upto 7 at %.

at 4.2°K. Later Pells and Montgomery measured the absorption as a function of photon energy from 1.7 to 5.9 eV for CuGe at two compositions. In both these measurements the main absorption edge at about 2.2 eV of pure copper moves upto higher energy on alloying with Ge. Rayne has observed that the main peak for pure copper at about 4.20eV shifts slightly to the higher energy in the alloy. Pells and Montgomery(102) find that the single peak near 5 eV in Cu is split into two peaks in the alloy. The low energy peak is not as pronounced as the high energy one. The high energy peak remains close to 5.4 eV and the low energy one moves to the lower energy as the Ge concentration increases. Optical and photoemission measurements have been made by Nilsson(103) on $Cu_{0.94}Ge_{0.06}$. His observations show the same broad features as found in the measurements of Pells and Montgomery. As seen earlier, L_2' lies about 0.5 eV below E_F which is depressed on alloying by an amount which depends on the total number of conduction electrons and the density of states. The Fermi energy should show a slow rise. Thus, in alloy $(L_2'-E_F)$ separation will be larger than in pure copper. From our calculation $(L_{32}-L_2')$ separation is about 2.067 eV in $Cu_{0.9}Ge_{0.1}$. This suggests that in the case of pure copper the absorption edge could be ascribed to transitions from the top of the d-band to E_F. Then two levels move apart as we alloy and this agrees with the observed movement to the higher energy. We adopt the interpretation of pure Cu from Pells and Shiga(104)

TABLE -3

Transitions	Cu		CuGe	
	Theory	Expt.	Theory	Expt.
L_{32}-$L_{2'}$	1.48[a] 1.20[d]	2.20[bc]	2.07	2.23[b]
$L_{2'}$-L_{12}	4.67[a] 4.87[d]	4.78[c]	4.37	4.0[e]
L_{11}-$L_{2'}$	4.98[a] 4.25[d]	5.32[c]	5.41	5.4[e]
X_5-$X_{4'}$	3.99[a] 3.84[d]	3.97[c]	4.09	--

for the absorption peaks. The lower energy peak is assumed to arise from the transitions in the neighbourhood of $(L_{2'}-L_{12})$ and the higher one to $(L_{11}-E_F)$. If we regard E_F to lie close to $L_{2'}$ the table 3 shows that the calculated values show surprisingly good agreement with experiment.

CuAl

This is a prototype of a noble metal alloyed with a free electron type metal. The band structures of both Cu and Al are well studied and this system is well-suited for optical studies because the conduction bands are supposed to shift substantially with increasing electron concentration by adding Al into copper. In the alloys studied earlier like CuZn and CuGe, the solute atoms Zn and Ge have their own d-bands well below the bottom of the conduction bands. It is not easy to find out how do they influence the band-structure of such alloys. While in the CuAl, such problem is not there.

Using the phase shift parametrization method we have calculated the energy bands in three principal directions for Cu and Al (shown in Figs.7(a) and 7(b)). The spectral functions are calculated for $Cu_{0.9}$ $Al_{0.1}$ at selected points of the Brillouin zone using the energy search method. The peak points of $\rho(E,\vec{k})$ are shown in Table 4, against the pure copper values. The muffin-tin zero of the pure copper is -11.797 eV for the Chodorow potential while for the alloy it is -11.078 eV (a virtual crystal muffin-tin-zero).

TABLE 4

	Cu	$Cu_{0.9}Al_{0.1}$
Γ_1	0.00	0.00
$\Gamma_{25'}$	5.42	5.31
Γ_{12}	6.24	6.14
X_1^{ℓ}	3.56	3.82
X_3	4.05	4.40
X_2	6.82	6.67
X_5	7.03	6.99
$X_{4'}$	11.13	10.98
X_1^u	16.47	-
L_1^{ℓ}	3.59	3.51
L_3^{ℓ}	5.37	5.30
L_3^u	6.85	6.75
$L_{2'}$	8.44	8.48
L_1^u	13.07	12.87

There are measurements on the optical reflectivity for this alloy by Rea and DeReggi(105) and Hummel et al.(100). The inter-band contributions to ε_2 for Cu and CuAl alloys due to Rea and DeReggi are shown in Fig.12a.The vertical lines (A,B,C and D) show the movements of the thresholds of transitions which one can compare with the critical energy transitions of Hummel et al. The edge at 2.2 eV is due to transition from the top of the d-band to the Fermi level. This increases on alloying and for 10 at %. of Al we find the change in $|L_{32}-L_{2'}|$ gap is 0.137 eV. Hummel et al. have observed this change to be 0.14 eV. The line CB starts nearly from 4.4 eV and decreases on increasing Al. This transition is due to $(L_{2'}(E_F)-L_1)$. Our calculated shift is 0.246 eV against the observation 0.82 eV. The remaining transition which is seen at 5.2 eV, its energy decreases as the concentration of Al increases upto 7.5 at %. of Al and then it increases. The differential spectrogram of Hummel et al. shows two structures around 3.1 eV and 5.2 eV which were also reported by Fong et al.(106) for pure copper using wave length modulation technique. Although 3.1 eV structure disappears on increasing concentration of Al, the one at 5.2 eV shifts to lower energy. This transition may be due to $|X_1-E_F|.|X_5-X_{4'}|$ transition is observed by Hummel et al. which decreases by 1.2 eV as Al concentration increases to 10 at %. . We find this shift is 0.11 eV. For these interpretations of optical transitions, we could not calculate the Fermi level of the alloy.

But as in pure copper E_F lies about 0.5 eV above L_2, point, the filling of the d-band by additional electrons due to Al is assumed to have the same amount of upward shift of the Fermi level.

The possible assignment to the direct optical transitions are no doubt speculative, unless we do the detailed calculation of the dielectric functions.

CHAPTER-IV

ELECTRON STRUCTURE OF BINARY ALLOYS IN A TIGHT-BINDING MODEL

We have discussed in the last chapter the coherent potential approximation in the framework of multiple scattering theory, its single site version and other possible extensions with some typical results in relation to realistic experimental measurements. What is significantly important in the theory of disordered binary alloy is the effect of fluctuation in the alloy potential. It has been pointed out earlier that the fluctuations are neglected in the self-consistent single site theories. Recently Edwards and Loveluck(107) have proposed an approach within a tight binding framework, which appears promising for taking into account the effect of fluctuations of the alloy potential. In this theory the electronic structure is described as usual in terms of the configurationally averaged Green function. A partial summation for the averaged perturbation series was performed diagrammatically to get information about the electronic states. Some of the unsatisfactory features of such a partial summation was eliminated through a partially renormalised perturbation expansion. In their analysis Edwards and Loveluck (EL) replaced the hopping matrix element by its average value before the configurational averaging of the series is carried out for each term of the perturbation expansion in order to simplify the formulation. Such an approximation is not satisfactory

for an alloy whose constituents have significantly different potentials. In the present chapter we shall consider explicitly and exactly the configuration dependence of the hopping term (108). Necessarily this modification in the present formulation will lead to a more complicated analysis than the one made by EL.

1. MODEL HAMILTONIAN AND THE GREEN FUNCTION

We consider a simple model Hamiltonian for substitutional disordered binary alloy. This is the same model Hamiltonian as used by Edwards and Loveluck. The ions are randomly distributed, therefore, a particular type of ion has equal probability for the occupation of any lattice site which is equal to the concentration of that type of ion. We further assume that each ion has only one electron with eigenvalue E_o^i for the ion of type i (i=1,2). In the tight-binding approximation the Hamiltonian for the system will be written as

$$H = \sum_{\alpha}^{i} c_\alpha^i \, E_o^i \, a_\alpha^+ \, a_\alpha + \sum_{\alpha\beta}^{ij} c_\alpha^i \, a_\alpha^+ \, T_{\alpha\beta}^{ij} \, a_\beta \, c_\beta^j \, , \qquad \ldots (4.1)$$

where a_α^+ and a_α are the creation and annihilation operators respectively for an electron at the αth site, $T_{\alpha\beta}^{ij}$ is the hopping (transfer) matrix element between the αth site (with the ion of type i) and βth site (with ion of type j). The transfer matrix $T_{\alpha\beta}^{ij}$ is related to the crystal potential $V(\vec{r})$ by

$$T^{ij}_{\alpha\beta} = \int d\bar{r}\ \phi^{i*}_{\alpha}(\bar{r})\left[V(\bar{r}) - U^{j}_{\beta}(\bar{r})\right]\phi^{j}_{\beta}(\bar{r}), \qquad \ldots (4.2)$$

$$\text{with } V(\bar{r}) = \sum_{\alpha}^{i} c^{i}_{\alpha}\, U^{i}_{\alpha}(\bar{r}), \qquad \ldots (4.3)$$

where we have designated the potential at position $\bar{r}$ associated with an ion of type i (i=1,2) centred at the lattice point $\bar{R}_\alpha$ by $U^i_\alpha(\bar{r})$. $\phi^i_\alpha(\bar{r})$ is the atomic wave function which corresponds to the ion at the site $\bar{R}_\alpha$. The coefficient c^i_α takes only one of the two values 1 or 0. If the lattice site $\bar{R}_\alpha$ is occupied by an ion of type i then c^i_α is equal to unity, otherwise zero. Since at a time only one type of ion can occupy a particular lattice site, c^i_α and c^j_α satisfy the following condition,

$$c^{i}_{\alpha}\, c^{j}_{\alpha} = c^{i}_{\alpha}\, \delta_{ij} \qquad \ldots (4.4)$$

Let us now define the retarded single particle Green function and its Fourier transform by

$$g^{ij}_{\alpha\beta}(t-t') = -i\theta(t-t')\left\langle\left[c^{i}_{\alpha}\, a_{\alpha}(t),\ c^{j}_{\beta}\, a^{+}_{\beta}(t')\right]\right\rangle_{e} \qquad \ldots (4.5)$$

and

$$g^{ij}_{\alpha\beta}(E) = \frac{1}{2\pi}\int g^{ij}_{\alpha\beta}(t)\, \exp(iEt)\,dt \qquad \ldots (4.6)$$

respectively. Here $a_\alpha(t)$ is the operator in the Heisenberg representation for a_α and $\theta(t-t')$ is the Heaviside step-function defined by

$$\theta(t-t') = 1 \qquad \text{for } t > t'$$
$$= 0 \qquad \text{for } t < t'$$

$[\ \ ]$ represents an anticommulator and the angular brackets

$\langle\ \rangle_e$ indicate the average over the grand canonical ensemble,

$$\langle O\rangle_e = \mathrm{Tr}\ O\ e^{-\beta H}/\mathrm{Tr}\ e^{-\beta H}$$

The equation of motion for the Green function (4.5) can be now easily obtained by differentiating with respect to time. Using the property (4.4) of the coefficients the equation of motion is

$$(E-E_o^i)\ g_{\alpha\beta}^{ij}(E) = c_\alpha^i\ \delta_{\alpha\beta}^{ij} + c_\alpha^i \sum_\delta T_{\alpha\delta}^{il}\ g_{\delta\beta}^{lj}(E) \qquad \ldots (4.7)$$

we now introduce the atomic Green function

$$Y_{\alpha\beta}^{oij} = \frac{\delta_{\alpha\beta}^{ij}}{E-E_o^i} \qquad \ldots (4.8)$$

where $\delta_{\alpha\beta}^{ij}$ stands for the product of $\delta_{\alpha\beta}$ and δ_{ij}. The equation (4.7) with the help of the atomic Green function (4.8) can now be written in a more convenient and compact form

$$g_{\alpha\beta}^{ij}(E) = c_\alpha^i\ Y_{\alpha\beta}^{oij}(E) + \sum_{\lambda\delta}^{kl} c_\alpha^i\ Y_{\alpha\lambda}^{oik}(E)\ T_{\lambda\delta}^{kl}\ g_{\delta\beta}^{ij}(E) \qquad \ldots (4.9)$$

2. Perturbation Expansion and Diagram Technique

Our problem is to solve the Eq.(4.9) for the Green function $g_{\alpha\beta}^{ij}(E)$. Due to random distribution of ions it is not an easy task to get a solution. For a disordered lattice the crystal momentum $\bar{k}$ is not a good quantum number and we shall solve the equation for Green function in the direct lattice representation. We shall expand

equation (4.9) by successive iterations and then configurationally average it term by term. Thus

$$\langle g^{ij}_{\alpha\beta}(E)\rangle = \langle c^{i}_{\alpha}\, Y^{oij}_{\alpha\beta}\rangle + \langle \sum_{\nu\delta}^{kl} c^{i}_{\alpha}\, Y^{oik}_{\alpha\nu}\, T^{kl}_{\nu\delta}\, Y^{olj}_{\delta\beta}\rangle + \langle \sum_{\nu\delta\varepsilon\lambda}^{klmn} c^{i}_{\alpha}\, Y^{oik}_{\alpha\nu}\, T^{kl}_{\nu\delta}\, c^{l}_{\delta}\, Y^{olm}_{\delta\varepsilon} T^{mn}_{\varepsilon\lambda}\, c^{n}_{\lambda}\, Y^{onj}_{\lambda\beta}\rangle + \ldots \quad \ldots (4.10)$$

This is identical to the Eq.(3.16) of Edwards and Loveluck obtained by them by following a different procedure. Here $\langle\ \rangle$ denotes the configurational averaging. In Eq.(4.10) Edwards and Loveluck replaced $T^{ij}_{\alpha\beta}$ appearing in the expressions like $\langle c^{i}_{\alpha}\, T^{ij}_{\alpha\beta}\, c^{j}_{\beta}\rangle$ and the other higher order terms by the average value $\langle T^{ij}_{\alpha\beta}\rangle$, $\langle T^{ij}_{\alpha\beta}\rangle$ depends on $\bar{R}_{\alpha}$ and $\bar{R}_{\beta}$ through $|\bar{R}_{\alpha} - \bar{R}_{\beta}|$ and is designated by $k^{ij}_{\alpha-\beta}$.

In the present study we have tried to investigate the problem without resorting to such an approximation for $T^{ij}_{\alpha\beta}$. It is clear from the expression (4.2) that $T^{ij}_{\alpha\beta}$ depends on the coefficients c^{s}_{μ} through the expression of the crystal potential $V(\bar{r})$. We shall average the various terms in (4.10) without resorting to any approximation for the transfer matrix element $T^{ij}_{\alpha\beta}$. Except this difference we shall be closely following the work of Edwards and Loveluck. In order to accomplish this we rewrite $T^{ij}_{\alpha\beta}$ in a slightly modified form using equations (4.2) and (4.3).

$$T^{ij}_{\alpha\beta} = \sum_{\mu}^{s} (c^{s}_{\mu} - \delta^{sj}_{\mu\beta})\, V^{isj}_{\alpha\mu\beta},$$

where,

where,

$$V^{isj}_{\alpha\mu\beta} = \int d\bar{r}\ \phi^{i*}_{\alpha}(\bar{r})\ U^{s}_{\mu}(\bar{r})\ \phi^{j}_{\beta}(\bar{r}). \qquad .. (4.12)$$

We now substitute (4.11) into (4.12) and obtain

$$\langle g^{ij}_{\alpha\beta}\rangle = c^{i}_{\alpha}\ Y^{oij}_{\alpha\beta} + \sum_{\nu\mu\delta}^{ksl} Y^{oik}_{\alpha\nu}\ V^{ksl}_{\nu\mu\delta}\ Y^{olj}_{\delta\beta}$$

$$(\langle c^{i}_{\alpha}\ c^{s}_{\mu}\ c^{l}_{\delta}\rangle - \delta^{sl}_{\mu\delta}\langle c^{i}_{\alpha}\ c^{l}_{\delta}\rangle + \sum_{\nu\mu\delta\varepsilon\eta\lambda}^{kslmpn} Y^{oik}_{\alpha\nu}\ V^{ksl}_{\nu\mu\delta}\ Y^{olm}_{\delta\varepsilon}$$

$$V^{mpn}_{\varepsilon\eta\lambda}\ Y^{onj}_{\lambda\beta}\langle c^{i}_{\alpha}(c^{s}_{\mu}-\delta^{sl}_{\mu\delta})\ c^{l}_{\delta}(c^{p}_{\eta}-\delta^{pn}_{\eta\lambda})\ c^{n}_{\lambda}\rangle + \ldots \qquad \ldots (4.13)$$

Now it is clear from the perturbation expansion (4.13) that the task of evaluating the averages is to evaluate the averages of the products of the coefficients c^{i}_{α} (for example: $\langle c^{i}_{\alpha}\ c^{s}_{\mu}\ c^{l}_{\delta}\rangle\langle c^{i}_{\alpha}\ c^{s}_{\mu}\ c^{l}_{\eta}\ c^{p}_{\lambda}\ c^{n}_{\beta}\rangle$ etc.). These averages can be easily evaluated if we adopt a diagrammatic approach. Of course, one can easily get the first few terms by algebra without resorting to diagrams, but the higher order terms in the perturbation series (4.13) will become more and more complicated and it is difficult to evaluate them without using the diagram technique. These diagrams can be constructed by following certain rules which are derived from algebra. The rules are discussed in detail by Edwards and Loveluck and we will not repeat them here. Wherever necessary we shall point out the modifications or extension of their rules so as to deal with the problem at hand here.

In the perturbation expansion (4.13) the first term on the right hand side contains only a single coefficient

c_α^i, and its average in the case of complete disorder is equal to n^i the concentration of the ith type of ion. The second term in (4.13) contains three c's and two c's. In order to evaluate these averages, following Edwards and Loveluck we first construct the dot diagrams which are given below

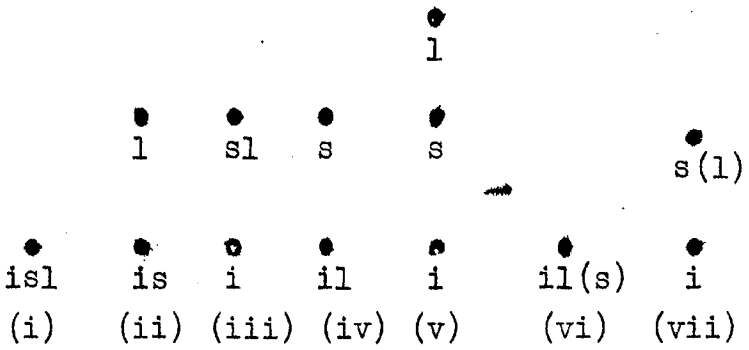

Here l(s) stands for δ^{ls} which is explicitly present in the second term of (4.13). A moments reflection shows that out of these dot diagrams (i) and (iii) are cancelled by (vi) and (vii) respectively, and only three dot diagrams survive. Once the dot diagrams are made, one has to do horizontal grouping over the various lattice indices α, μ and δ, and the diagrams can be easily constructed. The diagrams corresponding to the second term (4.13) are shown in Fig.13.

On comparison with the first order (in $\langle T \rangle$ diagrams corresponding to the perturbation expansion (3.17) of Edwards and Loveluck, one finds that the diagrams except (3,6,9) in Fig.13 are completely new. These new diagrams arise due to the fact that we took out explicitly the

coefficients c_μ^s from the expression of the transfer matrix element $T_{\alpha\beta}^{ij}$, while this was not considered by Edwards and Loveluck. These new diagrams lead to changes in the self-energy part of the Green function, which will be discussed in succeeding sections.

In addition to the rules given by Edwards and Loveluck, the following points need mention.

(a) In the present case the curly line, which has been used to represent the potential strength, incorporates three lattice sites. In the interpretation of a particular diagram a summation has to be introduced over the intermediate indices for the lattice site and atomic type.

(b) In case two lattice sites are connected by a dotted line, a δ-function has to be introduced.

Keeping these and other rules in mind the contribution of the above diagrams to the total Green function is found to be

$$\sum_{\mu}^{s} \frac{1}{E-E_o^i}\Big[\delta_{\alpha\mu}^{is}(1-\delta_{\alpha\beta})n^i n^j+\delta_{\alpha\beta}^{ij}(1-\delta_{\alpha\mu})n^i n^s$$
$$+n^i n^s n^j+2n^i n^s n^j \delta_{\alpha\mu}\delta_{\beta\mu}\delta_{\alpha\beta}-n^i n^s n^j(\delta_{\mu\beta}+\delta_{\mu\alpha}+\delta_{\alpha\beta})\Big]$$
$$\times \frac{1}{E-E_o^j} V_{\alpha\mu\beta}^{isj}$$
$$= \frac{1}{E-E_o^i} n^i S_{\alpha\beta}^{ij} \frac{1}{E-E_o^j}, \qquad \ldots (4.14)$$

where the meaning of $S_{\alpha\beta}^{ij}$ is obvious. In the approximation

of Edwards and Loveluck:

$$T^{ij}_{\alpha\beta} \rightarrow \langle T^{ij}_{\alpha\beta} \rangle = \rho^{ij}_{\alpha-\beta} = \sum_{\mu}^{S} n^s \, V^{isj}_{\alpha\mu\beta} - V^{ijj}_{\alpha\beta\beta}$$

They get for the contribution from diagrams of first order in $\langle T \rangle$ and expression identical to (4.14) except $S^{ij}_{1\alpha\beta}$ replaced by $\bar{S}^{ij}_{1\alpha\beta}$ where,

$$\bar{S}^{ij}_{\alpha\beta} = \rho^{ij}_{\alpha\beta}\delta^{ij}_{\alpha\beta} + n^j \rho^{ij}_{\alpha\beta}(1-\delta_{\alpha\beta})$$

$$= \left[\delta^{ij}_{\alpha\beta}\left\{\sum_{\mu}^{S} n^s V^{isi}_{\alpha\mu\alpha} - V^{iii}_{\alpha\alpha\alpha}\right\} + n^j \sum_{\mu}^{S} n^s \, V^{isj}_{\alpha\mu\beta}(1-\delta_{\alpha\beta}) \right.$$

$$\left. - n^j V^{ijj}_{\alpha\beta\beta}(1-\delta_{\alpha\beta})\right] \qquad \ldots (4.15)$$

Comparing (4.14) and (4.15) we obtain

$$S^{ij} = \bar{S}^{ij}_{1\alpha\beta} + n^j V^{iij}_{\alpha\alpha\beta}(1-\delta_{\alpha\beta})\delta + n^j V^{ijj}_{\alpha\beta\beta}(1-\delta_{\alpha\beta}) + v^{iii}_{\alpha\alpha\alpha}\delta^{ij}_{\alpha\beta} - \delta^{ij}_{\alpha\beta}$$

$$\sum_{\mu}^{S} n^s V^{isi}_{\alpha\mu\alpha}\delta_{\alpha\mu} + 2n^j \, \delta_{\alpha\beta} \sum^{S} n^s \, V^{isj}_{\alpha\alpha\alpha} - n^j \sum^{S} n^s (V^{isj}_{\alpha\beta\beta} + V^{isj}_{\alpha\alpha\beta})$$

$$\ldots (4.16)$$

We observe here that $S^{ij}_{\alpha\beta}$ depends on α and β only through $|\bar{R}_\alpha - \bar{R}_\beta|$ so we may define the space Fourier transform as

$$S^{ij}_{1\alpha\beta} = \frac{1}{N} \sum_{\bar{k}} e^{-i\bar{k}(\bar{R}_\alpha - \bar{R}_\beta)} \, S^{ij}_1(\bar{k}). \qquad \ldots (4.17)$$

If we consider the tight binding approximation with the nearest neighbour hopping alone, we can write

$$S^{ij}(\bar{k}) = S^{ij}_1(\bar{k}) - \Delta S^{ij}(\bar{k}) \qquad \ldots (4.18)$$

such that

$$\Delta S_1^{ij}(\bar{k}) = n^j \beta(\bar{k}) \left[\rho^{ij}_{k_1(-)} + \rho^{ij}_{k_1(+)} \right] + \rho^{ij}_{k_o(a)} \delta^{ij} \qquad \ldots (4.19)$$

where,

$$\rho^{ij}_{k_1(+)} = \int \phi^{i*}(\bar{r}+\bar{a}_n) \left[\sum^{S} n^S U^S(\bar{r}) - U^j(\bar{r}) \right] \phi^j(\bar{r}) d\bar{r} \qquad \ldots (4.20a)$$

$$\rho^{ij}_{k_1(-)} = \int \phi^{i*}(\bar{r}) \left[\sum^{S} n^S U^S(\bar{r}) - U^j(\bar{r}) \right] \phi^j(\bar{r}-\bar{a}_n) d\bar{r} \qquad \ldots (4.20b)$$

$$\rho^{ij}_{k_o(a)} = \int \phi^{i*}(\bar{r}) \left[\sum^{S} n^S U^S(\bar{r}) - U^j(\bar{r}) \right] \phi^j(\bar{r}) d\bar{r} \qquad \ldots (4.20c)$$

and $\beta(\bar{k}) = \sum_{a_n} e^{i\bar{k}.\bar{a}_n}$

with $\bar{a}_n$ denoting nearest neighbour lattice vectors.

The diagrams corresponding to the third term of the perturbation expansion (4.13) can be constructed in a similar manner and contribution of each diagram can be written down. It is to be noted that the third term contains five c's and numerous diagrams will result. However, one can always choose the most relevant class of diagrams depending on the nature of the problem. After a laborious and tedious calculation one obtains the following series for the Fourier transform of the Green function.

$$\langle g(\bar{k},E) \rangle = nY^o(E) + nY^o(E)S(\bar{k})Y^o(E) + nY^o(E)S(\bar{k}) Y^o(E)S(\bar{k})Y^o(E) + \ldots\ldots$$

$$= nY^o(E) \; / \; (1-S(\bar{k})Y^o(E)), \qquad \ldots (4.21)$$

where we have defined

$$n^{ij} = n^i \delta^{ij} \qquad \ldots (4.22a)$$

and $$Y^{oij} = \frac{\delta^{ij}}{E - E_o^i} \qquad \ldots (4.22b)$$

The self-energy matrix $S(\bar{k})$ is given by

$$S(\bar{k}) = S_1(\bar{k}) + S_2 + \ldots \ldots$$

S_1, S_2, ... being contributions from first, second ..... order diagrams respectively.

The spectral function for the system is given by

$$\langle f(\bar{k}, E) \rangle = -\frac{1}{\pi} \operatorname{Im} \sum^{ij} \langle g^{ij}(\bar{k}, E) \rangle , \qquad \ldots (4.23)$$

which can be evaluated explicitly using the expression (4.21) for the averaged Green function. The mean field approximation consists in replacing $S(\bar{k})$ by $S_1(\bar{k})$ of (4.18). From (4.18), we observe that in the self-energy $S_1(\bar{k})$ is different from that given by Edwards and Loveluck to an explicit consideration of the coefficients c_α^i in the expression of the transfer matrix element $T_{\alpha\beta}^{ij}$. Because of this modification the band structure will change.In order to see this we shall consider the case in which the potential is assumed to be given by

$$\langle V(\bar{r}) \rangle = \sum^s n^s U^s(\bar{r}) \qquad \ldots (4.24)$$

i.e. the sum of the two types of the atomic potentials and in this approximation we obtain with the help of equations (4.18) and (4.19),

$$\bar{S}^{ij}(\bar{k}) = \underset{o(a)}{\rho^{ij}_{k}} \delta^{ij} + n^{j}\beta(\bar{k})\, \underset{1(+)}{\rho^{ij}_{k}} , \qquad \ldots (4.25)$$

we now substitute (4.25) into (4.18) and obtain

$$S^{ij}(k) = -n^{j}\beta(\bar{k})\, \underset{1(-)}{\rho^{ij}_{k}} \qquad \ldots (4.26)$$

As observed by Edwards and Loveluck the self-energy depends only on the overlap integral between the neighbouring ions. In the limit $|E_o^1 - E_o^2| \gg$ bandwidth, it can be shown (107) that $E_1(\bar{k})$ and $E_2(\bar{k})$ reduce approximately in the following form,

$$\begin{aligned} E_1(\bar{k}) &\simeq E_o^1 - n^1\beta(\bar{k})\, \rho_{k\,1(-)} \\ E_2(\bar{k}) &\simeq E_o^2 - n^2\beta(\bar{k})\, \rho_{k\,1(-)} \end{aligned} \qquad \ldots (4.27)$$

where we have assumed that the overlap integrals $\underset{1(-)}{\rho^{ij}_{k}}$ are independent of i, j for the sake of simplicity. On comparison with the corresponding expression (3.42) of Edwards and Loveluck we find a constant shift in the energy bands $E_1(\bar{k})$ and $E_2(\bar{k})$. For the case $|E_o^1 - E_o^2| \ll$ bandwidth, the theory does not exclude the possibilities that the density of state functions for the bands due to $E_1(\bar{k})$ and $E_2(\bar{k})$ overlap, and a gap may not necessarily be there in the mean field approximation. In the mean field approximation the self-energy is real. If one renormalises the perturbation expansion one finds that the renormalised self-energy is complex.

3. Partial Renormalized Perturbation Expansion

In the previous section we noticed that the life-time of the electronic states due to disorder does not show up in the mean field approximation. This is due to the fact that Y^o did not have any structure in wave-vector space, and we could introduce the idea of wave-vector $\bar{k}$ and a well defined relation between E vs $\bar{k}$ for the configurationally averaged system too. In order to renormalize the perturbation expansion one has to replace Y^o in (4.10) by the averaged Green function (4.21) as in Edwards and Loveluck. One has to renormalize the perturbation expansion(4.10)in such a way that the resulting series corresponds to the Green function(4.21)and at the same time the convergence of the expansion is improved.

We follow the procedure of Edwards and Loveluck and obtain the following result for the renormalized expansion of the Green function,

$$\begin{aligned}
\langle g^{ij}_{\alpha\beta}(E)\rangle = n^i Y^{ij}_{l\alpha\beta} &+ \sum_{\nu\mu\delta}^{ksl} Y^{ik}_{l\alpha\nu}\, V^{ksl}_{\nu\mu\delta}\, Y^{lj}_{l\delta\beta}\Big[\Big\{\langle c^i_\alpha c^s_\mu c^l_\delta\rangle - \delta^{sl}_{\mu\delta}\langle c^i_\alpha c^l_\delta\rangle \\
&- \frac{n^i}{n^k}\langle c^k_\mu c^s_\mu c^l_\delta\rangle - \delta^{sl}_{\mu\delta}\langle c^k_\nu c^l_\delta\rangle\Big] \\
&+ \sum_{\nu\delta\varepsilon\eta\mu\lambda}^{kslmpn} Y^{ik}_{l\alpha\nu}\, V^{ksl}_{\nu\mu\delta} Y^{lm}_{l\delta\varepsilon}\, V^{mpn} Y^{nj}_{l\lambda\beta}\Big[\langle c^i_\alpha (c^s_\mu - \delta^{sl}_{\mu\delta}) \\
&c^i_\delta (c^p_\eta - \delta^{pn}_{\eta\lambda}) c^n_\lambda\rangle - \langle c^i_\alpha (c^s_\mu - \delta^{sl}_{\mu\delta}) c^l_\delta\rangle \frac{1}{n^m} \\
&\langle c^m_\varepsilon (c^p_\eta - \delta^{pn}_{\eta\lambda}) c^n_\lambda\rangle - \langle c^i_\alpha (c^p_\eta - \delta^{pn}_{\eta\lambda}) c^n_\lambda\rangle \frac{1}{n^k} \\
&\langle c^k_\nu (c^s_\mu - \delta^{sl}_{\mu\delta}) c^l_\delta\rangle + \frac{n^i}{n^k}\langle c^k_\nu (c^s_\mu - \delta^{sl}_{\mu\delta} c^l_\delta\rangle \frac{1}{n^m} \\
&\langle c^m_\varepsilon (c^p_\eta - \delta^{pn}_{\eta\lambda}) c^n_\lambda\rangle\Big] + \ldots \qquad \ldots (4.28)
\end{aligned}$$

There exists a close similarity between the two perturbation expansion (4.10) and (4.28). It seems that one can obtain (4.28) by just replacing $T^{ij}_{\alpha\beta}$ by $T^{ij}_{\alpha\beta}\, c^{j}_{\beta} - \frac{1}{c^{i}_{\alpha}} \langle c^{i}_{\alpha} T^{ij}_{\alpha\beta} c^{j}_{\beta} \rangle$ and $Y^{ij}_{\alpha\beta}$ by $Y^{ij}_{1\alpha\beta}$ in the earlier perturbation expansion (4.10) Here Y_1 is the averaged propagator (4.21) in the mean field approximation without the multiplication factor n.

We observe that the renormalized perturbation expansion of the Green function (4.28) contains many complicated combinations of the coefficients c^{i}_{α} and their evaluation directly from algebra is a tedious task. However, various terms can be determined through diagrammatic technique by a method described by Edwards and Loveluck and used by us in the preceding section. The diagrams for the first order terms obtained in the direct lattice space are shown in Fig. 14.

These diagrams can be classified into the categories (i) the diagram starting with a Y_1 line and ending with a Y_1 line. Such type of diagrams will be called as $\sum$ - like. $\sum$ stands for the intermediate structure between the two Y_1 lines:

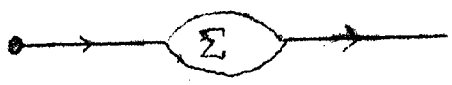

(ii) The diagram ending with a Y_1 line but not beginning with it. Such type of diagrams can be represented by

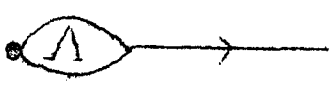

and will be called Λ-like. If we only consider the first order diagrams then Λ_1 and Σ_1 are represented in Fig.15.

On comparing the first-order renormalized diagrams of Edwards and Loveluck, we observe that in the present treatment five additional diagrams each for Λ_1-like and Σ_1 like diagrams. In the same way the second order diagrams corresponding to the third terms of (4.28) can be constructed. A large number of diagrams will appear in this case. A calculation shows that the first order diagrams even after renormalization do not contribute towards lifetime. Some of the second order diagrams are, however, found to lead to a complex self-energy. We shall categorise those diagrams in the following groups:

(1) The diagrams which can be represented by

$$Y_1 \Sigma_1 Y_1 \Sigma_1 Y_1 .$$

(2) The diagrams which are of the type

$$\Lambda_1 \Lambda_1 Y_1$$

(3) The diagrams which can be represented by

$$\Lambda_1 Y_1 \Sigma_1 Y_1$$

(4) The diagrams which are of the type $\Lambda_2 Y_1$. Those are the diagrams other than those in (2).

(5) There are some more diagrams other than of type (i) which start with a Y_1 line and end with Y_1-line. These

will be called Σ_2 like, Actually these are the diagrams which contribute towards the imaginary part of the self-energy. The second order diagrams are 35 in number.

The evaluation of $\Sigma_2(\bar{K},E)$ now needs the evaluation of the contribution of all 35 diagrams in the Appendix. These involve complicated type of integrals. We give below the algebraic equation for the self-energy considering only those diagrams which contribute to the life-time of the electronic states.

$$\sum_{2\nu\lambda}^{kn}(E) = \sum_{\mu\eta\delta\varepsilon}^{pslm} V_{\nu\mu\delta}^{ksl}\, Y_{l\delta\varepsilon}^{lm}\, V_{\varepsilon\eta\lambda}^{mpn}\Big[\, n^s n^l \delta_{\delta\lambda}^{ps}\delta_{\delta\lambda}^{ln}(1-\delta_{\mu\lambda}) + n^s n^l \delta_{\mu\lambda}^{sn}\delta_{\delta\eta}^{lp}(1-\delta_{\lambda\eta})$$

$$+2n^s n^p n^l \delta_{\lambda\mu}^{ns}\delta_{\eta\delta}\delta_{\mu\eta} + n^s n^p n^l \delta_{\lambda\mu}^{ns}(1-\delta_{\delta\mu}) - \delta_{\lambda\mu}^{ns}\delta_{\eta\delta} n^s n^l n^p$$

$$-n^s n^l n^p \delta_{\lambda\mu}^{ns}\delta_{\mu\eta} + 2n^s n^l n^n \delta_{\mu\eta}^{sp}\delta_{\eta\lambda} + 2n^s n^l n^p \delta_{\delta\lambda}^{nl}\delta_{\mu\delta}\delta_{\mu\eta}$$

$$+n^s n^l n^p \delta_{\lambda\delta}^{nl}(1-\delta_{\mu\eta}) - n^s n^n n^p \delta_{\delta\lambda}^{ln}\delta_{\lambda\eta} - n^s n^l n^p \delta_{\delta\lambda}^{ln}\delta_{\mu\lambda}$$

$$+2n^s n^l n^n \delta_{\delta\eta}^{lp}\delta_{\lambda\delta}\delta_{\delta\mu} + n^s n^p n^n \delta_{\delta\eta}^{lp}(1-\delta_{\eta\lambda}$$

$$-n^s n^p n^n \delta_{\delta\eta}^{lp}\delta_{\mu\delta} - n^s n^p n^n \delta_{\delta\eta}^{lp}\delta_{\lambda\mu} - 3n^s n^l n^p n^n \delta_{\lambda\eta}\delta_{\eta\delta}\delta_{\delta\mu}$$

$$+2n^s n^l n^p n^n \delta_{\lambda\delta}\delta_{\lambda\mu} + 2n^s n^l n^p n^n \delta_{\eta\delta}\delta_{\eta\mu} + 2n^s n^l n^p n^n \delta_{\delta\lambda}\delta_{\eta\lambda}$$

$$+2n^s n^l n^p n^n \delta_{\lambda\eta}\delta_{\eta\mu} + n^s n^l n^p n^n \delta_{\mu\lambda}\delta_{\delta\eta} + n^s n^l n^p n^n \delta_{\mu\eta}\delta_{\delta\lambda}$$

$$-n^s n^l n^p n^n \delta_{\mu\eta} - n^s n^l n^p n^n (\delta_{\eta\delta}+\delta_{\mu\lambda}+\delta_{\lambda\delta})\,\Big] \quad \ldots\ (4.29)$$

4. A LINEAR CHAIN

In order to see the difference between the present method and the approximation adopted by Edwards and Loveluck in their paper, we consider a linear chain having two different kinds of atoms which occupy the sites of the linear lattice in a random manner. The potentials of the ions of the type 1 and 2 are V^1 and V^2 respectively. Here we assume that in the nearest neighbour interaction only the integrals of the following types to survive:

$$\langle \phi_o^i | V_o^i | \phi_a^j \rangle = \langle \phi_o^j | V_a^i | \phi_a^i \rangle = \beta_i^{ij} \qquad \ldots (4.30)$$

and

$$\langle \phi_o^j | V_o^j | \phi_a^i \rangle = \langle \phi_o^i | V_a^j | \phi_a^j \rangle = \beta_j^{ij} \qquad \ldots (4.31)$$

Using these overlap integrals we calculate 35 diagrams given in the appendix. We also calculate 8 diagrams of Edwards and Loveluck carrying out of their second order correction to the self-energy having Σ_2 structure. On inspection one can find our diagrams (nos.16 and 35 of the appendix) are present as such in the set of a diagrams of Edwards and Loveluck.

We wish to show here when and where the calculation based on the present formulation will differ from that of Edwards and Loveluck. For this we shall calculate the changes in the widths $\Gamma(E,\bar{k})$ of the spectral function $\rho(E,\bar{k})$. The width is the imaginary part of the complex band structure $E(\bar{k})$ and it comes through the self-energy $\Sigma_2(E,\bar{k})$. Since we do not attempt here a

detailed band structure calculation, which is much more involved, we content ourselves with an order of magnitude estimate of the width by writing,

$$\Gamma(E,\bar{k}) \simeq \mathrm{Im}\,\overset{11}{\Sigma}(E,\bar{k}) + \mathrm{Im}\,\overset{22}{\Sigma}(E,\bar{k}), \qquad \cdots (4.32)$$

Using various parameter for the overlap integrals for ions of type 1 and 2, we illustrate in Fig.16 the difference of widths in our calculation from that of Edwards and Loveluck. We notice that for a small difference of the overlap integrals, the widths calculated by our approach and by the Edwards and Loveluck theory are nearly the same. But these widths differ significantly if the overlap integrals for the two types of ions differ a lot.

5. CONCLUSION

We have discussed the electronic structure of substitutionally disordered binary alloys closely following the work of Edwards and Loveluck and using a tight-binding description. Edwards and Loveluck have replaced the hopping matrix by the average value in order to obtain a simplified perturbation series. In view of the virtual crystal type approximation their theory does not give a correct description for an alloy having constituents whose potentials are very much different. The present approach does not suffer from such a drawback.Here the potential is constructed by superposition from all sites with the randomness duly taken care of in the formulation.

CHAPTER V

ELECTRONIC TRANSPORT IN BINARY ALLOYS

Uptil now we discussed about the equilibrium properties of disordered binary alloys. Compared to this the dynamical properties like conductivity have received much less attention. The most commonly approach to study electrical conductivity is by using the semiclassical Boltzmann equation(109) which is valid for the relaxation time being $> \hbar/E_F$. Another popular approach is based on the linear response formalism of Kubo(110).One solves there the Liouville equation for the density matrix to first order in the external field. Using this one electron Kubo formula Velický(65) studied the electrical conductivity for random binary alloys within the single band cell localised CPA. The formulation of Velický has been extended by Levin et al(111) to calculate some general transport coefficient: the thermopower, thermal conductivity and Hall coefficient. Chen et al(112) has studied the D.C. electrical resistivity and its temperature dependence introducing the thermal disorder in the single band CPA.

In the foregoing chapter we discussed an elaborate diagrammatic approach which is very useful in taking into account the fluctuations in the alloy potentials. A self-consistent version of this method is superior to

the widely used single site CPA, but it is obviously for more difficult than the CPA. However, we shall presently study(113) in this chapter the static electrical conductivity with the Kubo formula and using the tight binding formalism of Edwards and Loveluck(107).

1. EDWARDS-LOVELUCK THEORY

We shall borrow the results of EL and write for the Green function, after the renormalisation of the perturbation expansion about the mean field:

$$g(\omega,\bar{k}) = \frac{1}{I-\Lambda(\omega,\bar{k})}\,\frac{n}{Y^{-1}(\omega,\bar{k})-\Sigma(\omega,\bar{k})} \qquad \ldots (5.1)$$

with $$n = \begin{pmatrix} n^A & 0 \\ 0 & n^B \end{pmatrix} \qquad \ldots (5.2)$$

$\Sigma(\omega,\bar{k})$ is the self-energy matrix and $[I-\Lambda(\omega,\bar{k})]^{-1}$ is the weight factor. This weight factor is the outcome of the partial renormalisation. The treatment here is based on a perturbation approach; therefore the theory is valid only in the region $\Lambda^{ij} \ll 1$. Thus the poles of $[1-\Lambda(\omega,\bar{k})]^{-1}$ are of no significance. Here onwards we shall omit this factor for simplicity. This factor can be easily included in a calculation.

$Y(\omega,\bar{k})$ is defined by the equation

$$g_m(\omega,\bar{k}) = n\,Y(\omega,\bar{k}), \qquad \ldots (5.3)$$

In the mean-field approximation (denoted by the subscript m),

we have

$$g_m(\omega,\vec{k}) = \frac{1}{D}\begin{bmatrix} n^A(\omega-E_o^B-S_1^{BB}(\vec{k})) & n^A S_1^{AB}(\vec{k}) \\ n^B S_1^{BA}(\vec{k}) & n^B(\omega-E_o^A-S_1^{AA}(\vec{k})) \end{bmatrix} \quad \ldots (5.4)$$

where,

$$D = (\omega-E_o^A - S_1^{AA}(\vec{k}))(\omega-E_o^B-S_1^{BB}(\vec{k})) - S_1^{AB}(\vec{k})\, S_1^{BA}(\vec{k}) \quad .. (5.5)$$

and $$S_1^{ij}(\vec{k}) = \not{k}_o^{ij}\delta_{ij} + n^j \not{k}_1^{ij}\beta(\vec{k}) \quad .. (5.6)$$

Here,

$$\not{k}_o^{ij} = \int d\vec{r}\ \phi^{i*}(\vec{r})\left[\langle V(\vec{r})\rangle_{Av} - U^j(\vec{r})\right]\phi^j(\vec{r}) \quad \ldots (5.7)$$

$$\not{k}_1^{ij} = \int d\vec{r}\ \phi^{i*}(\vec{r}+\vec{a}_n)\left[\langle V(\vec{r})\rangle_{Av} - U^j(\vec{r})\right]\phi^j(\vec{r}) \quad \ldots (5.8)$$

and $$\beta(\vec{k}) = \sum_{\vec{a}_n} e^{i\vec{k}.\vec{a}_n} \quad \ldots (5.9)$$

with $\vec{a}_n$ as the direct lattice vector connecting the nearest neighbours.

An explicit expression for the self-energy $\sum(\omega,\vec{k})$ can be obtained from a partial summation of diagrams. In the first order approximation one can sum the diagrams which are of first order in the hopping matrix to give $\sum_1(\omega,\vec{k})$ for self-energy. A 'selective' summation over higher order diagrams could give

$$\sum(\omega,\vec{k}) = \frac{\not{k}_{\vec{k}}\, n}{I-\Lambda_1(\omega,\vec{k})}, \quad \ldots (5.10)$$

where,

$$\Lambda_1(\omega,\vec{k}) = \tilde{\Omega} - \Omega n \quad \ldots (5.11)$$

with

$$(\tilde{\Omega})^{ij} = \Omega\ \delta_{ij} \qquad \ldots (5.12)$$

and $$\Omega = \frac{1}{N} \sum_{\bar{q}}\ Y(\omega,\bar{q}) \rho_{\bar{q}} \qquad \ldots (5.13)$$

$\rho_{\bar{q}}$ being the Fourier transform of $\langle h^{ij}_{\alpha\beta} \rangle_{Av} = \rho^{ij}_{\alpha-\beta}$.

If we use the diagrammatic representation suggested by EL, $\rho_{\bar{k}}$n and $\sum_1(\omega,\bar{k})$ can be represented by the following diagrams in Fig.18. Edwards and Loveluck give a discussion of diagrams upto second order terms in the hopping matrix element $\rho_{\bar{k}}$, in the perturbation expansion of $\sum(\omega,\bar{k})$.

2. KUBO FORMULA FOR STATIC CONDUCTIVITY

In the linear response theory, the static electrical conductivity tensor σ is given by the familiar expression (110)

$$\sigma = \frac{1}{v} \int_0^\infty dt \int_0^\beta d\lambda \left\langle \bar{J}(o)\ \bar{J}(t+i\lambda) \right\rangle \qquad \ldots (5.14)$$

Here $\bar{J}(t)$ is the current operator in the unperturbed Heisenberg representation

$$\bar{J}(t) = \exp(iHt)\ \bar{J}(o)\ \exp(-iHt), \qquad \ldots (5.15)$$

i.e. H is the total Hamiltonian of the system before the field is switched on. v is the volume of the system, $\beta = 1/k_\beta T$, k_β is the Boltzmann constant and T is the absolute temperature. We write the current density operator in the form

$$\bar{J}(t) = -ie \sum_{\alpha\beta}^{ij} (\bar{R}_\alpha - \bar{R}_\beta)\, h_{\alpha\beta}^{ij}\, c_\alpha^i\, a_\alpha^+(t)\, a_\beta(t)\, c_\beta^j \qquad \ldots (5.16)$$

Now substituting (5.16) into (5.14) we obtain

$$= -\frac{e^2}{v} \int_o^\infty dt \int_o^\beta d\lambda \sum_{\alpha\beta\delta\eta}^{ijlp} (\tilde{R}_{\alpha\beta} h_{\alpha\beta}^{ij}).(\tilde{R}_{\delta\eta} h_{\delta\eta}^{lp})$$

$$x \langle c_\alpha^i a_\alpha^+(o) a_\beta(o) c_\beta^j c_\delta^l a_\delta^+(t+i\lambda) a_\eta(t+i\lambda) c_\eta^p \rangle$$

$$\ldots (3.17)$$

where,

$$\tilde{R}_{\alpha\beta} = \bar{R}_\alpha - \bar{R}_\beta \,.$$

This equation shows that the calculation of σ demands an evaluation of a two particle correlation function. The two particle correlation function can be obtained from the knowledge of the two particle Green functions. The equation of motion of two particle Green function involves still higher order Green functions. It is not possible to solve this hierarchy of equations, so one has to resort to some approximation. We adopt a simple method of decoupling the correlation functions(114).

$$\langle ABCD \rangle = \langle AB \rangle \langle CD \rangle + \langle AC \rangle \langle BD \rangle + \langle AD \rangle \langle BC \rangle \qquad \ldots (5.18)$$

When we apply the decoupling (5.18) to the correlation function in (5.17) and ignore the correlations between two creation or annihilation operators we obtain

$$\sigma = -\frac{e^2}{v} \sum_{\alpha\beta\delta\eta}^{ijlp} \int_o^\beta dt \int_o^\beta d\lambda (\tilde{R}_{\alpha\beta} h_{\alpha\beta}^{ij}).(\tilde{R}_{\delta\eta} h_{\delta\eta}^{lp})$$

$$\langle c_\alpha^i a_\alpha^+(o) a_\eta(t+i\lambda) c_\eta \rangle \langle c_\beta^j a_\beta(o) a_\delta^+(t+i\lambda) c_\delta^l \rangle$$

$$\ldots (5.19)$$

We define the spectral weight function $I(\omega)$ (34)

$$\langle c^{i}_{\alpha} a^{+}_{\alpha}(o) a_{\eta}(t+i\lambda) c^{p}_{\eta} \rangle = \int_{-\infty}^{+\infty} I^{pi}_{\eta\alpha}(\omega)\ e^{i(t+i\lambda)\omega}\, d\omega \quad \ldots (5.20)$$

Substituting (5.20) into (5.19) and integrating over t and λ we obtain

$$\sigma = -\frac{e^2}{v} \sum_{\alpha\beta\delta\eta}^{ijlp} C^{ij}_{\alpha\beta}.C^{pl}_{\delta\eta} \int_{-\infty}^{+\infty}\int_{-\infty}^{+\infty} d\omega\, d\omega'\ I^{pi}_{\eta\alpha}(\omega) I^{jl}_{\beta\delta}(\omega') \times \frac{\exp(\beta\omega)-\exp(\beta\omega')}{\omega-\omega'} \operatorname*{Lt}_{\varepsilon\to o} \frac{i}{\omega-\omega'+i\varepsilon}, \quad \ldots (5.21)$$

where,

$$\bar{C}^{ij}_{\alpha\beta} = \bar{R}_{\alpha\beta} h^{ij}_{\alpha\beta}. \quad \ldots (5.22)$$

We find that σ does not depend explicitly on ω and ω' and we can interchange them. This enables us to write

$$\sigma = -\frac{e^2}{v} \sum_{\alpha\beta\delta\eta}^{ijlp} \bar{C}^{ij}_{\alpha\beta}.\bar{C}^{lp}_{\delta\eta} \int_{-\infty}^{+\infty}\int_{-\infty}^{+\infty} d\omega\, d\omega'\ I^{pi}_{\eta\alpha}(\omega)\ I^{jl}_{\beta\delta}(\omega') \times \frac{\exp(\beta\omega)-\exp(\beta\omega')}{\omega-\omega'} \frac{1}{2} \operatorname*{Lt}_{\varepsilon\to o} \left[\frac{1}{\omega-\omega'+i\varepsilon} + \frac{1}{\omega'-\omega+i\varepsilon}\right] \quad \ldots (5.23)$$

Making use of the identity

$$\frac{1}{x+i\varepsilon} = \mathcal{P}\left(\frac{1}{x}\right) - i\pi\delta(x) \quad \ldots (5.24)$$

performing the integration over ω' and using

$$\lim_{\omega\to\omega'} \frac{\exp(\beta\omega)-\exp(\beta\omega')}{\omega-\omega'} = \lim_{\omega\to\omega'} \frac{\exp(\beta\omega')\{\exp[\beta(\omega-\omega')]-1\}}{\omega-\omega'} = \beta\exp(\beta\omega') , \quad \ldots (5.25)$$

The conductivity formula (5.23) reduces to

$$\sigma = -\frac{\beta\pi e^2}{v}\int_{-\infty}^{+\infty} d\omega \sum_{\alpha\beta\delta\eta}^{ijlp} (\tilde{C}^{ij}_{\alpha\beta}.\tilde{C}^{lp}_{\delta\eta})\, I^{pi}_{n\alpha}(\omega)\, I^{jl}_{\beta\delta}(\omega)\exp(\beta\omega). \quad \ldots (5.26)$$

The problem is therefore reduced to an evaluation of the spectral weight function $I(\omega)$. This can be obtained from the single particle Green function(34)

$$I(\omega) = \frac{i}{\exp(\beta\omega)+1}\left[g(\omega^+)-g(\omega^-)\right], \quad \ldots (5.27)$$

where $\omega^{\pm} = \omega\pm i\varepsilon$. Combining (5.27) with (5.26) we obtain

$$\sigma = \frac{\pi e^2}{v}\int_{-\infty}^{+\infty} d\omega \sum_{\alpha\beta\delta\eta}^{ijlp} \tilde{C}^{ij}_{\alpha\beta}.\tilde{C}^{lp}_{\delta\eta}\left(-\frac{df(\omega)}{d\omega}\right) \times \left[g^{pi}_{\eta\alpha}(\omega^+)g^{jl}_{\beta\delta}(\omega^+) + g^{pi}_{\eta\alpha}(\omega^-)g^{jl}_{\beta\delta}(\omega^-) - g^{pi}_{\eta\alpha}(\omega^-)g^{jl}_{\beta\delta}(\omega^+) - g^{pi}_{\eta\alpha}(\omega^+)g^{jl}_{\beta\delta}(\omega^-) \right] \quad \ldots (5.28)$$

where $f(\omega)$ is the Fermi distribution function.

For disordered alloys we have to configurationally average eq.(5.28) over all possible arrangements of ions in the lattice consistent with the given concentration of the constituents. In order to evaluate this we introduce

a quantity K,

$$K^{pl}_{\eta\delta}(\omega_1,\omega_2) = \sum_{\alpha\beta}^{ij} \langle g^{pi}_{\eta\alpha}(\omega_1)\ \tilde{C}^{ij}_{\alpha\beta}\ g^{jl}_{\beta\delta}(\omega_2)\rangle_{Av} \qquad \ldots (5.29)$$

On substituting (5.29) into (5.28) we are able to write

$$\sigma = \frac{\pi e^2}{v} \int_{-\infty}^{+\infty} d\omega \left(-\frac{df(\omega)}{d\omega}\right) D(\omega) \qquad \ldots (5.30)$$

where,

$$D(\omega) = \sum_{\eta\delta}^{pl} \left[K^{pl}_{\eta\delta}(\omega^+,\omega^+) + K^{pl}_{\eta\delta}(\omega^-,\omega^-) - K^{pl}_{\eta\delta}(\omega^-,\omega^+) - K^{pl}_{\eta\delta}(\omega^+,\omega^-)\right]$$

This is a convenient form of Kubo formula for a disordered system. We now need to evaluate K. K can be given a simple physical interpretation. K is the direct product of two propagators, describing the correlated motion of two electrons each specified by a single particle propagator.

3. EVALUATION OF $\langle gg\rangle_{Av}$ AND K.

We have found out that the expression for conductivity (5.31) requires the knowledge of K defined in (5.29). The quantity C defined in (5.22), which is sandwitched between the two propagators in the expression for K, does not depend on configurations when we use the approximation $\langle h^{ij}_{\alpha\beta}\rangle_{Av} = \rho^{ij}_{\alpha\beta}$. In this case K can be found out provided we know $\langle gg\rangle_{Av}$.

We are using the single particle description in

the same spirit as done by Velicky(65). The configurational averages reduce to averaging of a direct product of two electron Green function $\langle GG \rangle$. An extension to a linear response investigation basically involves the determination of the interference term known as vertex correction: ($\langle GG \rangle - \langle G \rangle \langle G \rangle$). Though the propagation of a single particle is statically independent, a correlation in the motion of two particles in a disordered medium not necessarily be ignored.

In the EL scheme a selfconsistent evaluation of the total self-energy Σ is an extremely complicated and involved process. This obviously means that one will have to resort to drastic approximations in solving for $\langle gg \rangle_{Av}$. In the low concentration limit Langer(114a) has discussed the equation for K in terms of the self-energy diagrams of the single particle propagators. The quantity K is found to satisfy an integral equation, which is the well-known Bethe-Salpeter equation(115). In the present problem of disordered alloy we do not **a-priori** assume that K will satisfy a Bethe-Salpeter type equation. We therefore make a detailed diagrammatic study for the propagation of the two particles and examine whether we can obtain a manageable expression for K and hence for the conductivity. With this motivation we go back to Edwards and Loveluck who partially renormalised the series expansion for $g(\omega)$ by replacing Y^{o} by Y and $\rho^{ij}_{k\alpha\beta}$ by $L^{ij}_{\alpha\beta}.L^{ij}_{\alpha\beta}$ is defined by

$$L^{ij}_{\alpha\beta} = \ell^{ij}_{k\alpha\beta}\, c^{j}_{\beta} - \frac{1}{n^{i}} \langle c^{i}_{\alpha} \ell^{ij}_{k\alpha\beta} c^{j}_{\beta} \rangle_{Av} \qquad \ldots (5.31)$$

The renormalised series expansion is now

$$g^{ij}_{\alpha\beta}(\omega) = c^{i}_{\alpha} Y^{ij}_{\alpha\beta}(\omega) + \sum_{\mu\delta}^{sl} c^{i}_{\alpha}\, Y^{is}_{\alpha\mu}(\omega)\, L^{sl}_{\mu\delta}\, Y^{lj}_{\delta\beta}(\omega) + \sum_{\mu\delta\eta\varepsilon}^{slpm} c^{i}_{\alpha}\, Y^{is}_{\alpha\mu}(\omega) L^{sl}_{\mu\delta} Y^{lp}_{\delta\eta}(\omega) L^{pm}_{\eta\varepsilon}\, Y^{mj}_{\varepsilon\beta}(\omega) + \ldots \qquad \ldots (5.32)$$

Using this equation we can write symbolically

$$\begin{aligned} \langle g(\omega) g(\omega') \rangle_{Av} = {} & \langle 11' \rangle_{Av} + \langle 12' \rangle_{Av} + \langle 13' \rangle_{Av} + \ldots . \\ & + \langle 21' \rangle_{Av} + \langle 22' \rangle_{Av} + \langle 23' \rangle_{Av} + \ldots . \\ & + \langle 31' \rangle_{Av} + \langle 32' \rangle_{Av} + \langle 33' \rangle_{Av} + \ldots . \\ & + \ldots \ldots \ldots \qquad \ldots (5.33) \end{aligned}$$

Here the numbers n (or n') denote the term in the perturbation expansion of $g(\omega)$ (or $g(\omega')$) of (5.32) used in constructing $\langle g(\omega) g(\omega') \rangle_{Av}$. Each term of the above series can now be evaluated following the rules discussed in EL. In the configurationally averaged single particle Green functions, the diagrams contributing to the life-time are of the type shown in Fig.19. Other diagrams (Λ-like) give either a shift in energy or a change in the weight factor, associated with the spectral functions. Therefore, we would draw only the diagrams of general structure like those as in Fig.19 which contribute to life-time and will not worry for the rest of them. Here

we shall use,

$$\langle c_\alpha^i c_\mu^s c_\delta^l c_n^p \ldots \rangle \simeq n^i \langle c_\mu^s c_\delta^l c_n^p \ldots \rangle_{Av} , \qquad \ldots (5.34)$$

and replace $\langle h_{\alpha\beta}^{ij} \rangle_{Av}$ by its average value $k_{\alpha\beta}^{ij}$ as mentioned earlier for drawing the diagrams. This way we have considerably reduced the labour by weeding out lot of diagrams. The first term $\langle 11' \rangle_{Av}$ of (5.33) corresponds to an uncorrelated motion of two electrons and is shown in Fig.(20a). The other terms of the first row of right hand side of (5.33) also represent uncorrelated motion. The total contribution from such term can be represented by Fig.(20b). Here the double line stands for the average single particle full propagator $\langle g \rangle_{Av}$. An examination of the various terms of (5.33) shows that the lowest order term that corresponds to the correlated motion of electrons is $\langle 33' \rangle_{Av}$ and the contribution from this are shown by diagrams in Fig.21.

In the above diagrams we observe that the two outgoing propagators are emerging from the same site, while the types of ions may be different.

The diagrams corresponding to the various terms of (5.33) can be drawn in a similar manner. From a careful study of these diagrams, we can write the equation for the two particle Green function in a compact form. We use the ladder approximation (116) and consider diagrams for the self-energy as discussed earlier. In this scheme some

of the diagrams corresponding to $\langle 66' \rangle_{Av}$ terms are shown in Fig.22 below.

With a proper selection of all the diagrams in a restricted ladder approximation in which two particles emerge out from the same point, we are able to write a Bethe-Salpeter type equation for the nondilute alloys within the Edwards-Loveluck scheme. Diagrammatically the appropriate equation is shown in Fig.23. The left hand side of Fig.23 shows the correlated two particle propagators. The first term in the right-hand side represents two independent single particle propagators and the hatched square is the vertex correction due to the correlated scattering of the two electrons. The equation corresponding to the above diagrammatic representation can be written as follows.

$$\langle g^{ij}_{\alpha\beta}(\omega_1)\; g^{i'j'}_{\alpha'\beta'}(\omega_2)\rangle_{Av} = \bar{g}^{ij}_{\alpha\beta}(\omega_1)\; \bar{g}^{i'j'}_{\alpha'\beta'}(\omega_2) + \sum_{\nu\nu'\eta}^{kk'p} \bar{g}^{ik}_{\alpha}(\omega_1)\; \bar{g}^{i'k'}_{\alpha'\nu'}(\omega_2)\; T^{kp}_{\nu\eta}(\omega_1) T^{k'p}_{\nu'\eta} \langle g^{pj}_{\eta\beta}(\omega_1) g^{pj'}_{\eta\beta'}(\omega_2)\rangle_{Av} \quad \ldots (5.35)$$

Here onwards we use a bar over the operators to show that they are also configurationally averaged,

We have written $T^{kp}_{\nu\eta}(\omega) = \frac{1}{\sqrt{np}} \sum^{kp}_{\nu\eta}(\omega)$., where $\sum^{kp}_{\nu\eta}(\omega)$ is the self-energy corresponding to the single particle Green function. With the help of eq.(5.35) we can

write a series for the two particle propagator.

$$\left\langle g^{ij}_{\alpha\beta}(\omega_1)\; g^{i'j'}_{\alpha'\beta'}(\omega_2)\right\rangle_{Av} = \bar{g}^{ij}_{\alpha\beta}(\omega_1)\; \bar{g}^{i'j'}_{\alpha'\beta'}(\omega_2) + \sum_{\nu\nu'\eta}^{kk'p} \bar{g}^{ik}_{\alpha\nu}(\omega_1)$$

$$\bar{g}^{i'k'}_{\alpha'\nu'}(\omega_2)\; T^{kp}_{\nu\eta}(\omega_1)\; T^{k'p}_{\nu'\eta}(\omega_2)$$

$$\Big\{\bar{g}^{pj}_{\eta\beta}(\omega_1)\; \bar{g}^{pj'}_{\eta\beta'}(\omega_2) + \sum_{\mu\mu'\delta}^{ss'l} \bar{g}^{ps}_{\eta\mu}(\omega_1)$$

$$\bar{g}^{ps'}_{\eta\mu'}(\omega_2)\; T^{sl}_{\mu\delta}(\omega_1)\; T^{s'l}_{\mu'\delta}(\omega_2)$$

$$\times\; \bar{g}^{lj}_{\delta\beta}(\omega_1)\; \bar{g}^{lj'}_{\delta\beta'}(\omega_2) + \ldots.\Big\} \qquad \ldots (5.36)$$

On multiplying by $C^{ji'}_{\beta\alpha'}$ (which is configuration independent) and rearranging various terms we obtain from (5.36)

$$K^{ij'}_{\alpha\beta'}(\omega_1,\omega_2)$$

$$= \left[\bar{g}(\omega_1)C\bar{g}(\omega_2)\right]^{ij'}_{\alpha\beta'} + \sum_{\nu\nu'\eta}^{kk'p} \bar{g}^{ik}_{\alpha\nu}(\omega_1)\; T^{kp}_{\nu\eta}(\omega_1)\left[\bar{g}(\omega_1)C\;\bar{g}(\omega_2)\right]^{pk'}_{\eta\nu'}$$

$$T^{k'p}_{\nu'\eta}(\omega_2)\; \bar{g}^{kj'}_{\eta\beta}(\omega_2) + \sum_{\nu\nu'\eta\mu\mu'\delta}^{kk'pss'l} \bar{g}^{ik}_{\alpha\nu}(\omega_1)\; T^{kl}_{\nu\delta}(\omega_1)\; \bar{g}^{ls}_{\delta\mu}(\omega_1)$$

$$T^{sp}_{\mu\eta}(\omega_1)\; \times \left[\bar{g}(\omega_1)\; C\bar{g}(\omega_2)\right]^{pk'}_{\eta\nu'}\; T^{k'l}_{\nu'\delta}(\omega_2)\bar{g}^{ls'}_{\delta\mu'}(\omega_2)\; T^{s'p}_{\mu'\eta}(\omega_2)$$

$$\bar{g}^{pj'}_{\eta\beta'}(\omega_2) + \ldots. \qquad \ldots (5.37)$$

We can therefore write

$$K = \bar{g}\left[C + \Gamma\right]\bar{g} \qquad \ldots (5.38)$$

such that

$$\Gamma^{kp}_{\nu\eta}(\omega_1,\omega_2) = \sum_{\nu'}^{k'} T^{kp}_{\nu\eta}(\omega_1)\left[\bar{g}(\omega_1)C\,\bar{g}(\omega_2)\right]^{pk'}_{\eta\nu'} T^{k'p}_{\nu'\eta}(\omega_2)$$
$$+ \sum_{\nu'\delta\mu\mu'}^{k'lss'} T^{kl}_{\nu\delta}(\omega_1)\,\bar{g}^{ls}_{\delta\mu}(\omega_1)\,T^{sp}_{\mu\eta}(\omega_1)\left[\bar{g}(\omega_1)C\bar{g}(\omega_2)\right]^{pk'}_{\eta\nu'}$$
$$\times\; T^{k's}_{\nu'\delta}(\omega_2)\,\bar{g}^{ls'}_{\delta\mu'}(\omega_2)\,T^{s'p}_{\mu'\eta}(\omega_2) + \ldots. \qquad \ldots (5.39)$$

The equation (5.38) can now be compared with the expression for K obtained by Velický(65) using the single site CPA. Although they resemble each other, they originate from quite different schemes. In the EL scheme it is not needed that the perturbation be cell localised as done in CPA(65) In order to evaluate the conductivity we have to solve (5.38) The solution in direct lattice representation is very tedious, therefore, we shall change over to the momentum representation.The Fourier transform of (5.38) is

$$K(\vec{k},\omega_1,\omega_2) = \bar{g}(\vec{k},\omega_1)C_{\vec{k}}\bar{g}(\vec{k},\omega_2) + \bar{g}(\vec{k},\omega_1)\,\Gamma(\omega_1,\omega_2)\,\bar{g}(\vec{k},\omega_2) \qquad \ldots (5.40)$$

where,

$$\Gamma(\omega_1,\omega_2) = \frac{1}{N}\sum_{\vec{q}} T_{\vec{q}}K(\vec{q};\omega_1,\omega_2)T_{\vec{q}} \qquad \ldots (5.41)$$

We shall use the principle of dynamical reversibility(117) which demands that

$$\varepsilon_{\vec{k}} = -\varepsilon_{\vec{k}} \qquad \ldots (5.42a)$$

and
$$C_{\vec{k}} = -C_{-\vec{k}} \qquad \ldots (5.42b)$$

Here $\bar{g}(\bar{q},\omega)$ and $T_{\bar{q}}$ are even functions of $\bar{q}$ while $C_{\bar{q}}$ is an odd function of $\bar{q}$. Hence $\Gamma(\omega_1,\omega_2)$ which involves a summation in $\bar{q}$, will vanish. Therefore,

$$K(\bar{k};\omega_1, \omega_2) = \bar{g}(\bar{k},\omega_1)\ \bar{C}_{\bar{k}}\ \bar{g}(\bar{k},\omega_2). \qquad \ldots (5.43)$$

These quantities are diagonal in $\bar{k}$. Thus we find that in the above approximation the average of the product of two Green functions becomes equal to the product of their averages,

$$\langle gg\rangle_{Av} = \bar{g}\ \bar{g} \qquad \ldots (5.44)$$

4. EVALUATION OF ELECTRICAL CONDUCTIVITY

We shall consider here a cubic lattice for which conductivity is isotropic. Using the Fourier transform of $\bar{C}^{ij}_{\alpha\beta}$ and $\bar{g}^{pi}_{\eta\alpha}$, we obtain from (5.29)

$$\sigma = \frac{\pi e^2}{3v}\int_{-\infty}^{+\infty} d\omega \sum_{\bar{k}}^{ijlp}\left(-\frac{df(\omega)}{d\omega}\right)\left(\nabla_{\bar{k}}\rho^{ij}_{\bar{k}}\right)\left(\nabla_{\bar{k}}\rho^{lp}_{\bar{k}}\right)$$

$$\times\left[\bar{g}^{\ pi}(\bar{k},\omega^+)-\bar{g}^{pi}(\bar{k},\omega^-)\right]\left[\bar{g}^{ij}(\bar{k},\omega^+)-\bar{g}^{jl}(\bar{k},\omega^-)\right] \qquad \ldots (5.45)$$

We shall now write the single particle Green function (5.1) in a convenient form (EL-eq.5.2).

$$\bar{g}(\bar{k},\omega) = \frac{A(\bar{k},\omega)}{\omega-\varepsilon_1(\bar{k},\omega)} + \frac{B(\bar{k},\omega)}{\omega-\varepsilon_2(\bar{k},\omega)} \qquad \ldots (5.46)$$

where,

$$A(\bar{k},\omega) = nM(\bar{k},\omega) \qquad \ldots (5.47)$$

and $$B(\bar{k},\omega) = nN(\bar{k},\omega) \qquad \ldots (5.48)$$

Here,

$$M(\bar{k},\omega) = \frac{1}{\varepsilon_2(\bar{k},\omega)-\varepsilon_1(\bar{k},\omega)} \begin{vmatrix} E_o^B - S_1^{BB} - \Sigma^{BB} - \varepsilon_1 & -S_1^{AB} - \Sigma^{AB} \\ -S_1^{BA} - \Sigma^{BA} & E_o^A - S_1^{AA} - \Sigma^{AA} - \varepsilon_2 \end{vmatrix} \qquad \ldots (5.49)$$

$$N(\bar{k},\omega) = \frac{1}{\varepsilon_1(\bar{k},\omega)-\varepsilon_2(\bar{k},\omega)} \begin{vmatrix} E_o^B - S_1^{BB} - \Sigma^{BB} - \varepsilon_2 & -S_1^{AB} - \Sigma^{AB} \\ -S_1^{BA} - \Sigma^{BA} & E_o^A - S_1^{AA} - \varepsilon_1 \end{vmatrix} \qquad \ldots (5.50)$$

$$\begin{matrix} \varepsilon_1(\bar{k},\omega) \\ \varepsilon_2(\bar{k},\omega) \end{matrix} = \frac{1}{2}\left[E_o^A + E_o^B + S_1^{AA}(\bar{k}) + S_1^{BB}(\bar{k}) + \Sigma^{AA}(\bar{k},\omega) + \Sigma^{BB}(\bar{k},\omega) \pm \Delta(\bar{k},\omega)\right] \qquad \ldots (5.51)$$

with

$$\Delta(\bar{k},\omega) = \Big[\left\{E_o^B - E_o^A - S_1^{BB}(\bar{k}) - S_1^{AA}(\bar{k}) + \Sigma^{BB}(\bar{k},\omega) - \Sigma^{AA}(\bar{k},\omega)\right\}^2 + 4\left\{S_1^{AB}(\bar{k}) + \Sigma^{AB}(\bar{k},\omega)\right\}\left\{S_1^{BA}(\bar{k}) + \Sigma^{BA}(\bar{k},\omega)\right\}\Big]^{1/2} \qquad \ldots (5.52)$$

We shall rewrite $\varepsilon_1(\bar{k},\omega)$ and $\varepsilon_2(\bar{k},\omega)$ in the form

$$\varepsilon_1(\bar{k},\omega) = E_1(\bar{k}) + \Sigma_1(\bar{k},\omega) \qquad \ldots (5.53)$$

and $$\varepsilon_2(\bar{k},\omega) = E_2(\bar{k}) + \Sigma_2(\bar{k},\omega) \qquad \ldots (5.54)$$

where,

$$\Sigma_1(\bar{k},\omega) = \frac{1}{2}\left[\Sigma^{AA}(\bar{k},\omega) + \Sigma^{BB}(\bar{k},\omega) + \Delta(\bar{k},\omega) - \tilde{\Delta}(\bar{k})\right] \quad \ldots (5.55)$$

and

$$\Sigma_2(\bar{k},\omega) = \frac{1}{2}\left[\Sigma^{AA}(\bar{k},\omega) + \Sigma^{BB}(\bar{k},\omega) + \Delta(\bar{k},\omega) + \tilde{\Delta}(\bar{k})\right] \quad \ldots (5.56)$$

$E_1(\bar{k})$ and $E_2(\bar{k})$ are the two roots of the equation (5.5) and $\tilde{\Delta}(k)$ is given by

$$\tilde{\Delta}(k) = \left[\left\{E_o^B - E_o^A + S_1^{BB}(\bar{k}) - S_1^{AA}(\bar{k})\right\}^2 + 4S_1^{AB}(\bar{k})S_1^{BA}(\bar{k})\right]^{1/2} \quad \ldots (5.57)$$

Let us resolve Σ, A and B into their real and imaginary parts,

$$\Sigma(\bar{k},\omega^{\pm}) = P(\bar{k},\omega^{\pm}) \mp i\Gamma(\bar{k},\omega^{\pm}) \quad \ldots (5.58)$$

$$A(\bar{k},\omega^{\pm}) = A_R(\bar{k},\omega^{\pm}) \mp iA_I(\bar{k},\omega^{\pm}) \quad \ldots (5.59)$$

$$B(\bar{k},\omega^{\pm}) = B_R(\bar{k},\omega^{\pm}) \mp iB_I(\bar{k},\omega^{\pm}) \quad \ldots (5.60)$$

In terms of these we can write

$$\left[\bar{g}(\bar{k},\omega^+) - \bar{g}(\bar{k},\omega^-)\right]$$
$$= -2i\left[\frac{\Gamma_1(\bar{k},\theta_1)A_R(\bar{k},\theta_1) + A_I(\bar{k},\theta_1)(\omega - E_1(\bar{k}) - P_1(\bar{k},\theta_1))}{\left[\omega - E_1(\bar{k}) - P_1(\bar{k},\theta_1)\right]^2 + \Gamma_1^2(\bar{k},\theta_1)}\right.$$
$$\left. + \frac{\Gamma_2(\bar{k},\theta_2)B_R(\bar{k},\theta_2) + B_I(\bar{k},\theta_2)(\omega - E_2(\bar{k}) - P_2(\bar{k},\theta_2))}{\left[\omega - E_2(\bar{k}) - P_2(\bar{k},\theta_2)\right]^2 + \Gamma_2^2(\bar{k},\theta_2)}\right] \quad \ldots (5.61)$$

where $\theta_{1,2} = \theta_{1,2}(\bar{k})$. The expression of the right hand side

of (5.61)shows that the functions are peaked at $\omega = E(\bar{k})+P(\bar{k},\theta)$. So we expect that the contributions to conductivity will arise mainly from near about this value of ω .This point has been emphasized by EL. Therefore,

$$\sigma = \frac{4\pi e^2}{3v} \int_{-\infty}^{+\infty} d\omega \sum_{\bar{k}}^{ijpl} \left(-\frac{df(\omega)}{d\omega}\right) (\nabla_{\bar{k}} \ell^i_{\bar{k}}{}^j)\,(\nabla_{\bar{k}} \ell^l_{\bar{k}}{}^p)$$

$$\times \left[\frac{\Gamma_1(\bar{k},\theta_1) A_R^{pi}(\bar{k},\theta_1)}{\left[\omega - E_1(\bar{k}) - P_1(\bar{k},\theta_1)\right]^2 + \Gamma_1^{\,2}(\bar{k},\theta_1)} \right.$$

$$\left. + \frac{\Gamma_2(\bar{k},\theta_2) B_R^{pi}(\bar{k},\theta_2)}{\left[\omega - E_2(\bar{k}) - P_2(\bar{k},\theta_2)\right]^2 + \Gamma_2^{\,2}(k,\theta_2)} \right]$$

$$\times \left[\frac{\Gamma_1(\bar{k},\theta_1) A_R^{jl}(\bar{k},\theta_1)}{\left[\omega - E_1(\bar{k}) - P_1(\bar{k},\theta_1)\right]^2 + \Gamma_1^{\,2}(\bar{k},\theta_1)} \right.$$

$$\left. + \frac{\Gamma_2(\bar{k},\theta_2) B_R^{jl}(\bar{k},\theta_2)}{\left[\omega - E_2(\bar{k}) - P_2(\bar{k},\theta_2)\right]^2 + \Gamma_2^{\,2}(\bar{k},\theta_2)} \right], \qquad \ldots (5.62)$$

where,

$$\theta_{1,2}(\bar{k}) = E_{1,2}(\bar{k}) + P_{1,2}(\bar{k}, E_{1,2}(\bar{k})). \qquad \ldots (5.63)$$

We can now write the expression for the electrical conductivity of a substitutionally disordered binary alloy in terms of the spectral density of state $\rho(\bar{k},\omega)$, defined by

$$\rho(\bar{k},\omega) = -\frac{1}{\pi}\,\mathrm{Im}\,\bar{g}(\bar{k},\omega) \qquad \ldots (5.64)$$

$$\sigma = \frac{4\pi e^2}{3v}\int_{-\infty}^{+\infty} d\omega \sum_{\bar{k}}^{ijpl}\left(-\frac{df(\omega)}{d\omega}\right)(\nabla_{\bar{k}}\rho^{ij}_{\bar{k}}),(\nabla_{\bar{k}}\rho^{pl}_{\bar{k}})$$

$$x\left[\rho_1(\bar{k},\omega)\ A_R^{pi}(\bar{k},\theta_1)+\rho_2(\bar{k},\omega)B_R^{pi}(\bar{k},\theta_2)\right]$$
$$x\left[\rho_1(\bar{k},\omega)\ A_R^{jl}(\bar{k},\theta_1)+\rho_2(\bar{k},\omega)\ B_R^{jl}(\bar{k},\theta_2)\right] \qquad \ldots (5.65)$$

We shall show below that this expression yields the known result in the weak scattering limit.

5. Weak Scattering Limit:

In the weak scattering limit the scattering matrix $\rho_{\bar{k}}$ is small. One can verify using (5.10) that $P(\bar{k},\theta)$ and $\Gamma(\bar{k},\theta)$ are proportional to $\rho_{\bar{k}}$. By using the identity

$$\underset{\varepsilon\to 0}{\mathrm{Lt}}\ \frac{\varepsilon}{x^2+\varepsilon^2} = \delta(x) \qquad \ldots (5.66)$$

the expression for the conductivity (5.65) will reduce to

$$\sigma = \frac{4\pi e^2}{3v}\int_{-\infty}^{+\infty} d\omega \sum_{\bar{k}}^{ijpl}\left(-\frac{df(\omega)}{d\omega}\right)(\nabla_{\bar{k}}\rho^{ij}_{\bar{k}}),(\nabla_{\bar{k}}\rho^{lp}_{\bar{k}})$$
$$x\ \alpha(\omega)\left[A_R^{jl}(\bar{k},\theta_1)\delta(\omega-\theta_1(\bar{k}))+B_R^{jl}(\bar{k},\theta_2)\delta(\omega-\theta_2(\bar{k}))\right] \qquad \ldots (5.67)$$

where,

$$\alpha(\omega) = \left[\rho_1(k,\omega)A_R^{pi}(k,\theta_1)+\rho_2(k,\omega)B_R^{pi}(k,\theta_2)\right] \qquad \ldots (5.68)$$

Integrating with respect to ω we get

$$\sigma = \frac{4\pi e^2}{3v} \sum_{\bar{k}}^{ijlp} (\nabla_{\bar{k}} \rho^{ij}_{\bar{k}}).(\nabla_{\bar{k}} \rho^{lp}_{\bar{k}}) \left[\left(-\frac{\partial f(\theta_1)}{\partial \theta_1}\right) \{\alpha(\theta_1) A^{jl}_R(\bar{k},\theta_1)\} + \left(-\frac{\partial f(\theta_2)}{\partial \theta_2}\right) \{\alpha(\theta_2)\ B^{jl}_R(\bar{k},\theta_2)\} \right] \quad \ldots (5.69)$$

Following EL, we have two distinct bands characterised by the spectral functions $\rho_1(\theta_1(\bar{k}))$ and $\rho_2(\theta_2(\bar{k}))$. These two bands in the reciprocal space will be separated by a gap, therefore $\rho_1(\theta_2(k))$ and $\rho_2(\theta_1(k))$ will vanish. Hence, we shall obtain

$$\sigma = \frac{4\pi e^2}{3v} \sum_{\bar{k}}^{ijlp} (\nabla_{\bar{k}} k^{ij}_{\bar{k}}).(\nabla_{k} k^{lp}_{\bar{k}}) \left[\left(-\frac{\partial f(\theta_1)}{\partial \theta_1}\right) \frac{A^{pj}_R(\theta_1) A^{jl}_R(\theta_1)}{\Gamma_1(\theta_1(\bar{k}))} + \left(-\frac{\partial f(\theta_2)}{\partial \theta_2}\right) \frac{B^{jl}_R(\theta_2) B^{pi}_R(\theta_2)}{\Gamma_2(\theta_2(\bar{k}))} \right] \quad \ldots (5.70)$$

The leading term in σ in the weak scattering limit is of the order of $\rho^2_{\bar{k}}$, which is physically obvious. The relaxation time (τ) for electrons resulting from the scattering due to disorder will be inversely proportional to the transition rate,

$$\tau \sim 1/\Gamma$$

If we retain only the lowest order term in the concentration, then we can show from (5.10) that

$$\Gamma \alpha\ n^A n^B = n^A(1-n^A) \quad \ldots (5.71)$$

Since the resistivity is proportional to Γ, we recover the Nordheim's rule, a well-known feature of the weak scattering theory[118].

6. SUMMARY

We have discussed the static electrical conductivity of a nondilute substitutionally disordered binary alloy using a simple tight binding model and Kubo's linear response theory. The two particle Green function is written in terms of single particle Green function within a restricted ladder approximation. In general one can perform a ladder sum to get the well known results of impurity conductivity as obtained by Ambegaonkar(115) in which a characteristic $(1-\cos\theta)$ factor occurs explicitly due to the vertex correction. The choice of restricted diagrams in the present treatment leads to the forward scattering approximation which is a reasonably good approximation for metallic binary alloys. From the knowledge of the self-energy correction to the single particle energies we obtained an expression for the electrical conductivity. In the weak scattering limit and in a first order approximation this theory gives the Nordheim rule.

It is necessary to point out that the formulation presented here is different from the work of Velický(65). Velický's theory has already been applied to calculate the transport coefficients in alloys (Levin et.al(111), Brouers and Vedyayev(119)). The Edwards-Loveluck approach

that we have used here is not based on the multiple scattering description adopted by Velický, but is formulated within a tight-binding framework. Also the formulation presented here is capable of taking into account the fluctuations in the alloy potential from site to site, whereas in the cell-localised disorder model used by Velický pure A and pure B are assumed to have the same band structure. We have to pay the price for the generalisation of the theory in terms of the complexity of the final expression that we obtain for the electrical conductivity. A calculation of the static electrical conductivity of a random substitutional binary alloy using the self-consistent version of Edwards and Loveluck theory will demand intensive computational effort.

CHAPTER VI

ELECTRONS IN POSITIONALLY DISORDERED SYSTEMS: LIQUID METALS

The description of the positionally disordered systems such as liquid metals and amorphous materials is extremely complicated compared to that of the cellular ones. In such systems the atomic species occupy random positions in space, hence there is no lattice structure to simplify the problem. In this chapter we shall discuss only the electronic states of liquid metals for which there exists a few numerical calculations.

In the theory of liquid metals there have been several approaches. Ziman(120a) has proposed a nearly free electron model analogous to that of Sommerfeld. This approach has been improved in several ways by using pseudo-potential perturbation theory and by invoking multiple scattering technique primarily based on the quasi-crystalline approximation(120b). Ziman's results were extended by Lloyd(121) who gave a formal expression for the average density of states in terms of the scattering phase shifts and radial distribution function for ions. From the expression of transition, T and reaction, K matrices, Bristol group(122) has calculated the density of states for some transition and noble liquid metals. Anderson and McMillan(85)

have devised an approach in which each ion is isolated within its Wigner-Seitz sphere and outside of it there is a complex (uniform) medium, which is determined by the condition that there is no forward scattering, parallel to the CPA condition. Using this method these authors have obtained the density of states for liquid Fe. Schwartz and Ehrenreich(123) have used the single site approximation and discussed the electronic theory of the liquid metals. They have calculated the complex band structure and density of states of liquid copper. Edwards(124) have developed the Green function theory to calculate the density of states from a perturbation expansion of the single particle Green function averaged over the possible atomic arrangements appropriate to the liquid state.

Ballentine(125) has used this approach to calculate the density of states of liquid Al and Zn which are free election like but predicted that density of states of liquid Be to differ significantly from the free electron parabola. He used a local pseudopotential for the electron-ion interaction derived from the Fermi energy shell matrix elements of the Heine-Abarenkov model potential. Shaw and Smith(126) have performed calculations for Li, Cd and In using nonlocal energy-dependent model potentials. In their result the Van Hove singularities are smoothed out and the density of states of Li is much different from free electron like density. Cyrot Lackmann(127) has developed a

tight binding approximation for the moments of the density of states. It is applicable to bound bands, since the moments do not exist for free bands.

A non-perturbative approach has been proposed recently by Rousseau et al.(128). In this chapter we outline the theory of independent pseudo-atoms and use that to calculate the density of states of liquid Al(129) and Be(130). Aluminum was chosen because for this system a number of calculations for the density of states have been attempted using other existing methods and there are some soft X-rays data. Be was chosen to compare our numerical calculation with the result of Rousseau et al. who used analytical method to obtain density of states by a model partition function.

1. OUTLINE OF THE THEORY OF INDEPENDENT PSEUDO-ATOMS

We shall summarise the theory of independent pseudo-atom due to Rousseau et al.(128) in order to establish the notation and provide a framework for the discussion of results. There are two essential steps in the calculation of the density of states in a liquid. First the partition function is obtained for a given configuration. Then the ensemble averaging is done to obtain the density of states.

The total potential $V(\bar{r})$ in the assembly is regarded as a sum of localised potentials $v(\bar{r})$ centred on $\bar{R}_i$, the position of ith ion:

$$V(\bar{r}) = \sum_{\bar{R}_i} v(\bar{r}-\bar{R}_i) \qquad \ldots (6.1)$$

The partition function is defined by

$$Z(\beta) = \sum_i e^{-\beta\varepsilon_i}$$

$$= \int C(\bar{r},\bar{r};\beta)d\bar{r} \qquad \ldots (6.2)$$

where ε is the ith eigenvalue of the single particle Hamiltonian $H = -\nabla^2+V(\bar{r})$, $\beta = 1/kT$ and $C(\mathbf{r},\mathbf{r}_o;\beta)$ is the canonical density matrix given by

$$C(\bar{r},\bar{r}_o;\beta) = \sum_i \psi_i^*(\bar{r})\psi_i(\bar{r}_o)\, e^{-\beta\varepsilon_i} \qquad \ldots (6.3)$$

If we have a slowly varying potential, the eigen values change by V whereas the wavefunctions remain essentially unchanged. Then for the potential given in eqn.(6.1), we can write

$$C(\bar{r},\bar{r}_o;\beta) = C_o(\bar{r},\bar{r}_o;\beta)\, \exp\left[-\beta \sum_i v(\bar{r}-\bar{R}_i)\right] \qquad \ldots (6.4)$$

where $C_o(\bar{r},\bar{r}_o;\beta)$ is the free-particle density matrix. Equation (6.4) is generalized to the form

$$C(\bar{r},\bar{r}_o;\beta) = C_o(\bar{r},\bar{r}_o;\beta)\, \exp\left[-\beta U(\bar{r},\bar{r}_o;\beta)\right] \qquad \ldots (6.5)$$

U is called the effective potential matrix and $U(\bar{r},\bar{r};\beta) \equiv U(\bar{r},\beta)$ defines the pseudo-atoms. We further write $U(\bar{r};\beta) = \sum_{R_i} u(\bar{r}-\bar{R}_i;\beta)$, so that the system is looked upon as a set of independent pseudo-atoms described by the above canonical density matrix involving effective potential U instead of actual potential $V(\bar{r})$.

A function analogous to the Mayer-function in classical statistical mechanics is introduced

$$f(\bar{r},\beta) = \exp\left[-\beta U(\bar{r},\beta)\right]-1 \qquad \ldots (6.6)$$

so that

$$C(\bar{r},\beta) = C_o(\bar{r},\beta)\Big[1 + \sum_i f(\bar{r}-\bar{R}_i);\beta) + \frac{1}{2!}\sum_i\sum_j f(\bar{r}-\bar{R}_i;\beta)\, f(\bar{r}-\bar{R}_j;\beta) + \ldots\Big] \qquad \ldots (6.7)$$

The series (6.7) has to ensemble-averaged.

In order to find the configurational averages for a set of correlated scatterers higher order correlation functions are needed. Three body correlation functions are expressed in terms of two body correlation functions by the Abe approximation

$$\rho^{(b)}(r_1, r_2, r_3) \simeq \frac{1}{3}\left[g(r_{12})g(r_{13})+g(r_{21})g(r_{23})+g(r_{31})g(r_{32})\right] \qquad \ldots (6.8)$$

Similarly the nth order correlation functions may be expressed in terms of $g(r_{ij})$. Thus

$$Z(\beta) = \frac{1}{(2\pi\beta)3/2}\Big[1+\rho\int d\bar{r}f(\bar{r},\beta)+\int d\bar{r}_1 f(\bar{r}_1,\beta) * \left\{\frac{1}{2!}\rho^2 G(\bar{r}_1) + \ldots + \frac{1}{n!}\rho^n G^{n-1}(\bar{r}_1)+ \ldots\right\}\Big] \qquad \ldots (6.9)$$

with $G(\bar{r}_1) = \int d\bar{r}_2\, f(\bar{r}_2;\beta)\, g(r_{12})$ and so on. The terms in series (6.9) can be summed to yield

$$Z(\beta) = \frac{1}{(2\pi\beta)^{3/2}}\left(1 + \int d\bar{r}_1 \frac{f(\bar{r}_1,\beta)\{\exp[\rho G(\bar{r}_1)] - 1\}}{G(\bar{r})}\right) \quad \ldots (6.10)$$

For the random pseudo-atom model $g(r)$ is replaced by unity, so that Eq.(6.10) reduces to

$$Z(\beta) = \frac{1}{(2\pi\beta)^{3/2}} \exp[\beta\alpha(\beta)] \quad \ldots (6.11)$$

where,

$$\alpha(\beta) = \frac{\rho}{\beta} \int d\bar{r}\ f(\bar{r};\beta)$$

and ρ is the number of ions per unit volume.

The partition function $Z(\beta)$ is related to the density of states $n(E)$ by the Laplace transformation

$$Z(\beta) = \int_0^{+\infty} n(E)\ e^{-\beta E}\ dE \quad \ldots (6.12)$$

2. APPLICATION TO ALUMINIUM AND BERYLLIUM

In order to calculate the electronic density of states we have to start with the suitable choice of a potential. Here we use a potential in the following analytical form due to Green et al.(131)

$$v(r) = \frac{2(N\gamma - z)}{r} \quad \ldots (6.13)$$

where,

$$\gamma = 1 - \left[\{\exp(\frac{r}{d}) - H\} + 1\right]^{-1} \quad \ldots (6.14)$$

z is the number of nuclear protons, N is the number of core electrons and H and d are two parameters. These parameters are determined by fitting the energy values and wave functions with those calculated from the Hartree-Fock Slater method by Herman-Skillman(132). This simple analytical form which yields the same energies and wave functions as the Herman-Skillman potential is thus a reasonable choice for the single-centre potential. With this choice the effective potential matrix can be determined in an analytical form.

Hilton et al.(133) have shown that in the linear approximation (ignoring $\nabla U(\bar{r})$) the effective potential matrix $U(\bar{r},\bar{r}_o;\beta)$ is written as

$$U(\bar{r},\bar{r}_o;\beta) = \int g(\bar{r},\bar{r}_o;\bar{r}')\ v(\bar{r}')d\bar{r}' \qquad \ldots (6.15)$$

with

$$g(\bar{r},\ \bar{r}_o,\bar{r}') = \frac{\exp\left[\ |\bar{r}-\bar{r}_o|^2/2\beta\ \right]}{2\pi\beta}\ \frac{\left[\ |\bar{r}-\bar{r}'|+|\bar{r}'-\bar{r}_o|\ \right]}{\left[\ |\bar{r}-\bar{r}'||\bar{r}'-\bar{r}_o|\ \right]}$$

$$\times\ \exp\left[\ -\left\{(\bar{r}-\bar{r}'|+|\bar{r}'-\bar{r}_o|\right\}^2\ /\ 2\beta\ \right] \qquad \ldots (6.16)$$

We are interested in the diagonal element $U(\bar{r},\beta)$ given by

$$U(\bar{r},\beta) = \frac{1}{\pi\beta}\int d\bar{r}'\ v(\bar{r}')\ \exp.\left(\frac{-2|\bar{r}-\bar{r}'|^2}{\beta}\right) \qquad \ldots (6.17)$$

Using the form (6.13) for $v(\bar{r})$ we obtain

$$U(r,\beta) = -\frac{2Nd}{(1-H)r\beta}\sqrt{\frac{\pi\beta}{2}}\sum_{n}(-1)^{n+1}\exp\left[-\frac{n^2}{2\beta d^2}\right]$$

$$\times \operatorname{erfc}\left[\sqrt{\frac{2}{\beta}}\left(r+\frac{n\beta}{4d}\right)\right]\left[\bar{d}^{n}\left\{\exp\left(\frac{nr}{d}\right)-\exp\left(\frac{-nr}{d}\right)\right\}\right] \quad \cdots \quad (6.18)$$

As we have mentioned in the foregoing section, that this approach is valid for a slowly varying potential or a weak potential, we cannot apply the method in this form for a real metal having strongly attractive potentials and possessing bound states. Hence it is necessary to orthogonalise the density matrix to the known bound states of the system following the method due to Hilton et al.(133). The orthogonalised density matrix approach is applicable for a strong scattering potential also (128).

Now the orthogonalised density matrix is used to calculate $Z(\beta)$ for both random and correlated assembly. In the latter case the required radial distribution functions are taken from the numerical solutions of Percus-Yevick equations of the hard-sphere assembly.(134)

In principle the inversion of the partition function gives the density of states, but difficulty arises in a calculation, because $Z(\beta)$ is known numerically for certain values of β. We perform the inversion by making use of the method of first order steepest descent due to Hoare et al. (135). They have showed that this method gives reasonably good results when compared to exact analytical solutions for some simple cases.

3. RESULTS

In Figs.24 and 25, we have plotted $\alpha(\beta)$ for both the random and correlated cases of liquid Al and Be. It is seen that the difference between the results for random and correlated assembly increases with increasing β. For small values of β the curves for the random assemblies lie close to that for the correlated ones.

The density of states is shown in Fig.26 for both the random and correlated systems for a wide range of energy for Al and in Fig.27 for Be. As mentioned before an analytical evaluation of the density of states from partition function is not possible here, therefore, we have calculated numerically the density of states by Laplace inversion of (6.16) using six values of β (β=0.3,0.5, 0.7, 0.9, 1.1 and 1.3 in atomic units). The density of states for liquid aluminum obtained by the present method is compared with the results of other calculations in Fig.28. The calculations by other workers were based on free electron scheme, Edward's theory(125), MonteCarlo calculations (136) and the pseudo-potential method (137). The density of states curve obtained from the soft x-ray emission measurements of Rooke(138) is also shown. The pseudo-atoms tend to lower the value of the density of states at higher energies as compared to free electron results. For locating the low energy conduction edge we shall have to undertake tedious calculations using values of $Z(\beta)$ at many values of β higher than those used here.

The singularities in the density of states are washed out in our calculations for the disordered assembly. We also find that our results for density of states are close to those for free electron scheme. This shows the nearly free-electron like behaviour of electrons in the liquid aluminum.

In case of Be(Fig.27) the density of states for the random assembly is found to be less than that of the correlated one upto 1 Ryd and then it increases and exceeds that of the correlated one beyond 1 Ryd. An interesting feature of this calculation is the tailing structure in the density of states curve for both cases while in the calculation of Rousseau et al. the random assembly possesses a long tail and the correlated liquid has a very insignificant tail (Fig.3 of Rousseau et al. (128)). We do not find any direct experimental measurement of the density of states for this system.In view of the disagreement of our result with that of Rousseau et al., we conclude that the method of Laplace inversion by steepest descent method is not a powerful one.

CHAPTER VII

SUMMARY AND CONCLUSIONS

We have discussed in some details the activities and main interests in the field of disordered systems, which essentially aim at obtaining the quasiparticle energy spectrum and the nature of the wavefunctions. Research in the problem dealing with the energy spectrum has mainly aimed at: calculating the electronic density of states or the spectral functions. We have mainly concentrated on the substitutional binary alloys, the simplest of all disordered systems. The coherent potential model (an effective medium theory) has been found tc be very useful. The equilibrium and the dynamical properties of a disordered system are described with the help of the effective field concept of the type used in CPA. It is not quite clear how one can incorporate the fluctuations in random potentials over the effective field. We have omitted the discussion of the problem of dilute impurities for which normal perturbation method sometimes works fairly well. This method in a sequence of development has finally resulted in the effective medium theory except the fact that the self-energy in the perturbative method has spurious poles. In table 5 below, the development of the theory is abstracted. There exists model calculation (60) in the first order perturbative treatment that gives analogous results like CPA.

TABLE 5

Expression for the self-energy and its characteristic features

Type of excitations			Self-energy	Features	
Electrons	Phonons	Excitons		Dual Symmetry	Spurious poles in Σ
Edwards Klauder Matsubara and Toyozawa Beeby			$\frac{x\delta}{1-F(z)\delta}$	Broken	Don't exist
	Takeno Elliot and Taylor		$\frac{x\delta}{1-(1-x)F(z)\delta}$	Broken	Don't exist
Sovel Yonezawa	Taylor	Onedora and Toyozawa	$\frac{x\delta}{1-F(z)(\delta-\sigma)}$	Full	Removed

Details are given in a recent review by Yonezawa, Suppl. to Prog. Th.Phys. No.53, p.1 (1973).

The fact that the virtual crystal approximation is good enough for the alloys (where the difference of potentials is small), is used as a quantitative tool for obtaining the bandstructure of disordered alloys. The effective medium method is a step ahead of it.This relies on the self-consistency of the complex potential of the medium. Because of certain obvious unavoidable reasons as shown in Chapter III, the first iteration leading to ATA result has been obtained. Except performing some refinements over this method (to be discussed below) there seems no improvement in the single site theory. Then the next candidate is the cluster approach. One does a model calculation withinthe first shell of a cluster. But a realistic cluster calculation is extremely expensive for which there exists only a few calculations by Johnson and coworkers(139) at MIT and Ziman and coworkers(122) at Bristol for small clusters. The tight-binding method as used in the recent days in the band structure calculation of transition metals(140) may be a good start for use in the theory as described in Chapter IV. This scheme is very useful for taking into account the fluctuation in the random alloy potential. Although a selfconsistent version of this method will be no doubt superior to single site CPA, this scheme will be very complicated for use in a realistic calculation. This tight binding method has been used to obtain the static electrical conductivity and paramagnetic spin

susceptibility(141) of disordered binary alloys. Then next structurally complicated system we consider, is a positionally disordered material: liquid metals. The question of the influence of local order has been thoroughly discussed by March and collaborators who use the Thomas Fermi theory for the effect of the environment and discuss in detail how the liquid theory can be based on the partition function of the liquid directly. Use of this theory has been found to be fruitful for the realistic systems.The problems of amorphous materials are much more difficult and involved compared to disordered systems(142) considered here. Now we discuss some of the refinements which one can incorporate in our calculations. Charge transfer(143) happens to be the most important one for calculating the alloy potential. One usually expects a charge transfer from one of the species to another, if the atomic potentials or the valencies of the constituents differ. Mott(144) has pointed out that if the charges on the atoms are too large, the Madelung energy gained by forming an ordered solid overcomes the entropic term which favours disorder and the alloy will order at sufficiently low temperature. If the net charge is small enough, the ordering temperature might be so low that kinetic effects will make the disordered phase favourable.That is why the transition and noble metal alloys have in the primary phase a substitutionally disordered structure.So the net charge transfer is quite

small i.e. $< 10\%$ for equiconcentrated alloy. We have not considered charge transfer effects. A view point exists that the transfer of electrons is related to the electronegativities of the species. When atoms are brought together to form a solid, the electronic charge density is compressed by causing a significant increase of local Fermi energy, which provides a useful scale of electronegativity, but the local fermi-energy is not a measurable quantity, so one relates it with the work function of the material. Efforts have been put to examine the effects of work function of metals or the contact potentials of the bi-metallic systems on the charge transfer.(145) Recently Ehrenreich and collaborators(146) have tried to incorporate the charge transfer in AgAu in a two band model tight-binding Hamiltonian through CPA. However, the calculation of the complex band is no doubt very complicated but people are worrying about the choice of a good alloy potential. If one uses the density functional argument (that tells that there exists a periodic potential $V(\bar{r}, E)$ for a given energy E), then it is feasible to work out an alloy potential, as a functional of energy dependent constituent potentials. This has the possibility of including the many body effects through the density dependent exchange-correlation potential. This apprcach via the partition function (147) will be a simpler workable scheme for the alloy band structure than the model Hamiltonian approach used extensively these days.

Appendix

We give the diagrams which contribute to the imaginary part of the self-energy $\Sigma_2(\bar{k})$ in Fig.17. The diagrams are drawn in direct lattice space. The weight factors and the sign of each diagram are also given.

It is to be noted that the sixteenth and last diagrams are the same as obtained in Edwards and Loveluck(107). The other diagrams are completely new.

REFERENCES

1. F. Seitz, The Modern Theory of Solids, McGraw-Hill, New York, (1940).

   N.F. Mott and H.Jones, The Theory of the Properties of Metals and Alloys, Dover, New York, 1958.

   J.M.Ziman, Proc. Roy.Soc.(London) A 318, 401(1970),

   N.H. March and J.C.Stoddart, Rep.Prog.Phys.31,533(1968).

   M.H.Cohen, Lectures at NATO Summer School on Amorphous Semi-Conductor, Ghent, Belgium(1969), (unpublished).

   Electrons in Disordered Systems, Kyoto Seminar, Sept. (1972), ISSP Technical Report No.15(1973).

2. W.A.Harrison and M.B.Webb(Ed), The Fermi Surface, John Wiley(1960)

   B.Alder, S.Fernbach and M.Rotenberg(Ed), Methods in Computational Physics, Vol.8, Energy Bands in Solids, Academic, New York(1968).

   P.M. Marcus, J.F.Janak and A.R.Williams(Ed), Computational Methods in Band Theory, Plenum, New York, London (1971).

   J.M. Ziman in Solid State Physics, Vol.26, Edited by F.Seitz, D.Turnbull and H.Ehrenreich, Academic, New York(1971); J.Res.74A, 241(1970)

   J.M. Ziman,(Ed), 'Electrons in Metals-I,Cambridge (1969)

3. J.C. Slater, Quantum Theory of Molecules and Solids, Vol.II, McGraw Hill, New York (1965)

4. R.G.Chambers in Solid State Physics Vol.I, Ed.- R.Haerring and W.Cochran, p.283(1968).

5. F.Abeles (Ed) Optical Properties of Solids, North Holland(1972).

   F.Wooten, Optical Properties of Solids, North Holland (1972).

6. H.Ehrenreich and P.R.Phillips, Phys.Rev.128,1622(1962).

7. W.E.Spicer, J.Research(NBS), 74A,397(1970)

8. C.N.Burglund and W.E.Spicer, Phys.Rev.136,1030(1964) See for example K.K.Thornber, Sci.Prog.(Oxf.), 57,149(1969).

9. S.Doniach, Phys.Rev.B2, 3898(1970).

10. H.Hermeking, J.Phys.(C) 6, 2898(1973).

11. U.Gerhardt, Phys.Rev.172, 651(1965).

12. M.Cardona, Suppl. to Solid State Physics, Vol.11, Ed., F.Seitz, D.Turnbull and H.Ehrenreich Academic, New York, (1972).

13. E.A.Stern, Phys. Rev.157, 544(1966).
J.M. Tracy and E.A.Stern, Phys.Rev.B8, 582(1973).

14a. D.J.Fabian and L.M. Watson(Ed.) Band Structure Spectroscopy of Metals and Alloys(Academic), London(1973).

14b. D.J.Fabian, L.M. Watson and C.A.M. Marshall, Rep.Prog. Phys. 34,601(1973).

15. K.Ulmer in Band Structure Spectroscopy of Metals and Alloys,Ref.(14a).

16. D.J.Fabian, J.Fuggle and L.M.Watson in Ref.14a, p.91.

17. D.Shirley, Phys.Rev.B5, 4709(1972).
S.Hüfner, G.K.Wertheim, N.V.Smith and M.M.Traum, Solid State Comm.11, 323(1972).

18. D.Hagstrum, Phys.Rev.150, 495(1966).

19. W.Kohn, Phys.Rev.Lett.2, 393(1959).
S.C.Ng and B.N.Brockhouse, Solid State Comm.5,79(1967)

20. A.T.Stewart and L.O. Roelling, (Ed), Positron Annhilation-Academic, New York(1967).
C.K.Majumdar in Theory of Condensed Matter, p.829, IAEA(Vienna)(1968).

21. L.F.Roberts, R.L. Becker, F.E.Obenshain and J.D.Thomson, Phys.Rev.137, A895(1963).

22. I.Yu Dekhtyar, Phys.Reports 9C(1974).

23. F.E.Wagner, G.Wortmann and G.M. Kalvins, Phys.Lett.42A, 483(1973).

24. L.H.Bennett, R.E.Watson and G.C.Carter, J.Research(NBS), 74A, 569(1970).

25. L.H.Bennett(Ed) Density of States (NBS) (1971) Menton Conference Report as found in J.de Physique 33, Suppl. No.5-6(1972).

26. G.F.Koster and J.C.Stater, Phys.Rev., 96, 1208(1954).

27. E.N.Economou, M.H.Cohen, K.Freed, and S.Kirkpatrick, in Amorphous and Liquid Semi-conductors, edited by J.Jauc Plenum(1971)

E.N.Economou in Recent Advances in Amorphous Semi-conductors, edited by P.R.Wallace, R.Harris and M.J.Zuckermann, Noordhoff, Int. Publ. Co.Leyden(1972).

28. J.M. Ziman, J.Phys.(C), 1, 1532(1969).

V.K.S.Shante and S.Kirkpatrick, Adv.Phys.20, 320(1972).

29. See for example S.Kirkpatrick in Kyoto Seminar Ref.1, p.18.

31. P.W.Anderson, Phys.Rev.109, 1492(1958)

32. N.F.Mott and W.D.. Twose, Adv.Phys.10,107(1961).

N.F.Mott and E.Davis, Electronic Porcesses in Non-crystalline Materials', Oxford(1972).

33. J.M.Ziman, J.Phys(C) 2, 1230(1969)

D.J. Thouless, J.Phys(C) 3, 1559(1970)

P.W.Anderson, Comm.Solid.St.Phys.2, 193(1970)

M.Kikuchi, J.Phys. Soc.Japan, 29, 296, (1970)

E.N.Economou and M.H.Cohen, Mat. Res. Bull. 5, 577(1970); Phys.Rev.B5, 2931(1972)

T.Lukes, J.Non-Cryst.Solids, 8-10, 470(1972).

A.R.Bishop, Phil.Mag.27, 651, 1489(1973).

R.Abou-Chachra, P.W.Anderson, D.J.Thouless, J.Phys.(C), 6, 1934(1973); 7, 65(1974).

34. D.N.Zubarev, Sov. Phys.(Usp), 3,320(1961).

35. T.Fujita and J.Hori, J.Phys.(C) 5,1059(1972).

36. P.W.Anderson, Proc. Natl. Acad.Sc.(U.S.A.),69, 1097 (1972).

K.Freed, Phys.Rev.B5, 4802(1972).

E.N.Economou and D.C.Licciardello, preprint(1974).

A.Mookerjee (Private Communication).

37. See for example Progress in Material Science, Vol.9,No.5, Edited by J.M.Silvertoen and M.E.Nicholson, Pergamon (London), (1961).

S.K.Joshi, Lectures in Summer Science Institute, Roorkee (1973) (Unpublished).

38. M.Hansen, Constitution of Binary Alloys, McGraw Hill (New York), (1958).

39. H.Jones, Proc. Roy.Soc.144A, 396(1934).

J.Friedel, Adv.Phys.3, 446(1954).

40. V.Heine and D.Weaire in Solid State Physics, Edited by F.Seitz, D.Turnbull and H.Ehrenreich, (Academic), New York,Vol.24, 224(1970).

41. K.P.Gupta, C.H.Cheng and P.Beck in Metallic Solid Solutions, XXV-I, edited by J.Friedel and A.Guinier, Benjamin (1963);Phys.Rev.133, A203(1964).

S.Hufner, G.K. Wertheim, R.L.Cohen and J.H.Wernick, Phys.Rev.Lett. 28, 488(1972).

42. H.Jones, Phys.Rev.134A, 958(1964)

P.G.Dawber, and R.E.Turner, Proc. Phys.Soc.88, 217(1966).

A.D. Brailford, Proc.Roy.Soc. 293A, 433(1966).

E.Haga, Proc.Phys.Soc.91, 169(1967).

43. L.Nordheim, Ann.Phys.9, 607(1931)

T.Muto, Science Papers Inst.Phys.Chem.Res.(Tokyo),34, 377(1938)

44. H.Paramenter, Phys.Rev.97, 587(1955).

45. D.Stroud and H.Ehrenreich, Phys.Rev.B2, 1676(1970)

46. H.Amar, K.H. Johnson and C.B.Sommers, Phys.Rev.153, 655(1967)
M.M. Pant and S.K.Joshi, Phys.Rev.184, 635(1969).
N.H.March, P.Gibbs, G.M.Stocks and J.S.Faulkner, J.de Physique, 33S, C3-259(1972)

47. M.H. Cohen and V.Heine, Adv. Phys. 7, 395(1958).

48. N.D.Lang and H.Ehrenreich, Phys.Rev.168,605(1968). J.Appl.Phys.40,1282(1969).

49. P.W.Andersen, Phys. Rev.124, 41(1961)
J. Friedel, Phil.Mag.43, 153(1952).

50. D.H.Seib and W.Spicer, Phys.Rev.B2, 1676(1970); B2,1694 (1970).

51. E.A.Stern, Physics, 1,255 ,(1964); Phys.Rev.B7,1303, 5062(1973).

52. E.A.Stern, Phys.Rev.144, 545(1966);
J.Rudnick and E.A.Stern, Phys.Rev.7, 5062(1973)

53. S.Takeno, Prog.Theo.Phys. 42, 1221(1969), and references cited therein.

54. See for example D.J.Thouless and E.N.Economou and M.H. Cohen in ref.33.

55. P.Soven, Phys.Rev.156, 809(1967); 178, 1136(1969).

56. B.Velický, S.Kirkpatrick and H.Ehrenreich, Phys.Rev. 175,747(1968).

57. J.L.Beeby, Phys. Rev.135, A130(1964);Proc.Roy.Soc.279A, 82(1964).

58. L.Schwartz, F.Brouers, A.V.Vedyayev and E.Ehrenreich Phys.Rev.B4, 3383(1971).

59. F.Yonezawa, Prog.Theo.Phys.40, 734(1968) and references cited therein.

60. M.P.Das and S.K.Joshi, Phys. Rev.B4, 4363(1971).

61. P.L. Leath, Phys.Rev.171, 725(1968).

62. D.W.Taylor, Phys. Rev.156, 1017(1967).

63. Y.Onedora and Y.Toyozawa, J.Phys.Soc. Japan,24,341(1968)

64. L.M.Roth, Phys.Lett. 31A,440(1970).

65. B.Velický, Phys.Rev.184, 614(1969).

66. S.Kirkpatrick, B.Velický and H.Ehrenreich, Phys.Rev.B1, 3250(1970).

67. G.M. Stocks, A.R.Williams and J.S.Faulkner, Phys.Rev. Lett.26, 253(1971);Phys.Rev.B4, 4390(1971); J.Phys.(F), 3, 1688, (1973).
G.M.Stocks, Int.J.Quant.Chem.5, 553(1971).

68. F.Leoni and F.Sacchetti, Nuovo Cimento, 21B, 97(1974)
H.Hasegawa and J.Kanamori, J.Phys.Soc. Japan,32,1665(1972); 33, 1599(1972).

69. E.A.Stern, Phys.Rev.Lett. 26, 1630(1974);Phys.Rev.B7, 5054(1973).

69a. R.H.Lasseter and P.Soven, Phys.Rev. B8, 2476(1973).

70. F.Cyrot Lackmann and F.Ducastelle, Phys. Rev.Lett.27, 287(1971).

71. L.Schwartz and H.Ehrenreich, Phys.Rev.B6, 2923(1972).

72. B.Mozer, D.T.Keating and S.C.Moss, Phys.Rev.175, 868(1968); S.C.Moss, Phys.Rev.Lett.23, 381(1969).

73. K.Freed and M.H.Cohen, Phys.Rev.B3, 3400(1970).

74. W.H.Butler and W.Kohn, J.Research (NBS) 74A, 443(1970)

75. B.G.Nickel and J.A.Krumhansl, Phys.Rev.B4, 4354(1971).
L.Schwartz and E.Siggia, Phys.Rev.B5, 383(1972).
F.Ducastelle, J.Phys.(F) 2, 468(1972).

H.Shiba, Prog.Th.Phys. 46, 77(1971)

W.H.Butler, Phys.Lett.39A,203(1972), Phys.Rev.B8, 4499(1973).

M.Tsukada, J.Phys.Soc.Japan, 32, 1475(1972).

R.G.Wooley, and R.D.Mattuck, J.Phys(F), 3,75(1973).

F.Cyrot-Lackmann and M.Cyrot, J.Phys.(C) 5, L-209(1972).

E.N.Foo and M.Ausloos, J.Non-Cryst. Solid, 8-10, 134(1972).

E.Hartmann-Müeller, Solid State Comm.12,1269(1973).

B.G.Nickel and W.H.Butler, Phys.Rev.Lett. 30,373(1973).

E.N.Foo, S.M.Bose and M.Ausloos, Phys.Rev.B7,3454(1973).

V.Čápek, Phys.Stat.Solidi 52(b), 399(1972); Cz.J.Phys. B21,997(1971).

J.Sanders and H.Harris Solid State Comm.12, 219(1973)

K.Niizeki, Solidstate Comm.12, 267(1973).

F. Yonezawa, and M.Nakamura, 47, 1124(1972).

P.L.Leath, J.Phys(C) 6, 1559(1973).

I.Takahashi and M.Shimizu, Prog.Th.Phys.51,1678(1974).

D.C.Licciardello and E.N.Economou, Solid State Comm. 12, 1275(1973)

F.Ducastelle, (Preprint), (1974).

J.Zittartz, Z.Physik, 267, 243(1974).

76. J.C.Slater, Phys.Rev.145, 595(1966).
P.Soven, Phys.Rev.151, 539(1966).

77. M.M. Pant and S.K.Joshi, Phys.Rev.B2, 1704(1970)
M.P. Das and S.K.Joshi,Canad..J.Phys.50,2856(1972)

78. J.Korringa, Physica 13, 392(1947)

79. W.Kohn and N.Rostoker, Phys.Rev.94, 1111(1954).

80. P.Soven, Phys.Rev.B2, 4715(1970)

81. B.Gyorffy, Phys. Rev.B5, 2382(1972).

82. A.B.Chen, Phys.Rev.B7, 2230(1973).

83. A.Bansil and L.Schwartz, Preprint(1974).

84. R.Bass, Preprint (1974).

85. P.W.Anderson and W.L.McMillan, Proc. Int.Sch.Phys. 'Enrico Fermi', 37, 50(1967).

86. G.Gilat and L.J.Raubenheimer, Phys.Rev.144, 390(1966).

87. F.M.Mueller, J.W.Garland, M.H.Cohen and K.H.Bennemann-Argonne Report ANL-7556.

88. A.Balderschi, Phys.Rev.B7, 5212(1973).

89. Methods in Computational Physics of Ref.2, Chapter 7.

90. H.L.Davis in Computatinnal Methods in Band Theory of Ref.2, p.183.

91. L.F.Mattheiss, Phys.Rev.134, A 970(1964).

92. B.R.Cooper, E.L.Kreiger and B.Segall, Gen. Elastic Rep.No.71-C-085(1971).

93. M.P.Das and S.K.Joshi, J.Phys.(F) 2, L-42(1972).

94. M.P.Das and S.K.Joshi, Phys.Rev.B8, 4039(1973).

95. M.A.Biondi and J.A.Rayne, Phys.Rev.115, 1522(1959).

96. A.H.Lettington, Phil.Mag.11, 863(1965).

97. B.Segall, Phys.Rev.125, 109(1962).

98. B.R.Cooper, H.Ehrenreich and H.R.Phillips, Phys.Rev. 138, A494(1965).

99. D.Beaglehole, Proc.Phys.Soc.85, 1007(1965).

99a. F.M.Mueller and J.C.Phillips, Phys.Rev.157,600(1967).

99b. U.Gerhardt, D.Beaglehole and R.Sandrock, Phys.Rev.Lett. 19, 309 (1967).

100. R.E.Hummel, D.B.Dove and J.A.Holbrook, Phys.Rev.Lett. 25, 290(1970).

R.E.Hummel, J.A.Holbrook and J.B.Andrews, Surf.Sci.37, 717(1973).

R.E.Hummel and J.B.Andrews, Phys.Rev.B8, 2449(1973).

101. J.A.Rayne, Phys.Rev.121, 456(1961).

102. G.P.Pells, and H.Montgomery, J.Phys(C), Suppl.3, S-330(1970).

103. P.O.Nilsson, Physica Scripta,1, 189(1970).

104. G.P.Pells and M.Shiga, J.Phys.(C) 2, 1835(1969).

105. R.S.Rea and A.S.DeReggi, Phys.Rev.Lett.30, 549(1973); Phys.Rev.B9, 3285(1974).

106. C.Y.Fong, M.L.Cohen, R.R.L.Zucca, J.Stockes and Y.R.Shen, Phys.Rev.Lett. 25, 1486(1970).

107. S.F.Edwards and J.M.Loveluck, J.Phys.(C), Suppl.3, S261(1970).

108. R.S.Tripathi, M.P.Das and S.K.Joshi, J.Physics(F), 3, 944(1973).

109. J.M.Ziman, Principles of the Theory of Solids, Oxford Univ.Press, England(1965).

110. R.Kubo, J.Phys.Soc.Japan, 12, 570(1957).

111. K.Levin, B.Velicky and H.Ehrenreich, Phys.Rev.B2, 1771(1970).

112. A.B.Chen, G.Weisz and A.Sher, Phys.Rev.B5,2897(1972).

113. R.S.Tripathi, M.P.Das and S.K.Joshi, J.Phys.(F), 4, 717(1974).

114. C.Bloch and C.DeDominicis, Nucl.Phys.7, 459(1956).

114a. J.Langer, Phys.Rev.124, 1003(1961), Phys.Rev.128, 110(1962).

115. V.Ambegaonkar, in Astro-Physics and Many Body Problem,Edited by A.A.Maraduddin, et al.(Benzamin) (1964).

116. A.L.Fetter and J.P.Walecka, Quantum Theory of Many Particle Systems, McGraw Hill, New York,1971.

117. R.C.Tolman, Principles of Statistical Mechanics, Oxford(1950).

118. See for Example N.F.Mott and H.Jones, in Ref.1.

119. F.Brouers and A.V.Vedyayev, Phys.Rev.B5, 348(1972).

120a. J.M.Ziman, Phil.Mag.6, 1013(1961).

120b. J.M.Ziman, Proc.Phys.Soc.88, 387(1966).

121. P.Lloyd, Proc.Phys.Soc.90,207, 217(1967).

122. J.Keller and P.V.Smith, J.Phys.(C) 5, 1109(1972).
J.Keller and R.Jones, J.Phys.(F),1, L33(1972).
J.Keller and J.M.Ziman, J.Non-cryst.Solids, 8-10, 111(1972).
J.Klima, T.C.McGill and J.M.Ziman, Discussion of the Faraday Soc.No.50,20(1970).

123. L.Schwartz andH.Ehrenreich, Ann.Phys.(U.S.A.) 64, 100 (1971).

124. S.F.Edwards, Phil.Mag 6, 617(1961); Proc.Roy.Soc. 267A, 578(1962).

125. L.E.Ballentine, Canad.J.Phys.44, 2533(1966).

126. R.W.Shaw, Jr. and N.V.Smith, Phys.Rev.178, 985(1969).

127. F.Cyrot Lackmann, Adv.Phys.16,393 (1968); J.de Physique 27, 627(1966).

128. J.Rousseau, J.C.Stoddart and N.H.March, Proc. Roy. Soc.London, 317A,211(1970).

129. M.M.Pant, M.P.Das and S.K.Joshi, Phys.Rev.B4, 4379(1971).

130. M.M.Pant, M.P.Das and S.K.Joshi, Phys.Rev.B7, 4741(1973).

131. A.E.S.Green, D.L.Sellin and A.S.Zachor, Phys.Rev.184, 1(1969).

132. F.Herman and S.Skillman, Atomic Structure Calculations, Prentice Hall, Englewood Cliffs,N.J.(1963).

133. D.Hilton, N.H.March and A.R.Curtis, Proc.Roy.Soc. (London), 300A,391(1967).

134. G.J.Throop and R.J.Bearman, J.Chem.Phys.42, 2408(1965).

135. M.R.Hoare and Th.W.Ruijgrok, J.Chem.Phys.52, 113(1970).

136. D.Brust, Phys.Rev.B2, 818(1970).

137. N.W.Ashcroft in Soft X-ray Band Spectra, Ed.by D. J.Fabian, p.59, (in paper by G.Wiech), Academic(1968).

138. G.A.Rooke, in Optical Properties and Electronic Structure of Metals and Alloys, Edited by F.Abeles, p.336(in paper by Wooten et al.)North Holland(1966).

139. K.H.Johnson, J.de Phys.33S, 195(1972)

140. J.Langlinais, and J.C.Callaway, Phys.Rev.5B, 124(1974).

141. R.S.Tripathi, M.P.Das and S.K.Joshi, Nucl.Phys. and Solid State Physics Symposium, Bangalore(1973).

142. J.M.Ziman in Electrons in Dis-ordered System of Ref.1.

143. L.H.Bennett and R.H.Willens (ed), Charge Transfer and Electronic Structure of Alloys ,Proceedings of the 1973 Twin Symposium(1974).

144. N.F.Mott, Proc. Phys.Soc.(London), 49, 258(1937).

145. A.R.Miedema, F.R.de Boer and P.F.de Chatel, J.Phys.(F), 3, 1558(1973).

146. C.D.Gelatt and H.Ehrenreich, preprint(1974).

147. N.H.March, (Private Communication).

LIST OF PAPERS

1. Electronic States in a Disordered Binary Alloy- Phys.Rev.B4,4363,1971.

2. Density of Electronic States in Liquid Aluminium- Phys.Rev.B4, 4379,1971.

3. Electronic Structure of Disordered Binary Alloys-α-Brass- Canad.J.Phys.50, 2856, 1972.

4. The Optical Spectra of α-Brass- J.Phys.(F), Metal Physics,2,L42,1972.

5. Density of Electronic States in Liquid Beryllium- Phys.Rev.B7, 4741, 1973.

6. Electronic Structure of Disordered Binary Alloys- J.Phys(F), Metal Physics, 3,944,1973.

7. Electronic Transitions in α-Phase CuGe Alloys Phys.Rev.B8,4039,1973.

8. Electronic Transport in Disordered Binary Alloys- J.Phys.(F), Metal Physics,4,717,1974.

9. A note on 'Pseudo-Green Function methods for Energy Bands of Metals and Alloys-Technical Report, Department of Physics,Indian Institute of Technology, Kanpur(India), No.31/70.

10. Work-functions for Alkali Metals- ICTP(Trieste) Preprint No.32,1974, and to be published in J.Phys(F) 1975,

11. On the Magnetization in Metallic Films- ICTP(Trieste), Preprint No.77,1974 and to be published.

12. Electronic Structure of a Disordered Binary Alloy-α-CuAl- (communicated)

13. A note on 'Spin Susceptibility in Disordered Binary Alloys' (communicated)

14. Electronic Structure and Adhesive energies at the Bimetallic Interface- (to be published)

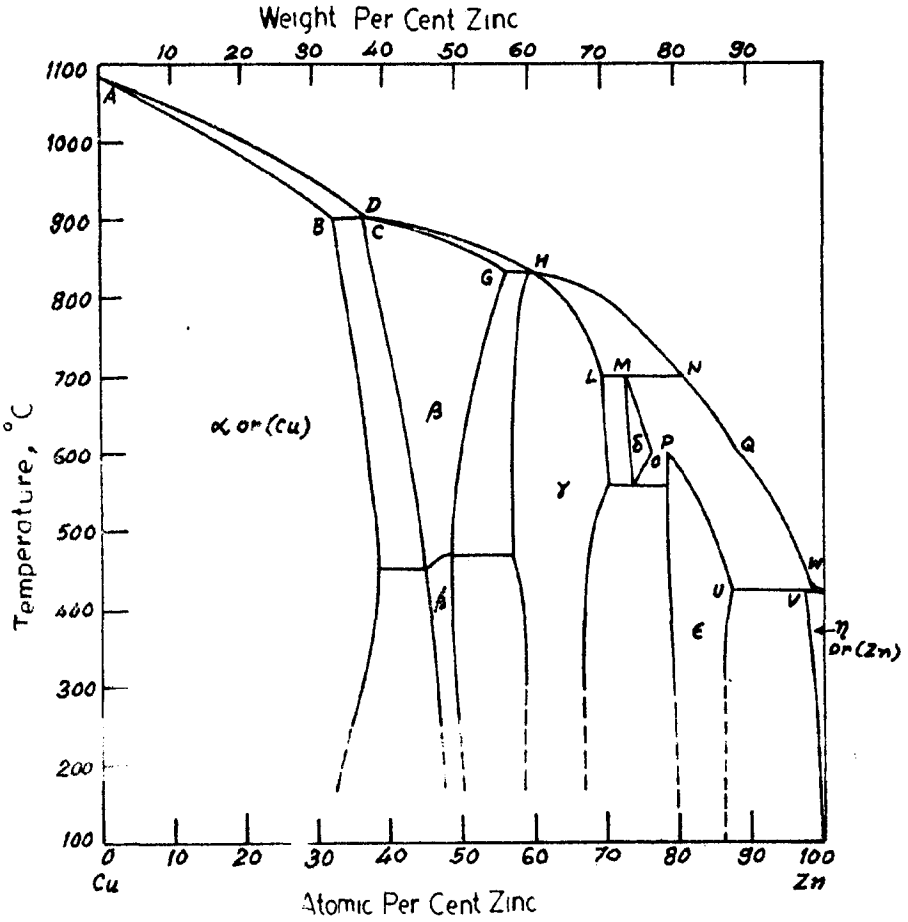
Weight Per Cent Zinc
10 20 30 40 50 60 70 80 90
1100
1000
900
800
700
600
500
400
300
200
100
Temperature, °C
A
B
C
D
G
H
L
M
N
P
Q
R
U
V
W
α or (Cu)
β
γ
δ
ε
η or (Zn)
0 10 20 30 40 50 60 70 80 90 100
Cu
Zn
Atomic Per Cent Zinc

FIG. 1(a)

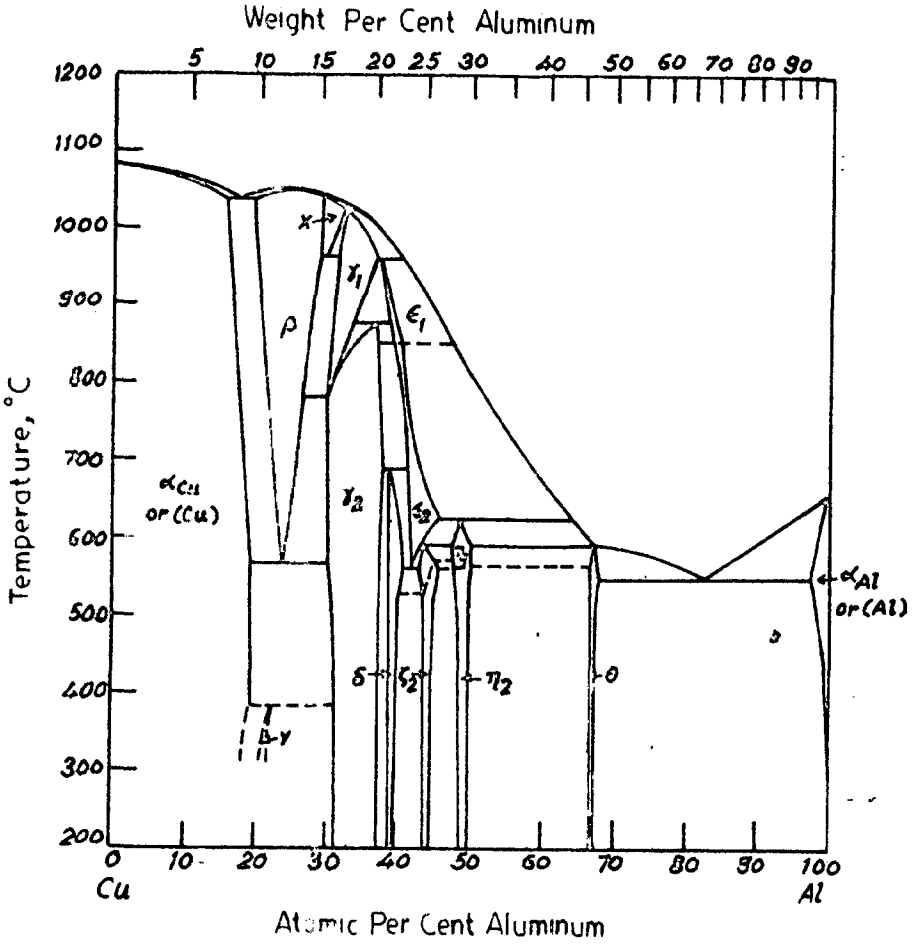
Weight Per Cent Aluminum
5 10 15 20 25 30 40 50 60 70 80 90
1200
1100
1000
900
800
700
600
500
400
300
200
Temperature, °C
x
γ1
ρ
ε1
αCu or (Cu)
γ2
ζ2
δ
ζ2
η2
θ
αAl or (Al)
L+γ
0 10 20 30 40 50 60 70 80 90 100
Cu
Al
Atomic Per Cent Aluminum

FIG.1(b)

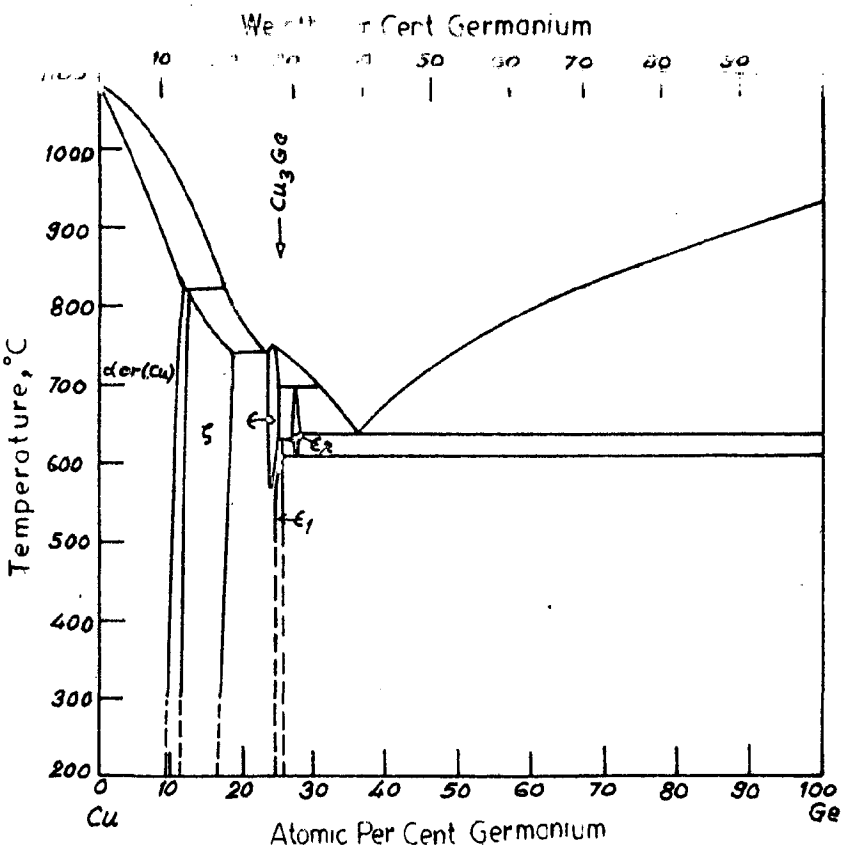
Cu3Ge
1000
900
800
700
600
500
400
300
200
Temperature, °C
α or (Cu)
ζ
ε
ε2
ε1
0 10 20 30 40 50 60 70 80 90 100
Cu
Ge
Atomic Per Cent Germanium

FIG.1(c)

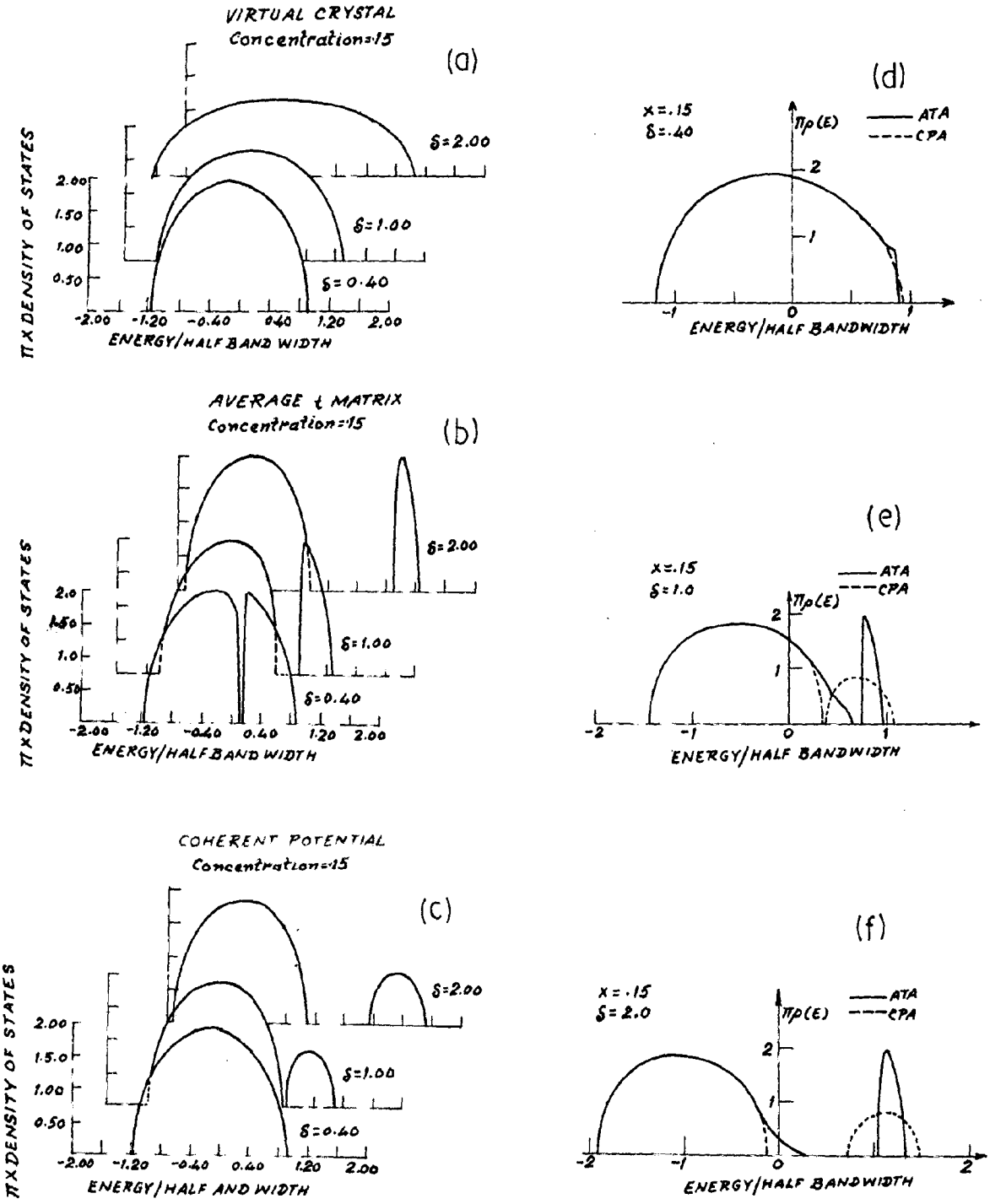
VIRTUAL CRYSTAL
Concentration=.15
(a)
δ=2.00
δ=1.00
δ=0.40
πX DENSITY OF STATES
2.00
1.50
1.00
0.50
-2.00 -1.20 -0.40 0.40 1.20 2.00
ENERGY/HALF BAND WIDTH
AVERAGE t MATRIX
Concentration=.15
(b)
δ=2.00
δ=1.00
δ=0.40
πX DENSITY OF STATES
2.0
1.50
1.0
0.50
-2.00 -1.20 -0.40 0.40 1.20 2.00
ENERGY/HALF BAND WIDTH
COHERENT POTENTIAL
Concentration=.15
(c)
δ=2.00
δ=1.00
δ=0.40
πX DENSITY OF STATES
2.00
1.5.0
1.00
0.50
-2.00 -1.20 -0.40 0.40 1.20 2.00
ENERGY/HALF AND WIDTH
(d)
x=.15
δ=.40
πρ(E)
ATA
CPA
2
1
-1 0 1
ENERGY/HALF BANDWIDTH
(e)
x=.15
δ=1.0
πρ(E)
ATA
CPA
2
1
-2 -1 0 1
ENERGY/HALF BANDWIDTH
(f)
x=.15
δ=2.0
πρ(E)
ATA
CPA
2
1
-2 -1 0 2
ENERGY/HALF BANDWIDTH

FIG.2

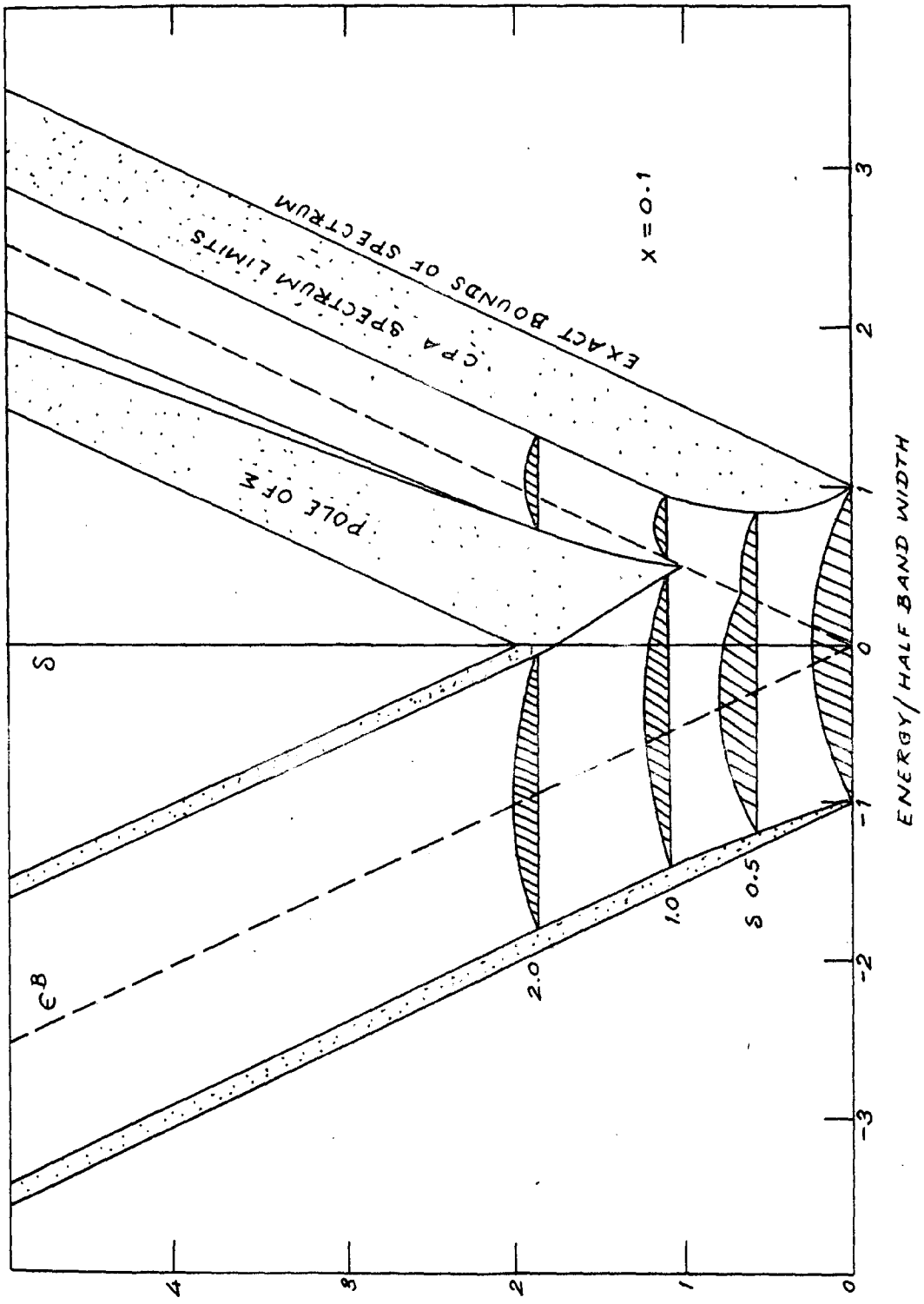
EXACT BOUNDS OF SPECTRUM
CPA SPECTRUM LIMITS
POLE OF Σ
x = 0.1
S
ϵ^B
2.0
1.0
S 0.5
ENERGY/HALF BAND WIDTH
4
3
2
1
0
3
2
1
0
-1
-2
-3

FIG.3

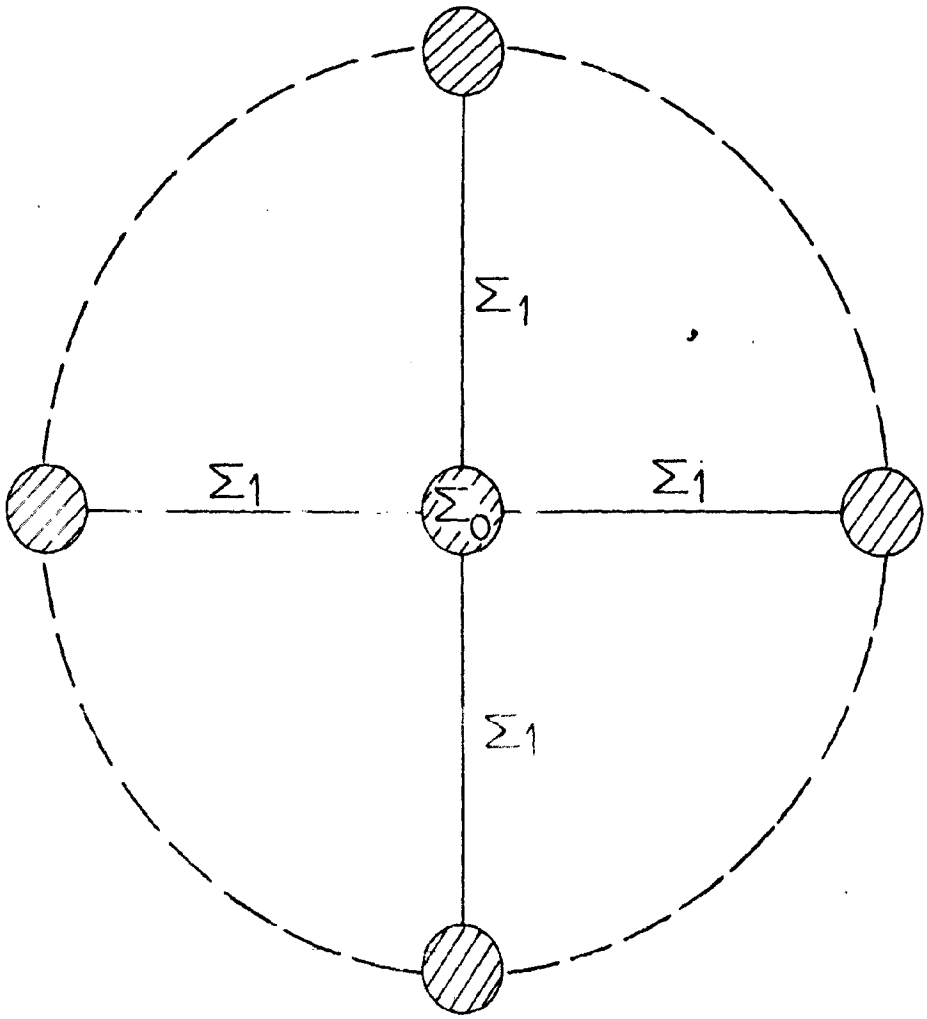

FIG.4

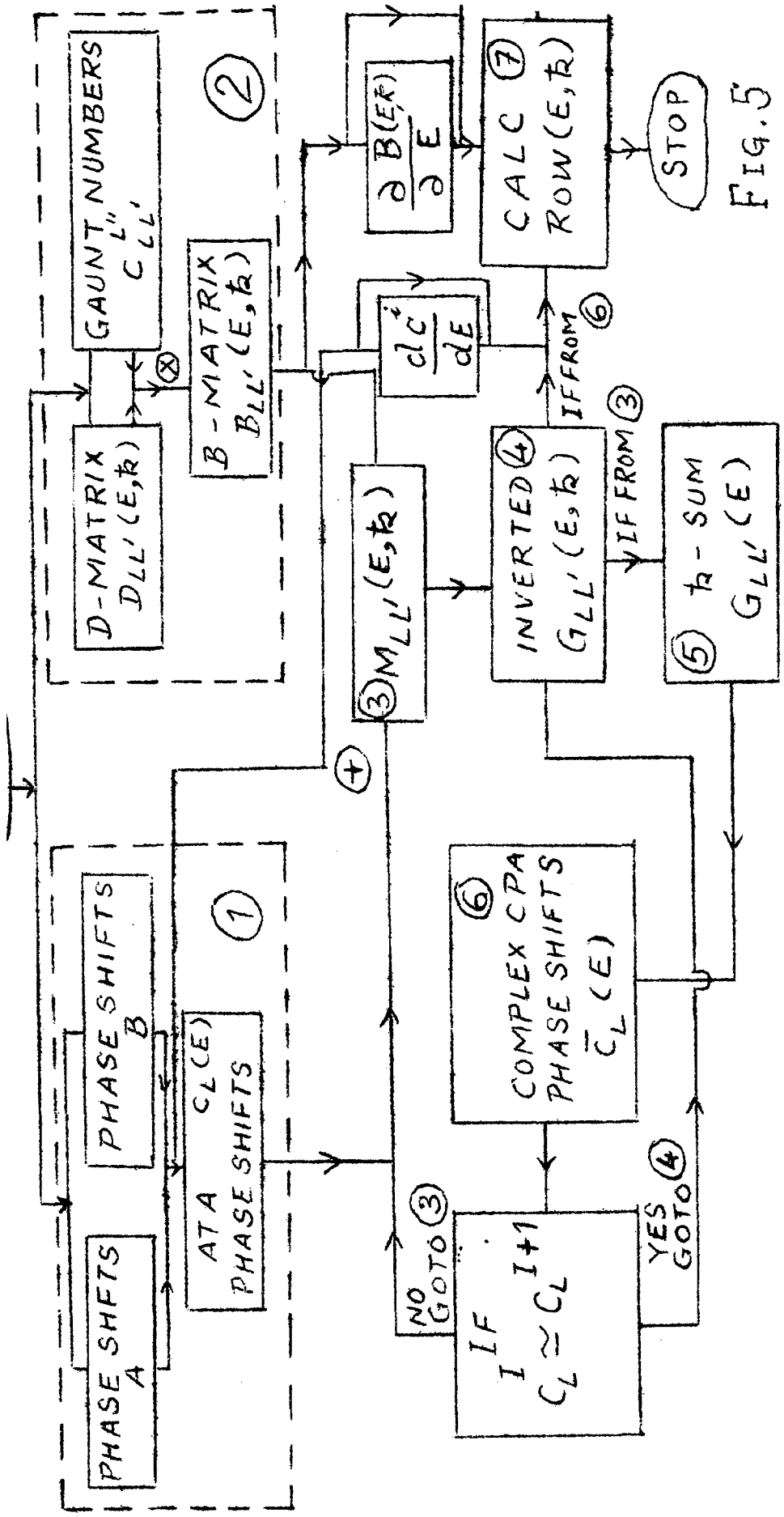
PHASE SHIFTS A
PHASE SHIFTS B
ATA PHASE SHIFTS $C_L(E)$
1
D-MATRIX $D_{LL'}(E,k)$
GAUNT NUMBERS $C_{LL'}^{L''}$
B-MATRIX $B_{LL'}(E,k)$
2
$M_{LL'}(E,k)$
3
$\frac{\partial B(E,k)}{\partial E}$
$\frac{dC_L}{dE}$
INVERTED $G_{LL'}(E,k)$
4
IF FROM 3
IF FROM 6
k - SUM $G_{LL'}(E)$
5
CALC ROW(E,k)
7
STOP
COMPLEX CPA PHASE SHIFTS $\bar{C}_L(E)$
6
IF $C_L \simeq C_L^{I+1}$
NO GOTO 3
YES GOTO 4

FIG. 5

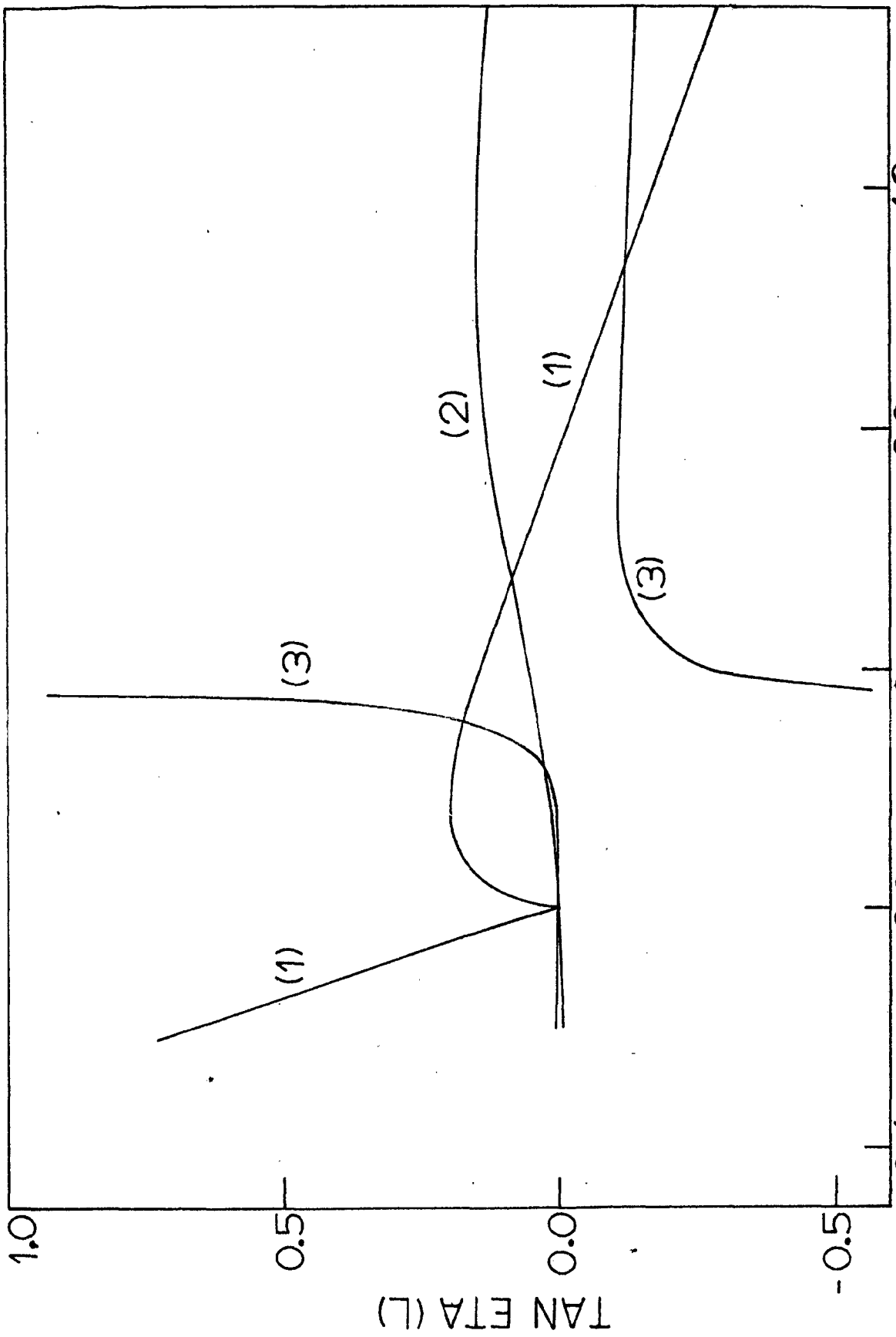

FIG.6(a)

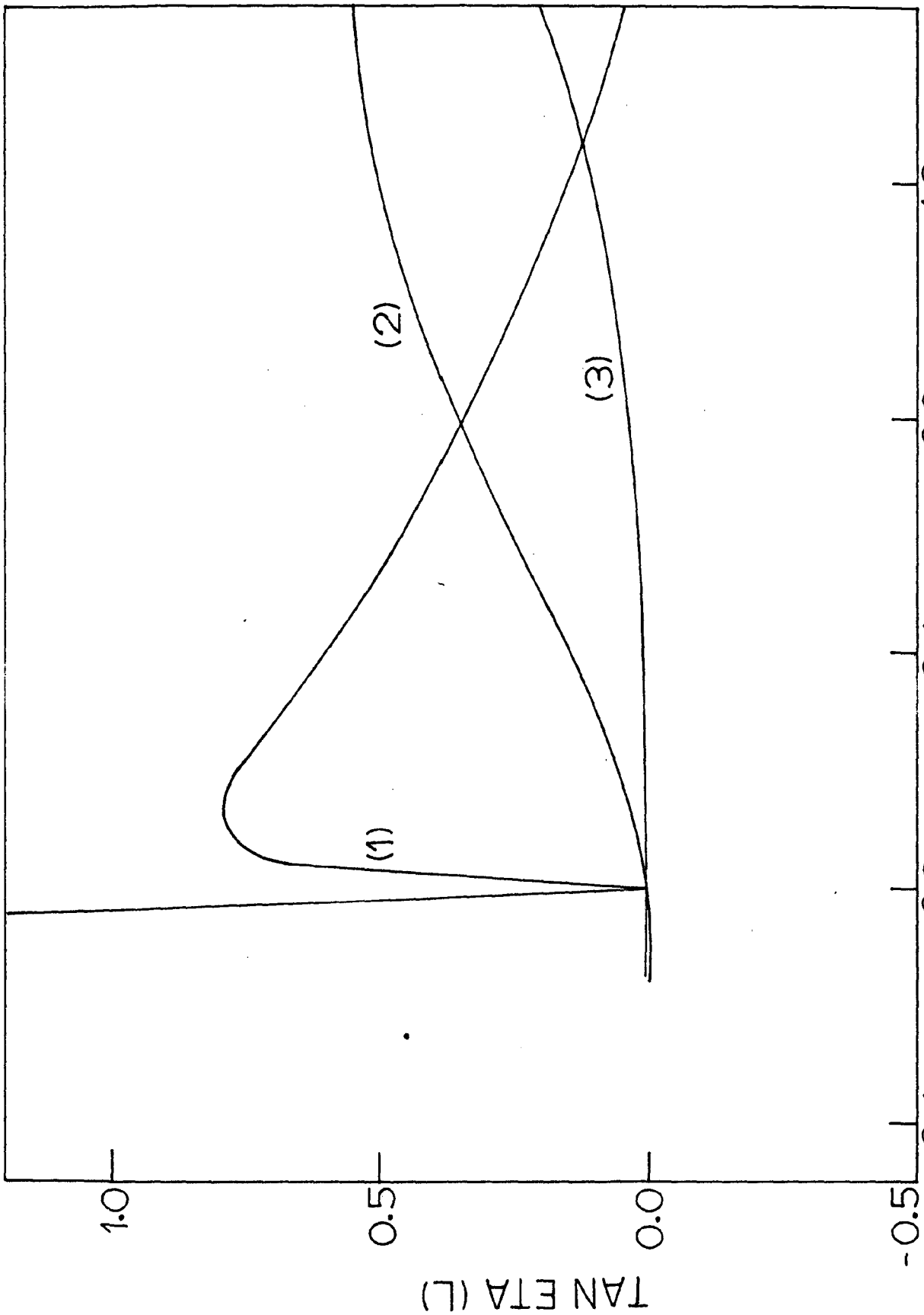

FIG.6(b)

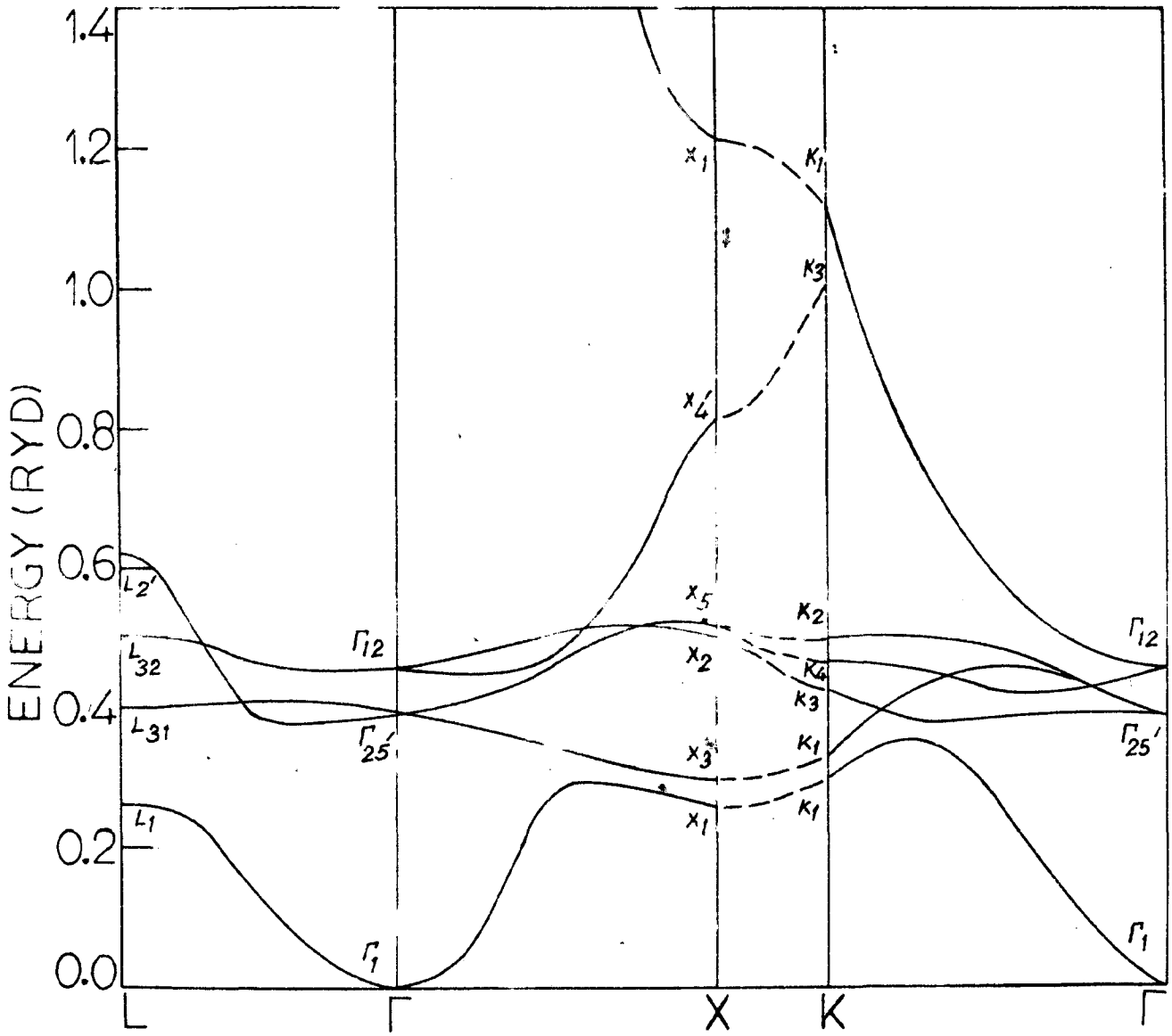
ENERGY (RYD)
1.4
1.2
1.0
0.8
0.6
0.4
0.2
0.0
L
Γ
X
K
Γ
$L_{2'}$
L_{32}
L_{31}
L_1
Γ_{12}
$\Gamma_{25'}$
Γ_1
X_1
X_4'
X_5
X_2
X_3
X_1
K_1
K_3
K_2
K_4
K_3
K_1
K_1
Γ_{12}
$\Gamma_{25'}$
Γ_1

FIG.7(a)

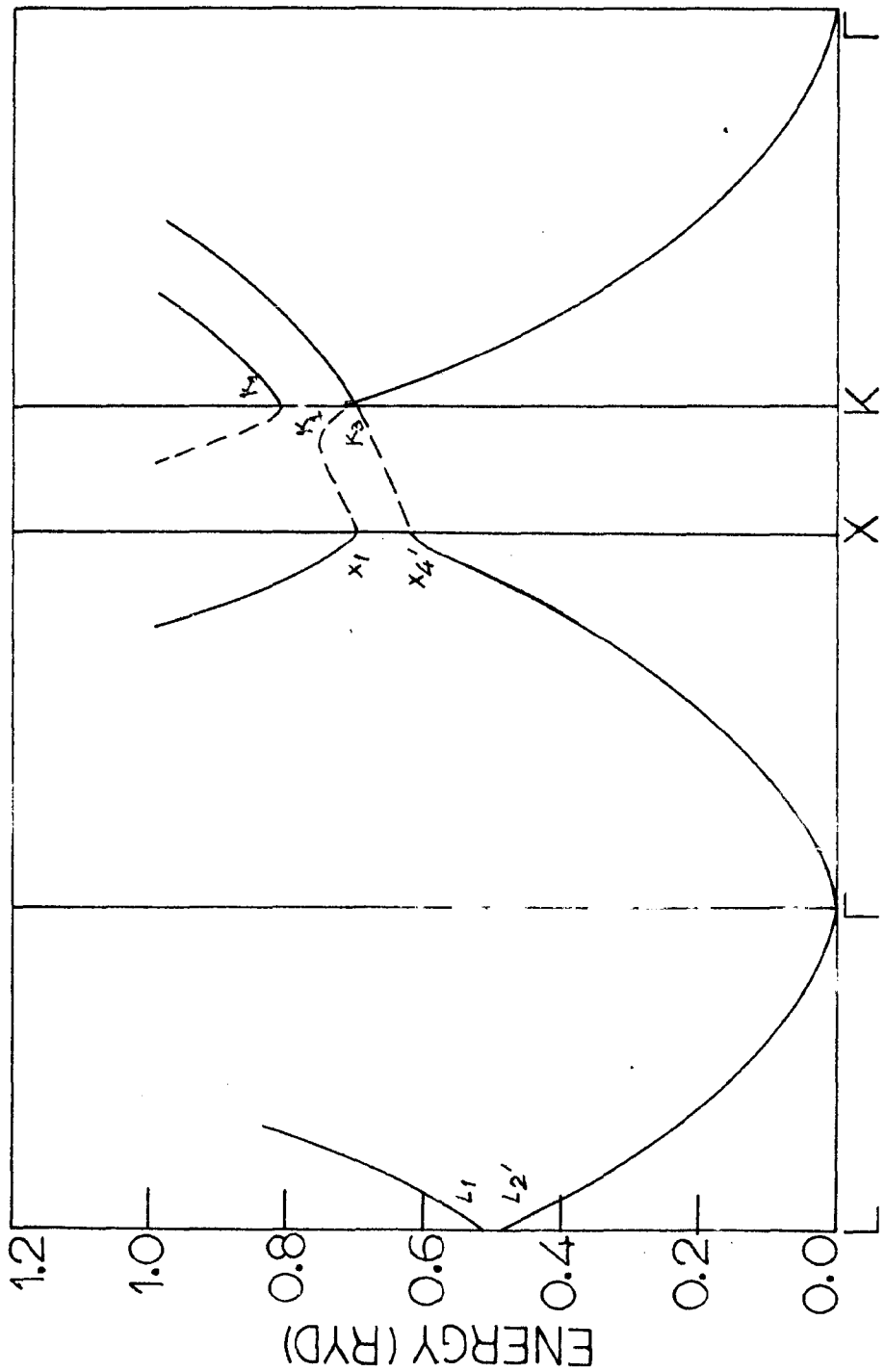

FIG.7(b)

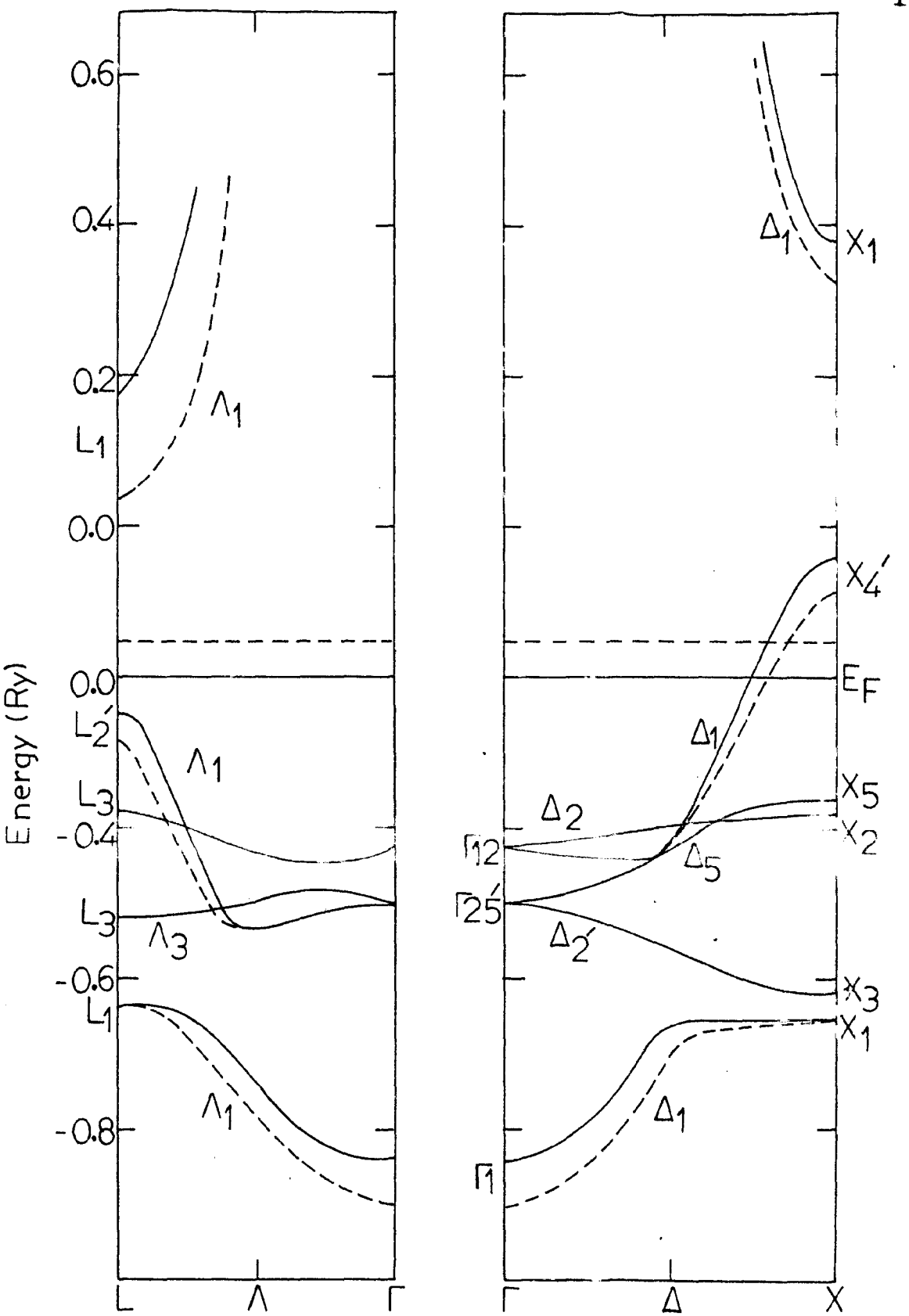
Energy (Ry)
0.6
0.4
0.2
0.0
-0.4
-0.6
-0.8
L1
Λ1
L2'
L3
L3
Λ3
L1
Λ1
Λ1
L
Λ
Γ
Δ1
X1
X4'
EF
Δ1
X5
Δ2
X2
Γ12
Δ5
Γ25'
Δ2'
X3
X1
Δ1
Γ1
Γ
Δ
X

FIG.8

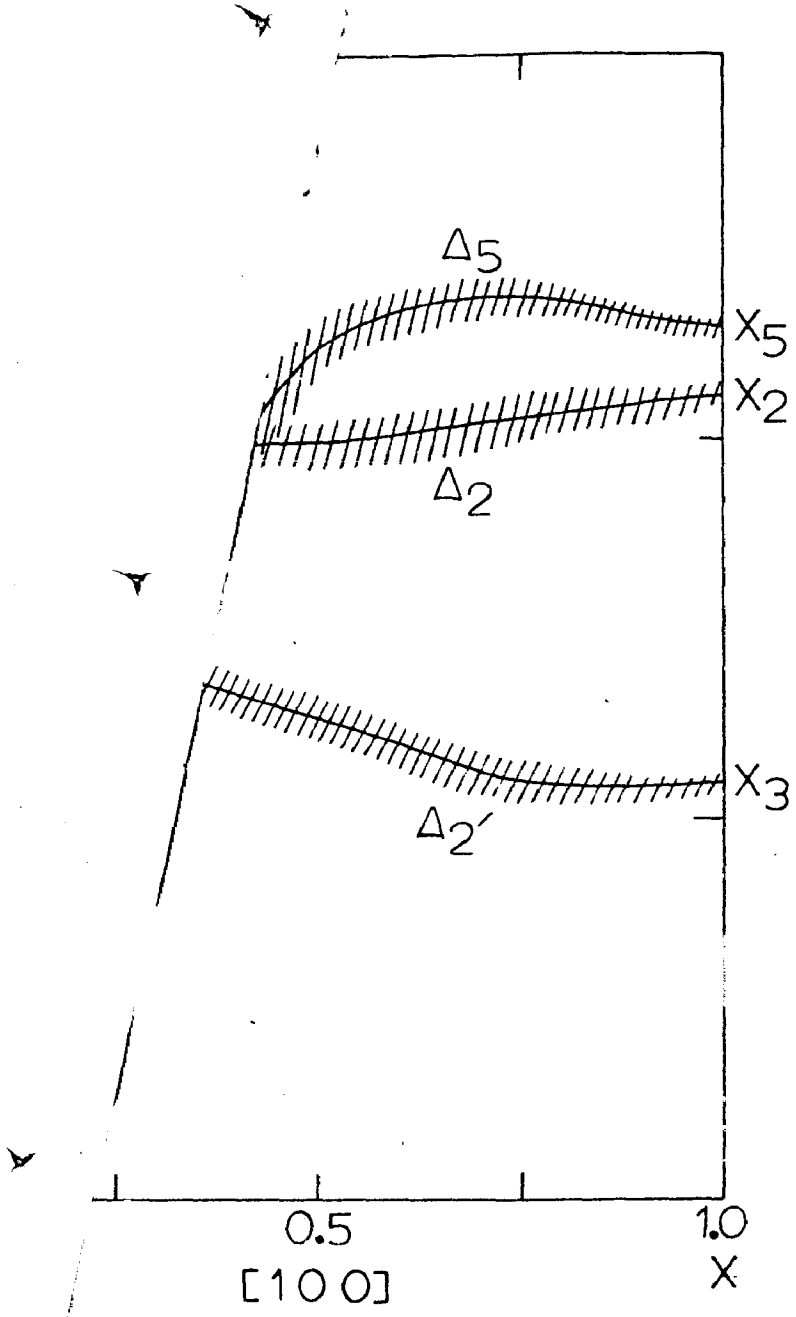

FIG. 9

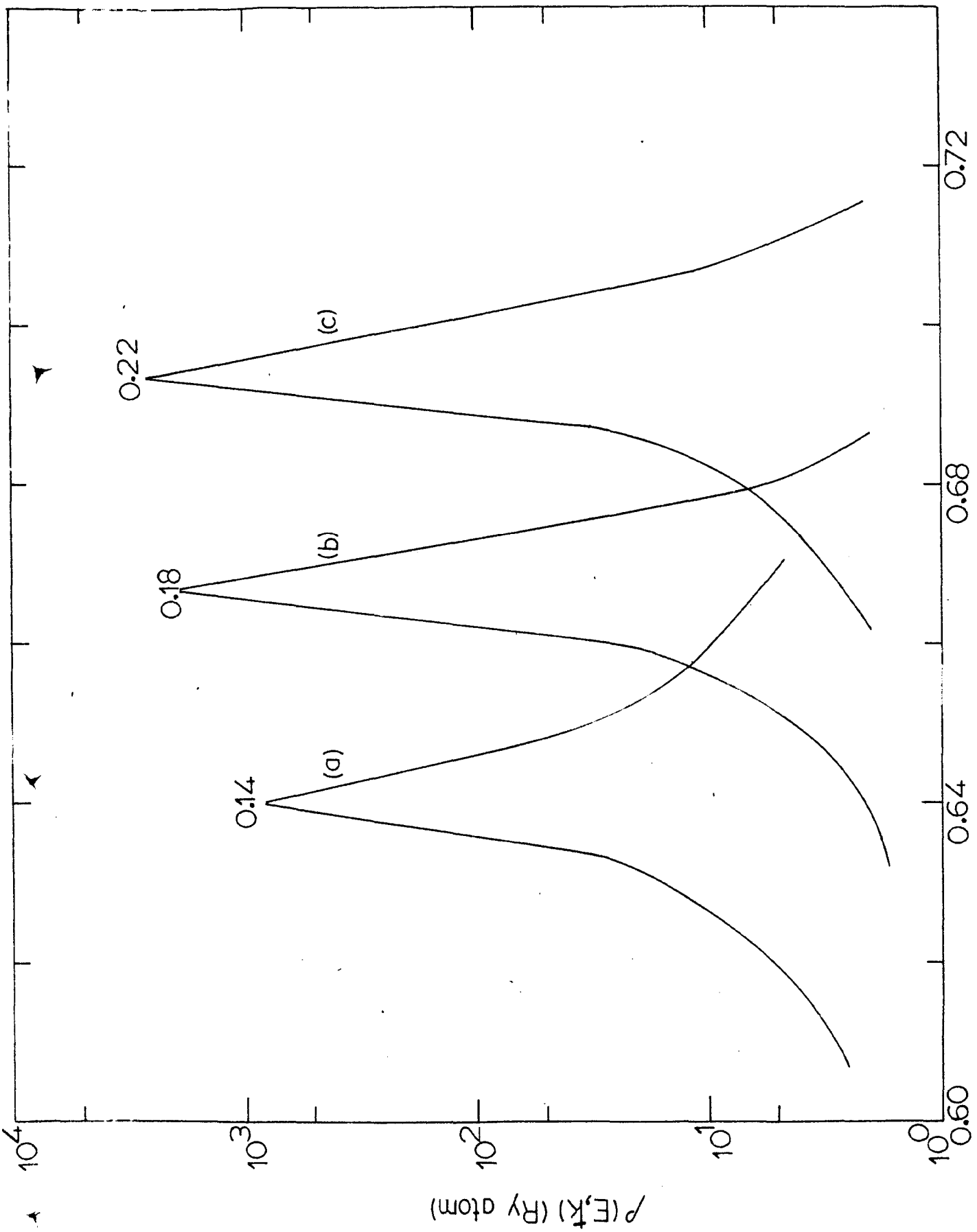
ρ (E,k) (Ry atom)
10^4
10^3
10^2
10^1
10^0
0.60
0.64
0.68
0.72
k (in units of 2π/a)
0.14
0.18
0.22
(a)
(b)
(c)

FIG.10

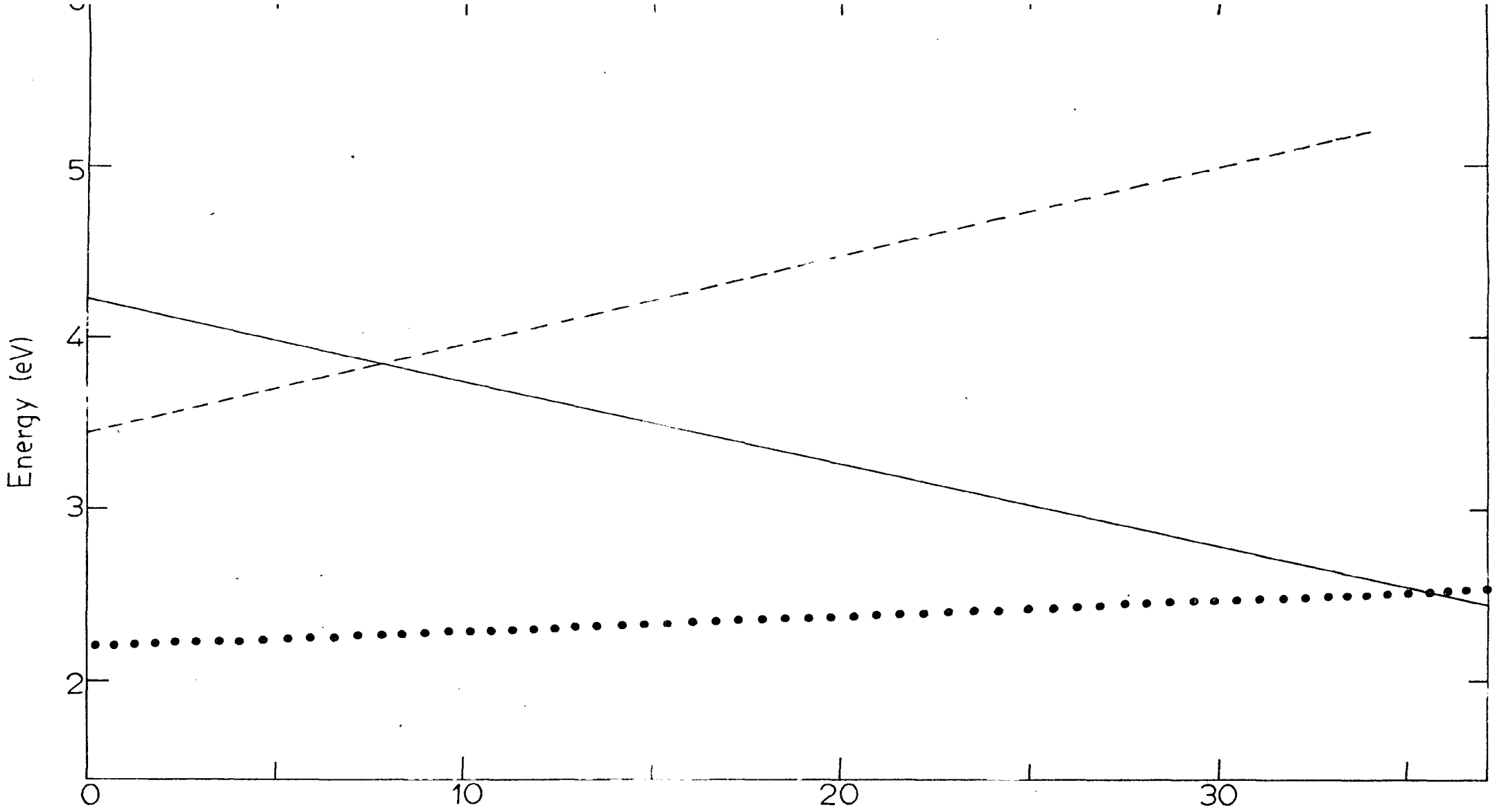

FIG.11

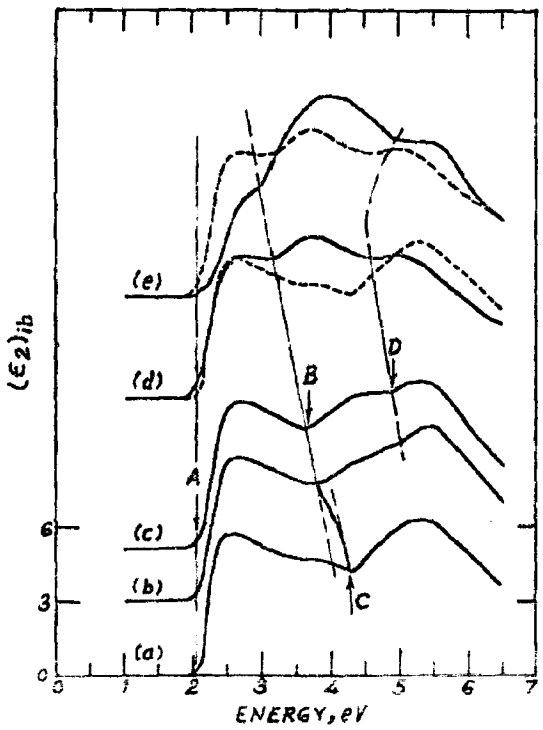

FIG.12(a)

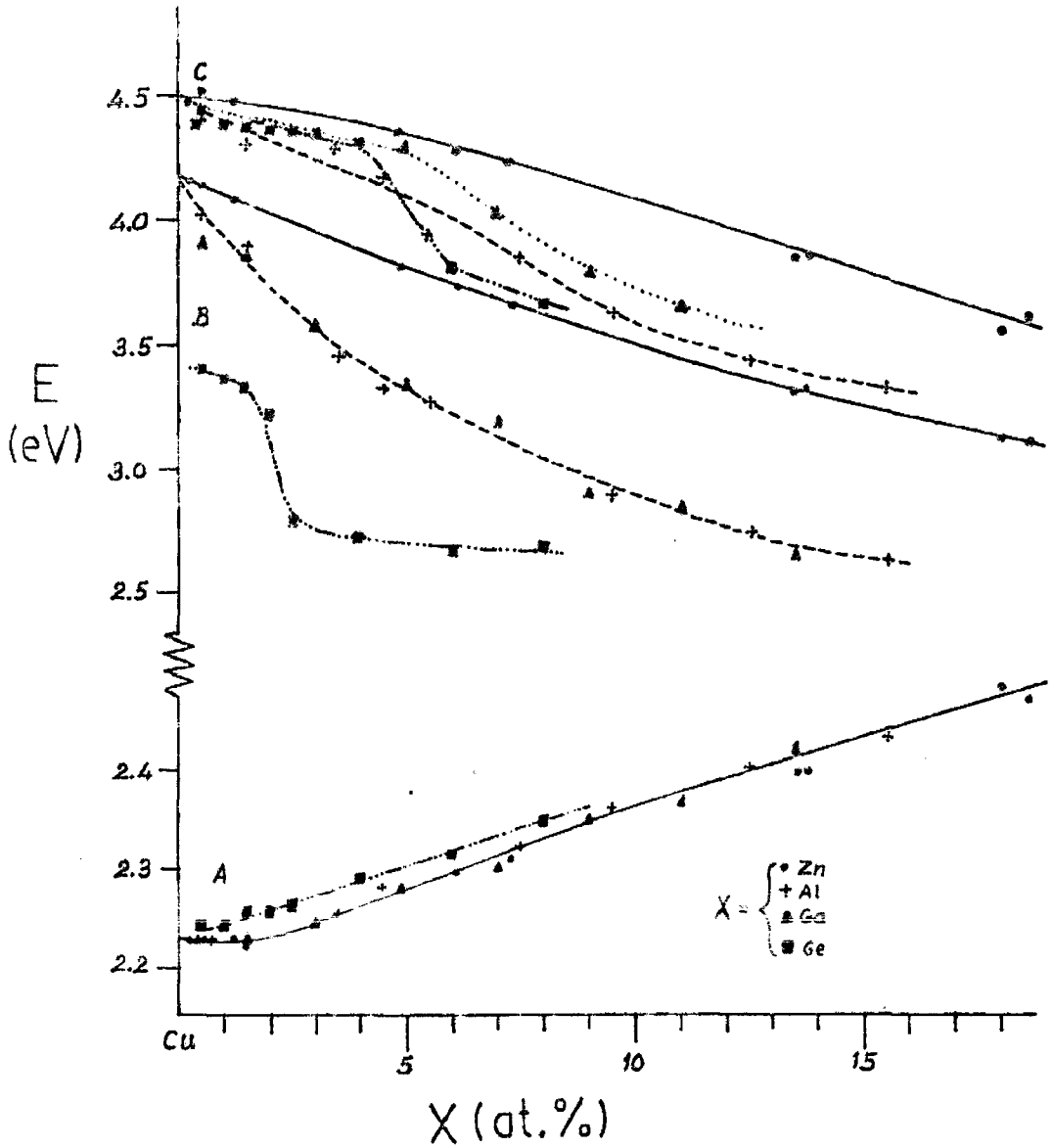

FIG.12(b)

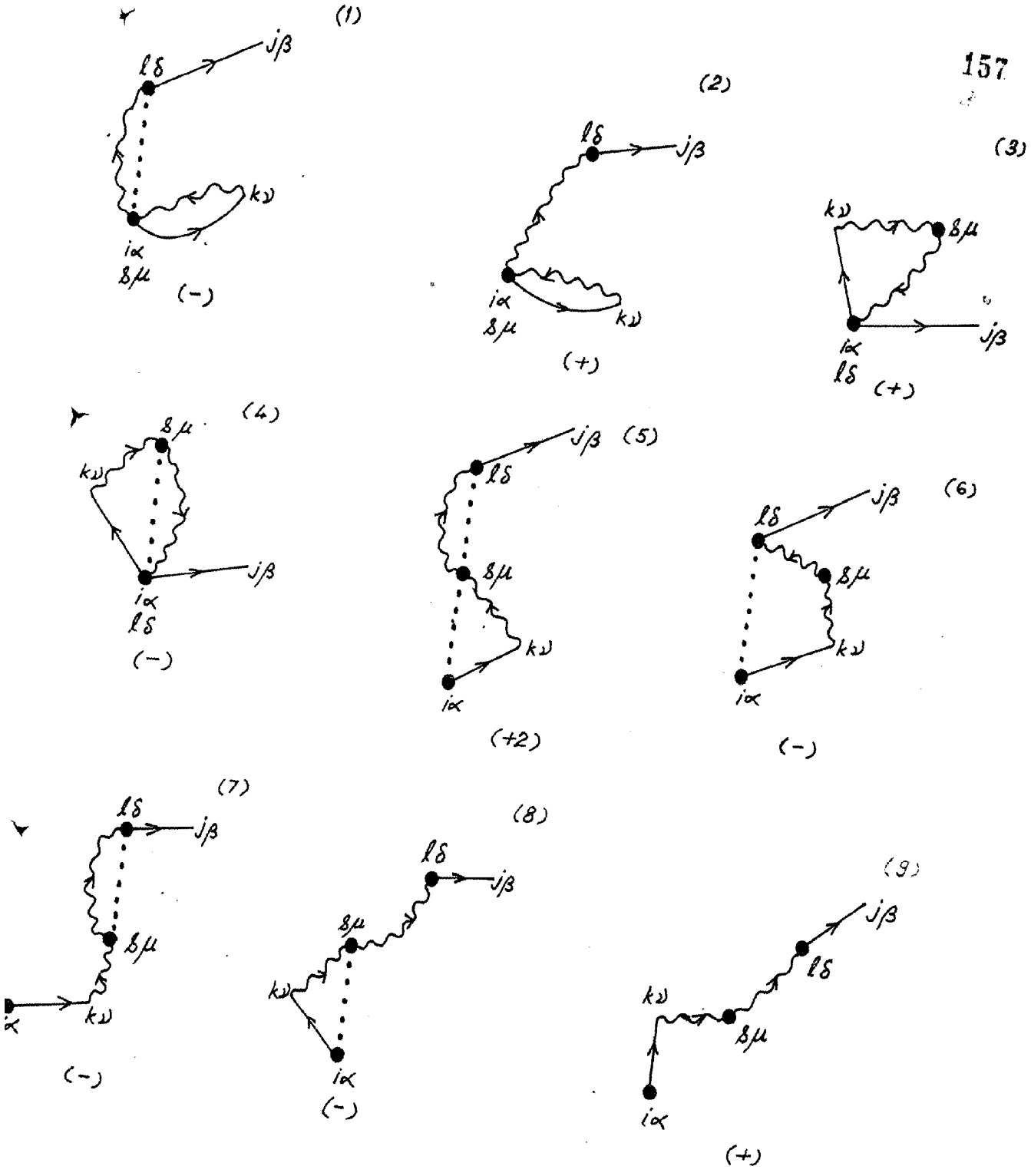
(1)
lδ
jβ
kν
iα
δμ
(−)
(2)
lδ
jβ
iα
δμ
kν
(+)
(3)
kν
δμ
jβ
iα
lδ
(+)
(4)
δμ
kν
jβ
iα
lδ
(−)
(5)
jβ
lδ
δμ
kν
iα
(+2)
(6)
lδ
jβ
δμ
kν
iα
(−)
(7)
lδ
jβ
δμ
α
kν
(−)
(8)
lδ
jβ
δμ
kν
iα
(−)
(9)
jβ
lδ
kν
δμ
iα
(+)

FIG.13

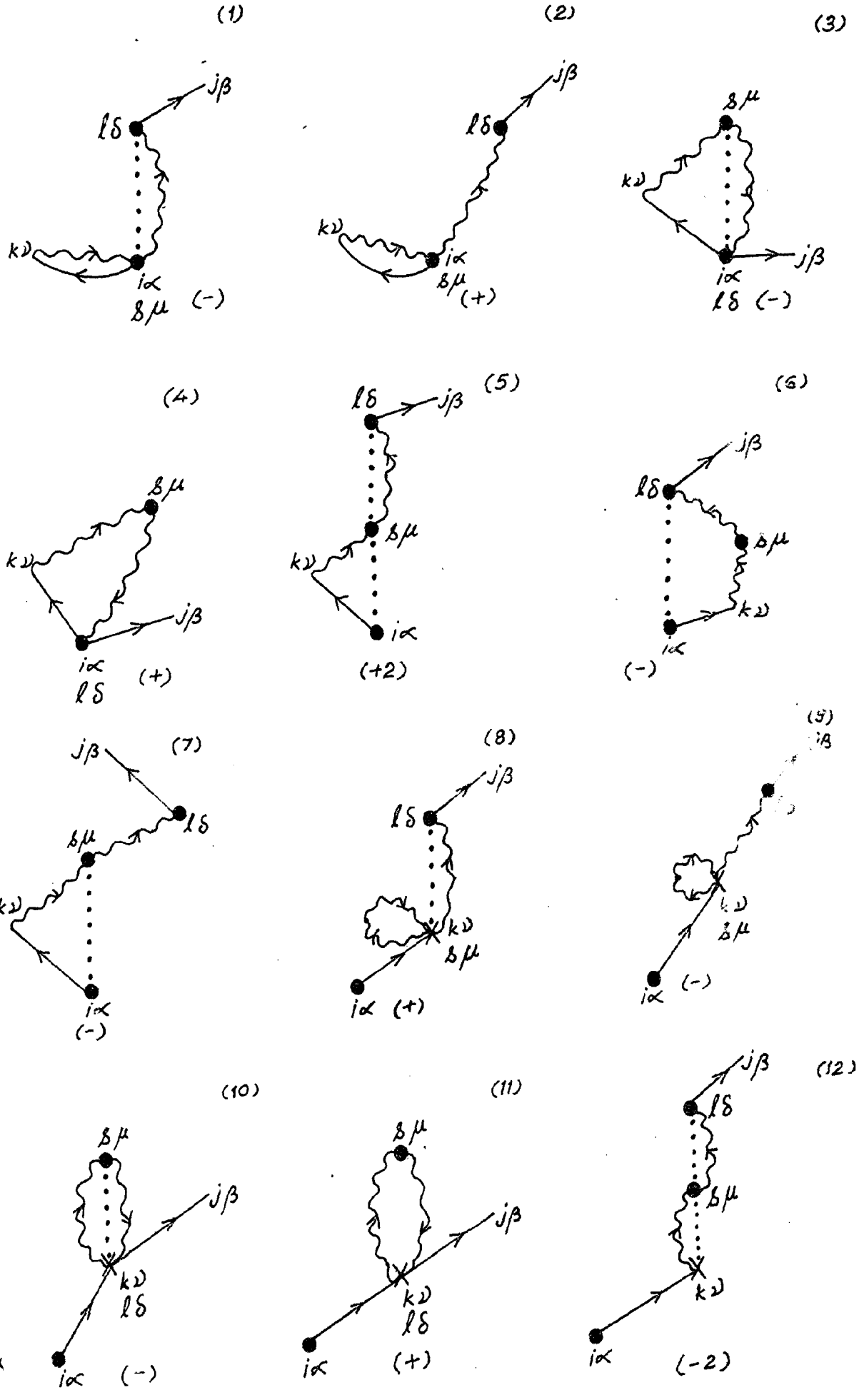
(1)
jβ
lδ
kν
iα
δμ
(-)
(2)
jβ
lδ
kν
iα
δμ
(+)
(3)
δμ
kν
jβ
iα
lδ
(-)
(4)
δμ
kν
jβ
iα
lδ
(+)
(5)
lδ
jβ
δμ
kν
iα
(+2)
(6)
jβ
lδ
δμ
kν
iα
(-)
(7)
jβ
lδ
δμ
kν
iα
(-)
(8)
jβ
lδ
kν
δμ
iα
(+)
(9)
jβ
kν
δμ
iα
(-)
(10)
δμ
jβ
kν
lδ
iα
(-)
(11)
δμ
jβ
kν
lδ
iα
(+)
(12)
jβ
lδ
δμ
kν
iα
(-2)

FIG.14(0)

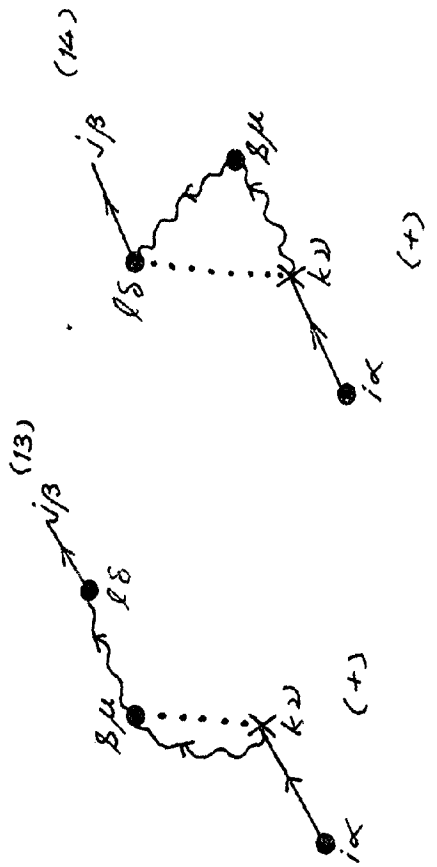

FIG.14(b)

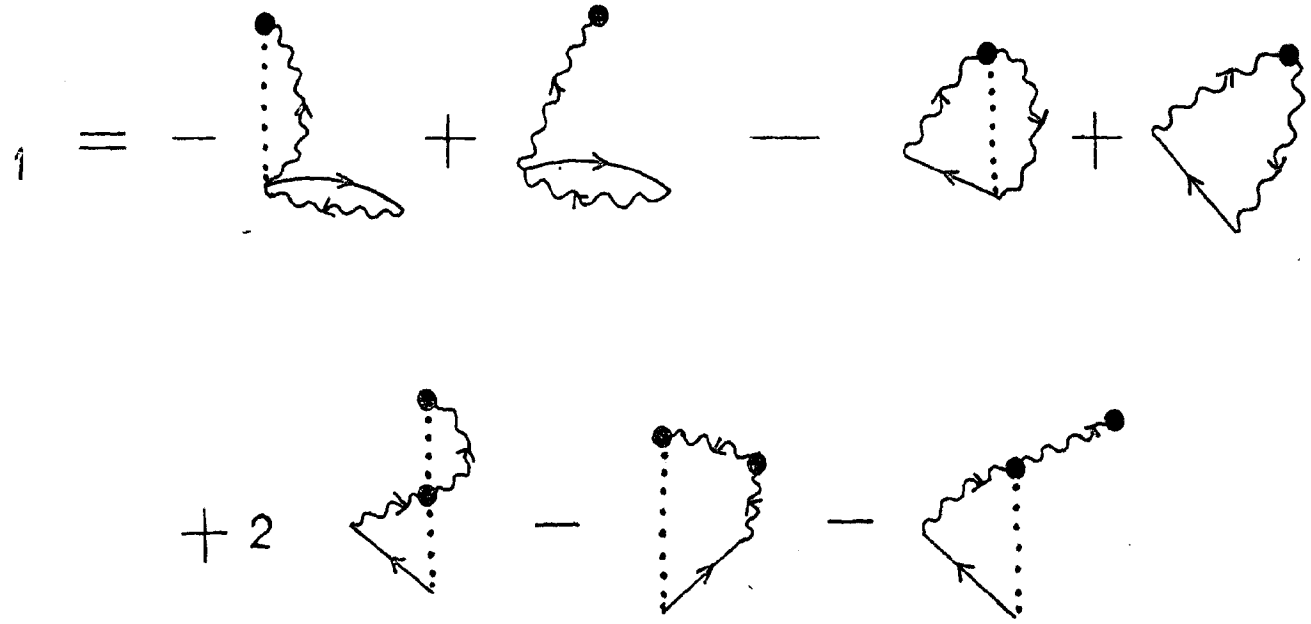

FIG.15(a)

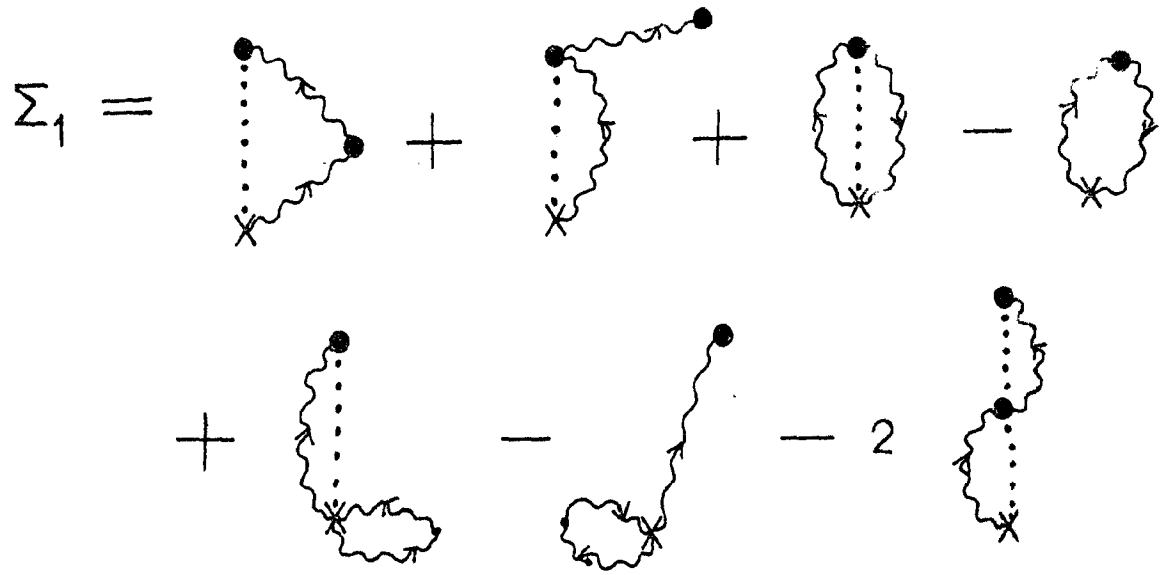

FIG.15(b)

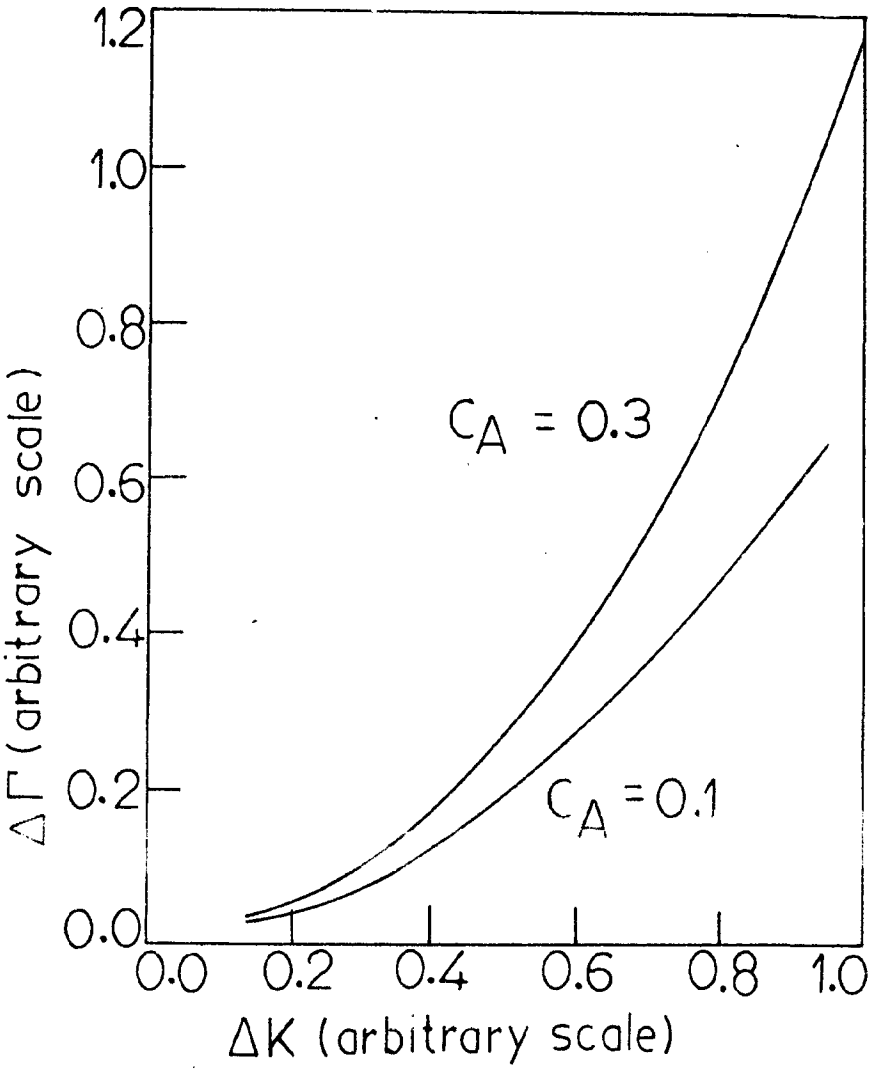
1.2
1.0
0.8
0.6
0.4
0.2
0.0
ΔΓ (arbitrary scale)
C_A = 0.3
C_A = 0.1
0.0
0.2
0.4
0.6
0.8
1.0
ΔK (arbitrary scale)

FIG.16

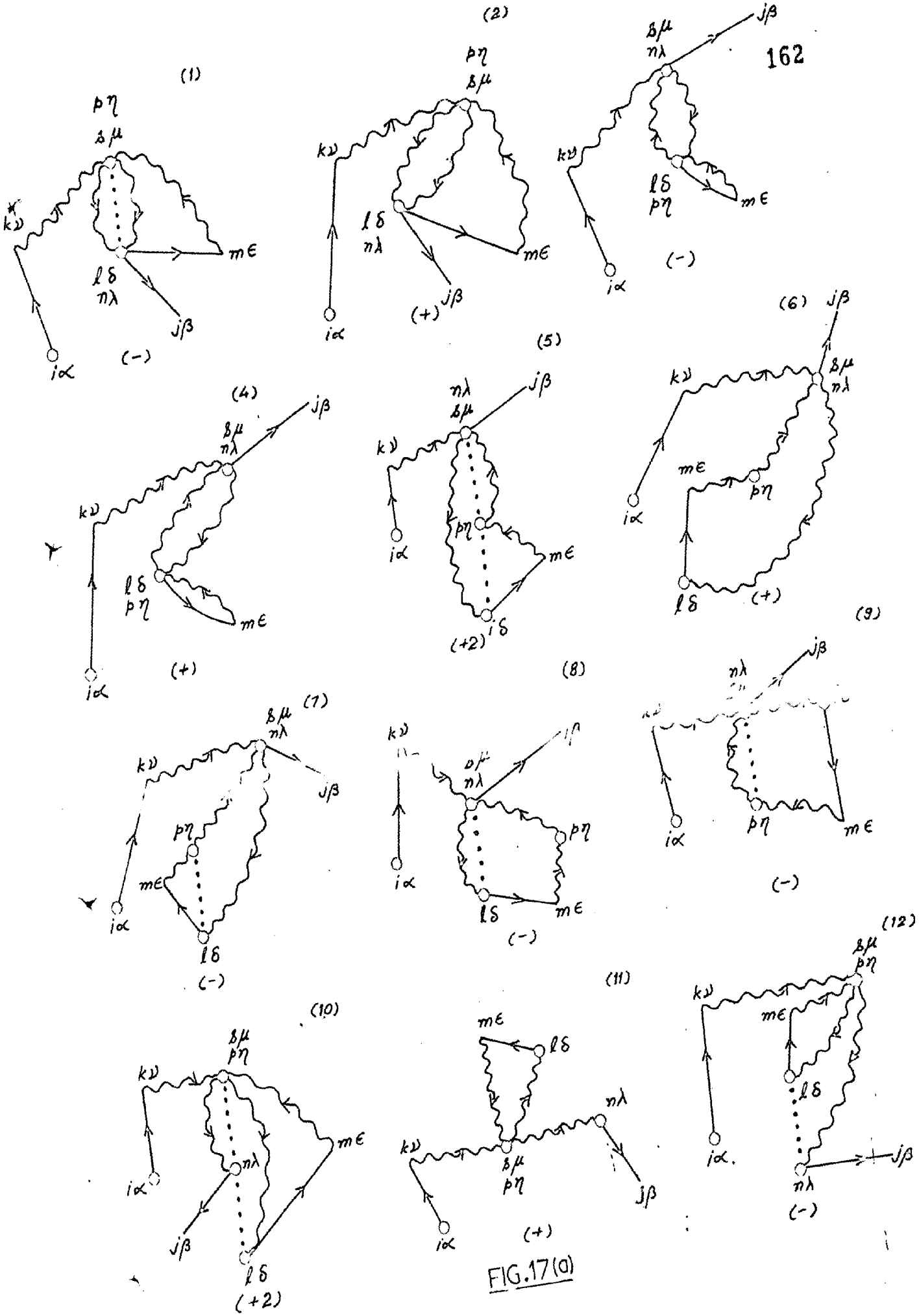
(1)
pη
sμ
kν
mϵ
lδ
nλ
jβ
iα
(−)
(2)
pη
sμ
kν
lδ
nλ
mϵ
(+)
jβ
iα
(3)
sμ
nλ
jβ
kν
lδ
pη
mϵ
iα
(−)
(4)
jβ
sμ
nλ
kν
lδ
pη
mϵ
(+)
iα
(5)
nλ
sμ
jβ
kν
pη
mϵ
iδ
(+2)
iα
(6)
jβ
sμ
nλ
kν
mϵ
pη
lδ
(+)
iα
(7)
sμ
nλ
kν
jβ
pη
mϵ
lδ
(−)
iα
(8)
kν
sμ
nλ
jβ
pη
lδ
mϵ
(−)
iα
(9)
nλ
jβ
pη
mϵ
(−)
iα
(10)
sμ
pη
kν
mϵ
nλ
jβ
lδ
(+2)
iα
(11)
mϵ
lδ
nλ
kν
sμ
pη
jβ
(+)
iα
(12)
sμ
pη
kν
mϵ
lδ
jβ
nλ
(−)
iα

FIG.17(a)

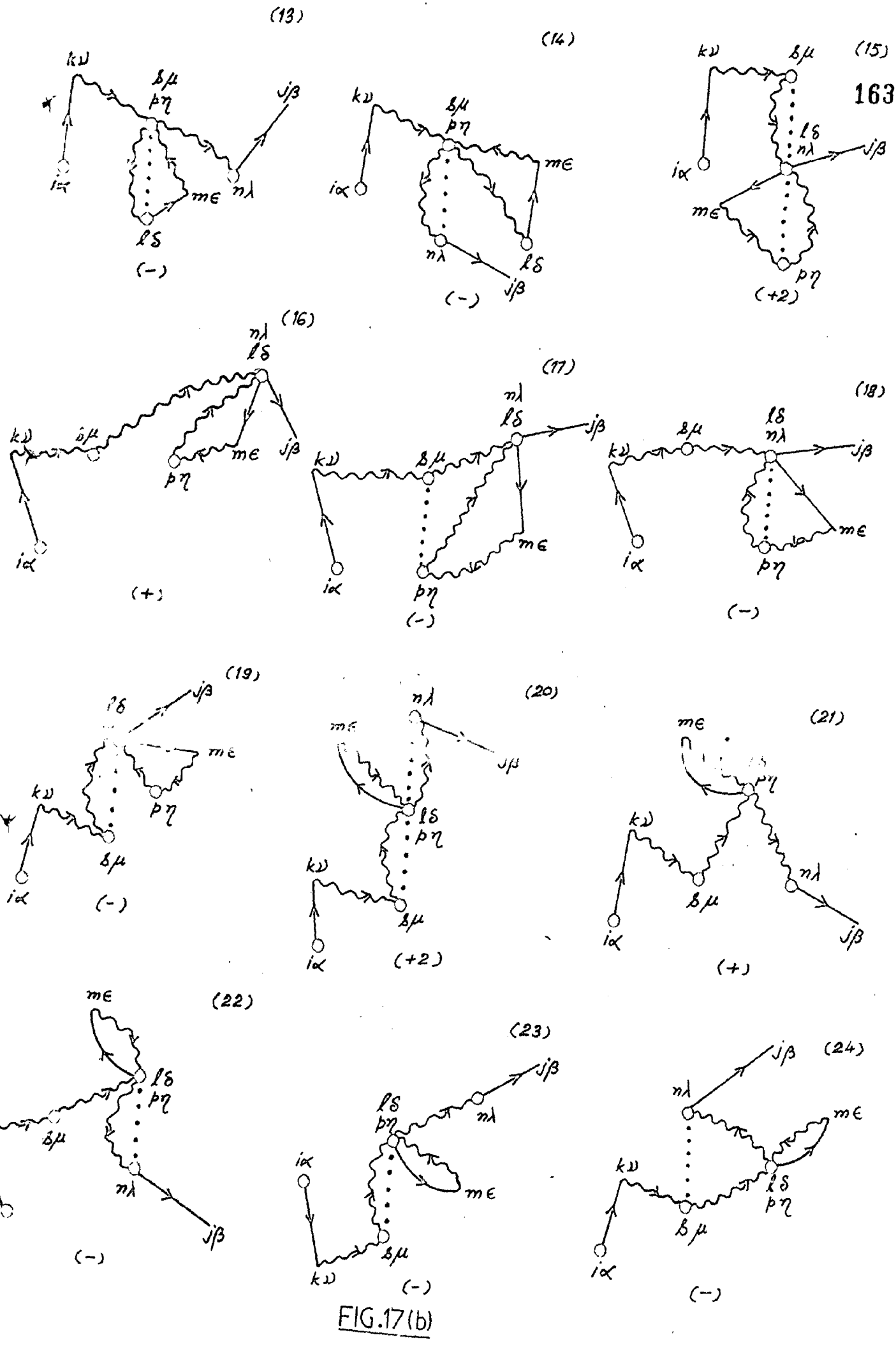
(13)
kν
δμ
pη
jβ
iα
mε
nλ
lδ
(−)
(14)
kν
δμ
pη
mε
iα
nλ
lδ
jβ
(−)
(15)
kν
δμ
lδ
nλ
jβ
iα
mε
pη
(+2)
(16)
nλ
lδ
kν
δμ
mε
jβ
pη
iα
(+)
(17)
nλ
lδ
jβ
kν
δμ
mε
iα
pη
(−)
(18)
δμ
lδ
nλ
jβ
kν
mε
iα
pη
(−)
(19)
lδ
jβ
mε
pη
kν
δμ
iα
(−)
(20)
nλ
mε
jβ
lδ
pη
kν
δμ
iα
(+2)
(21)
mε
pη
kν
nλ
δμ
iα
jβ
(+)
(22)
mε
lδ
pη
kν
δμ
nλ
jβ
(−)
(23)
jβ
lδ
pη
nλ
iα
mε
δμ
kν
(−)
(24)
jβ
nλ
mε
kν
lδ
pη
δμ
iα
(−)

FIG.17(b)

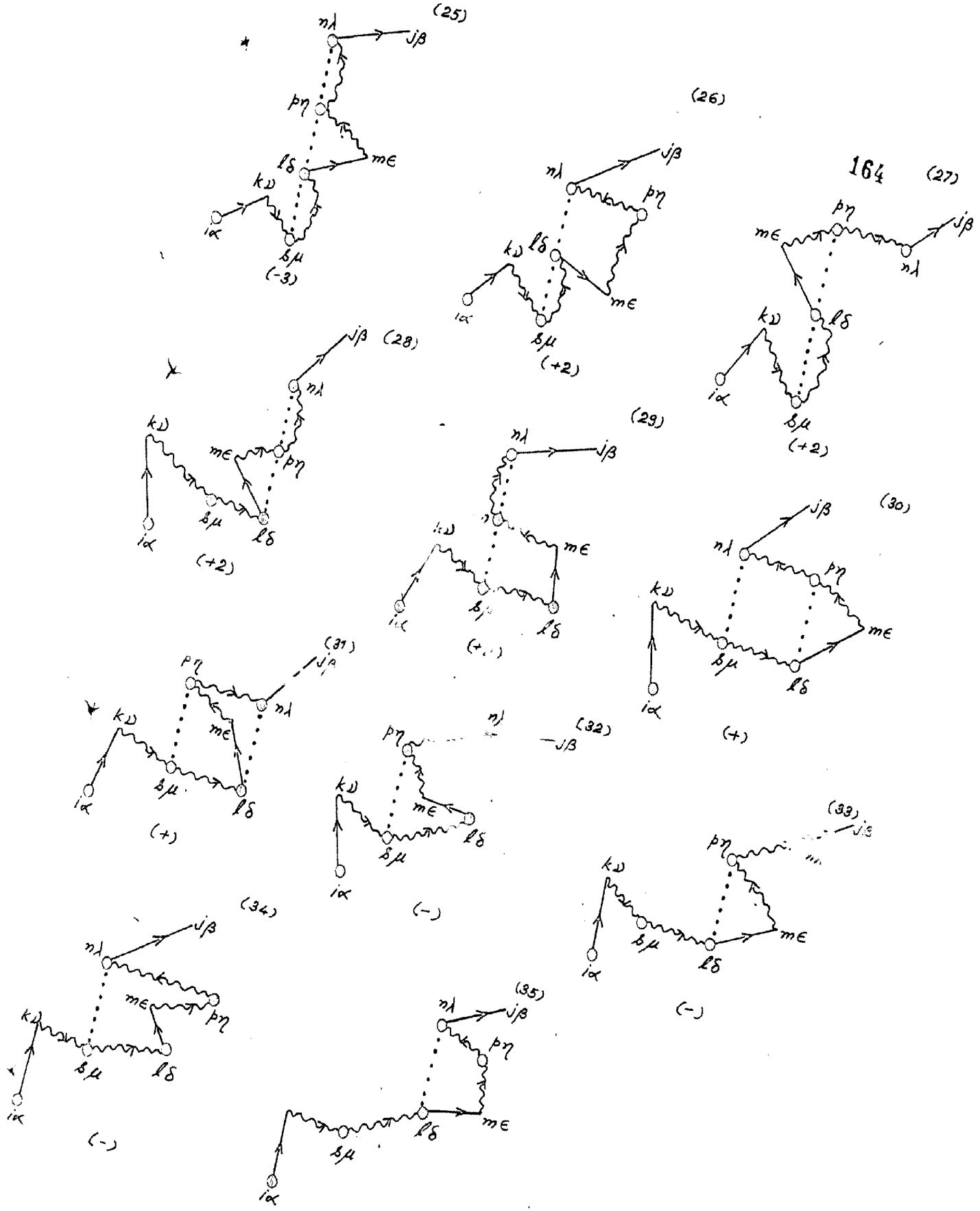
(25)
nλ
jβ
pη
lδ
mε
kν
iα
δμ
(-3)
(26)
nλ
jβ
pη
lδ
kν
mε
iα
δμ
(+2)
(27)
pη
mε
jβ
nλ
kν
lδ
iα
δμ
(+2)
(28)
jβ
nλ
kν
mε
pη
iα
δμ
lδ
(+2)
(29)
nλ
jβ
kν
mε
iα
δμ
lδ
(+)
(30)
jβ
nλ
pη
kν
mε
δμ
iα
lδ
(+)
(31)
pη
jβ
nλ
kν
mε
iα
δμ
lδ
(+)
nλ
(32)
pη
jβ
kν
mε
lδ
iα
δμ
(-)
(33)
jβ
pη
kν
δμ
mε
iα
lδ
(-)
(34)
jβ
nλ
mε
pη
kν
δμ
lδ
iα
(-)
(35)
nλ
jβ
pη
lδ
mε
δμ
iα
(-)

FIG.17(c)

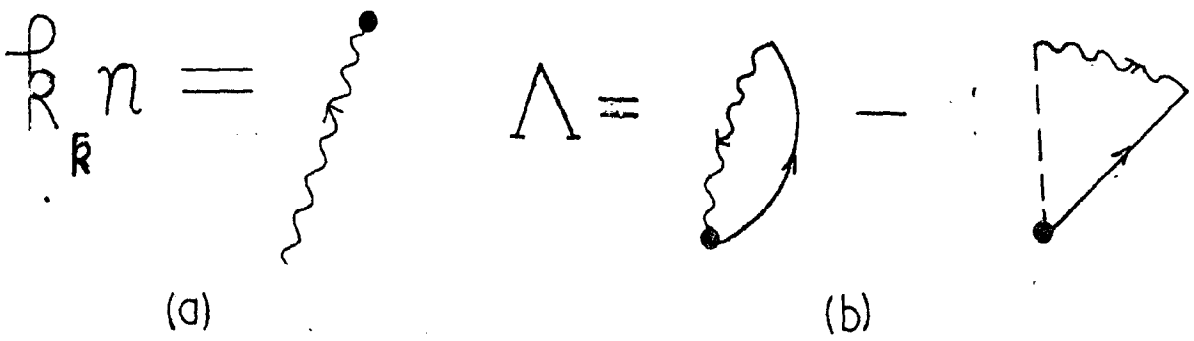

FIG.18

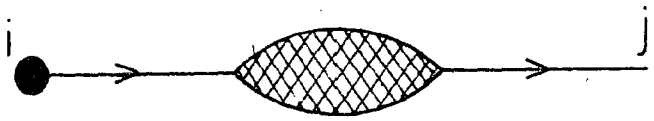

FIG.19

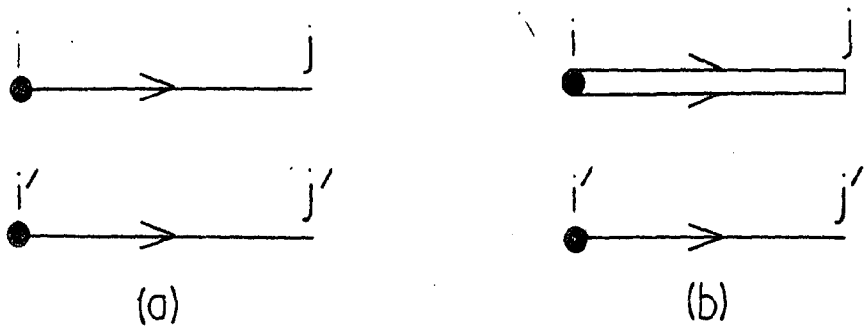

FIG.20

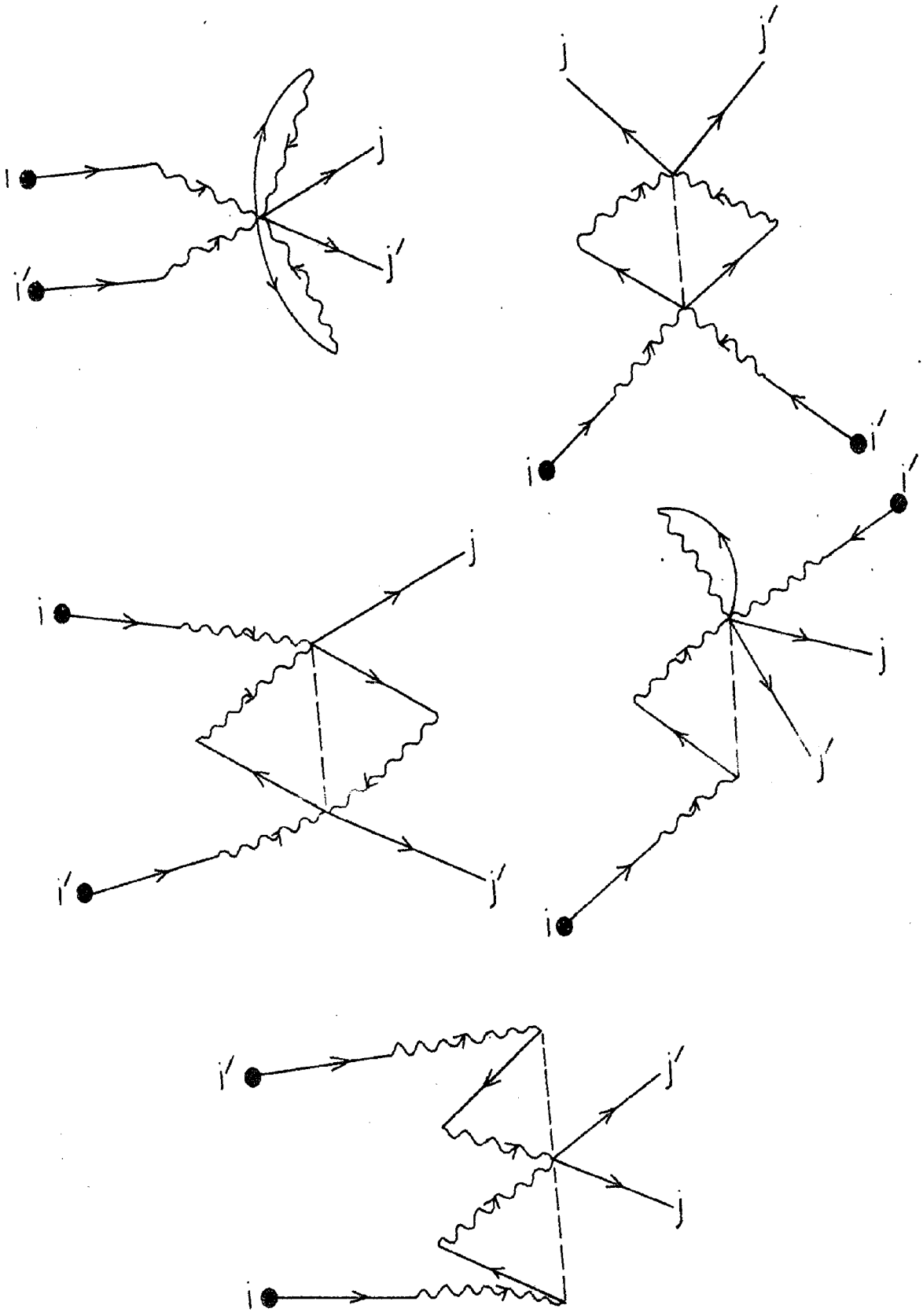

FIG. 21

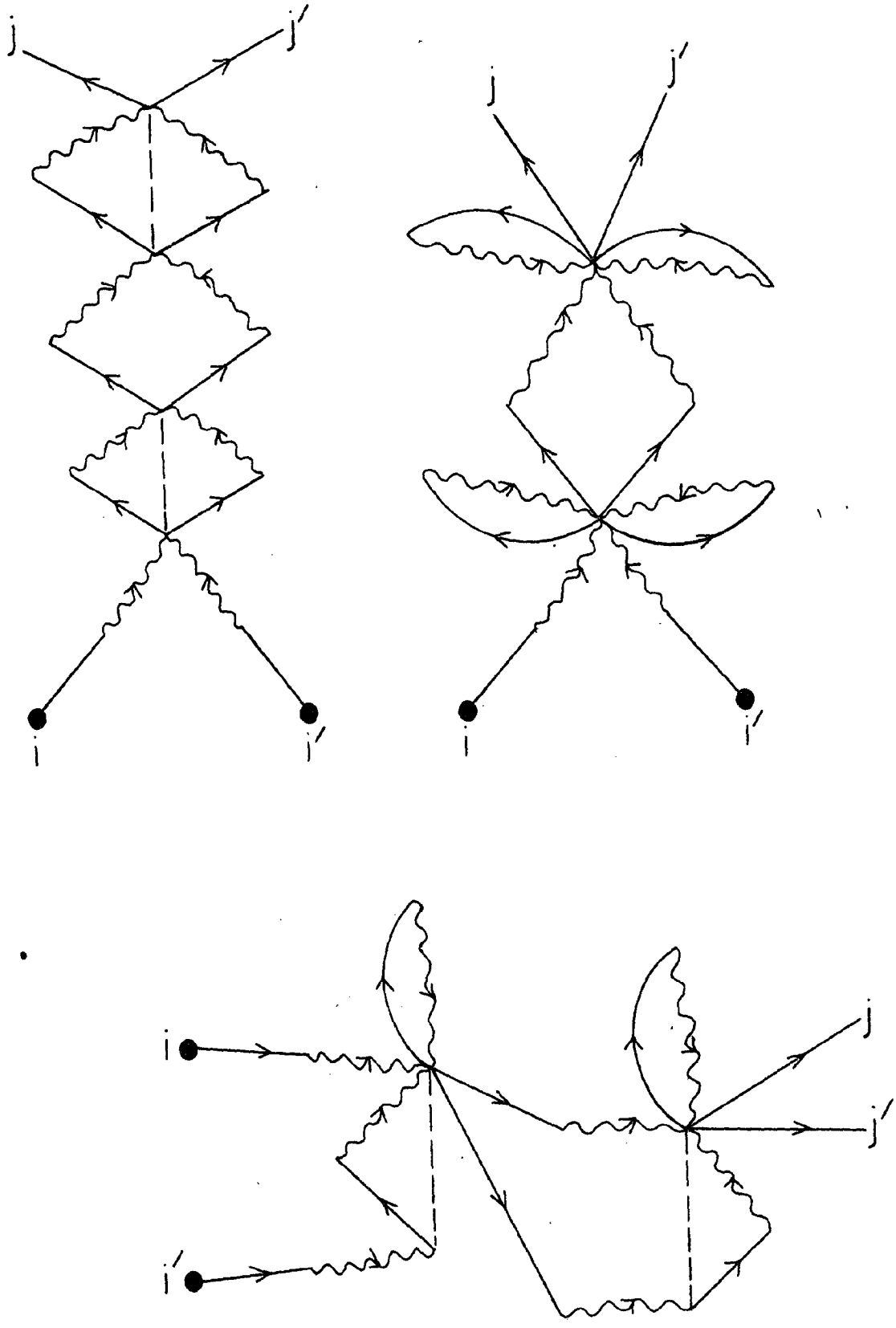

FIG.22

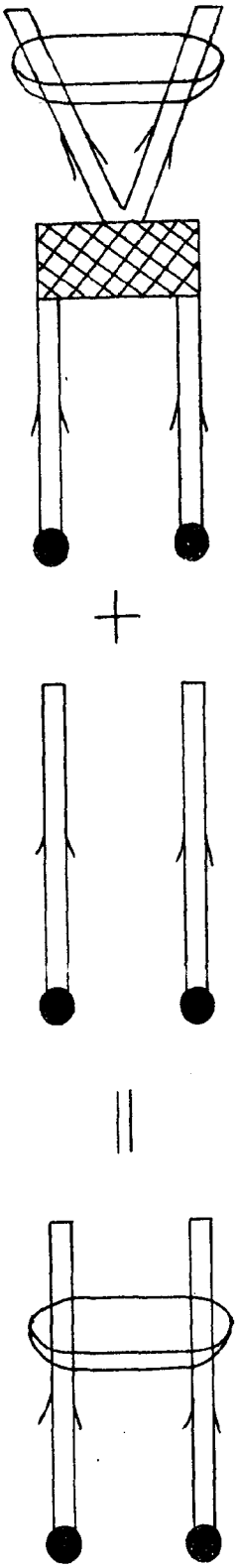

FIG.23

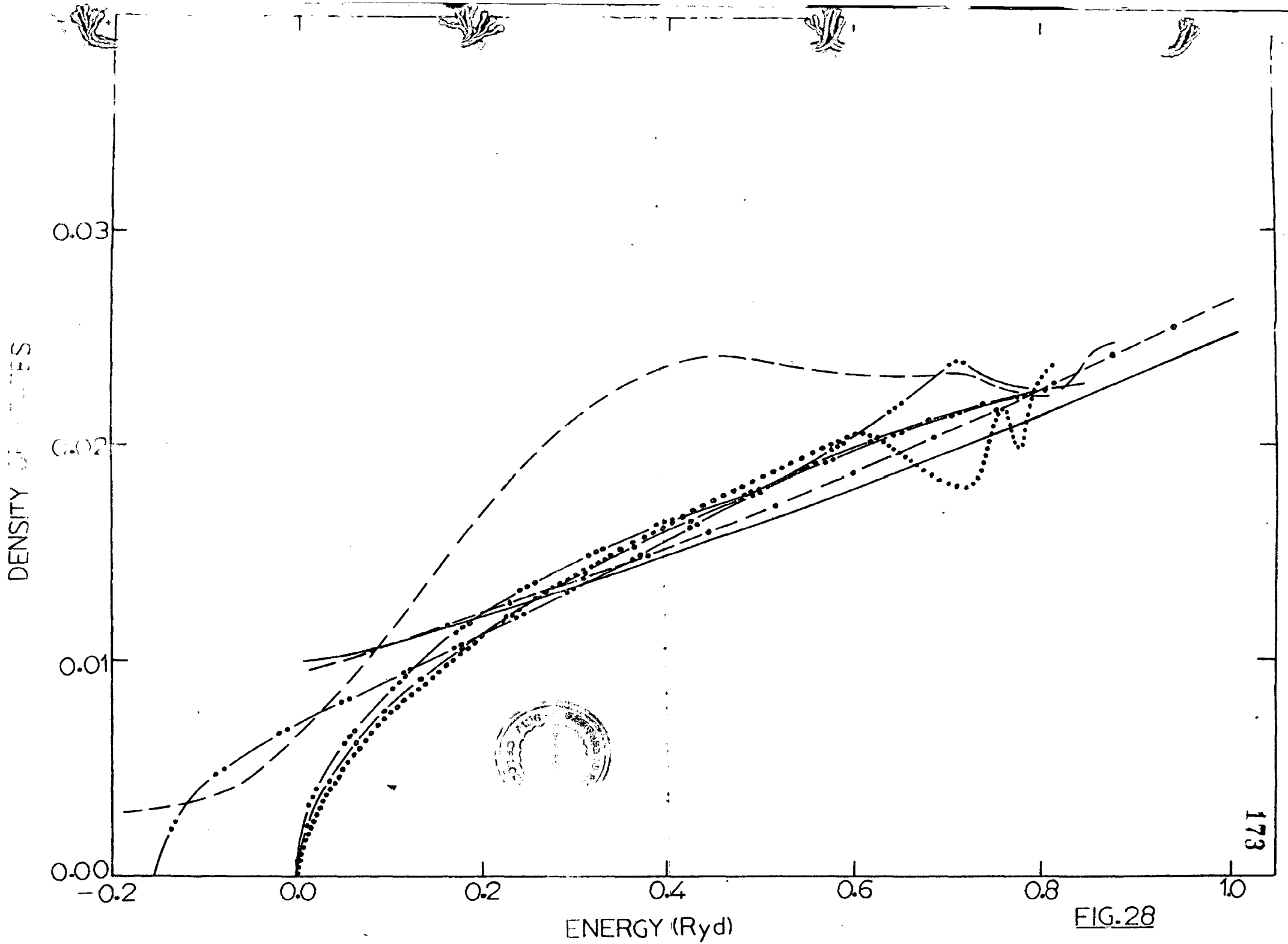

FIG. 28

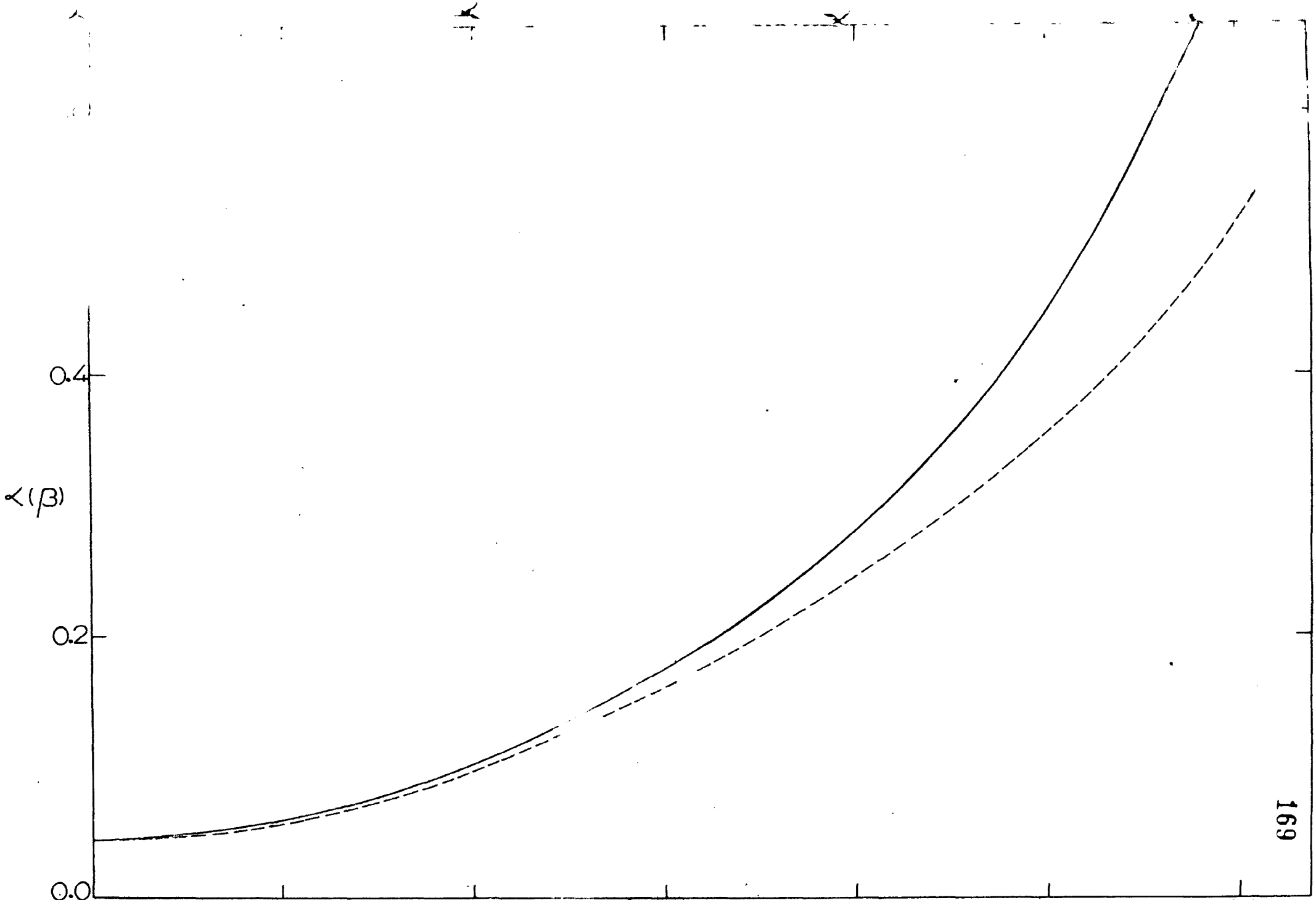

FIG. 2 4

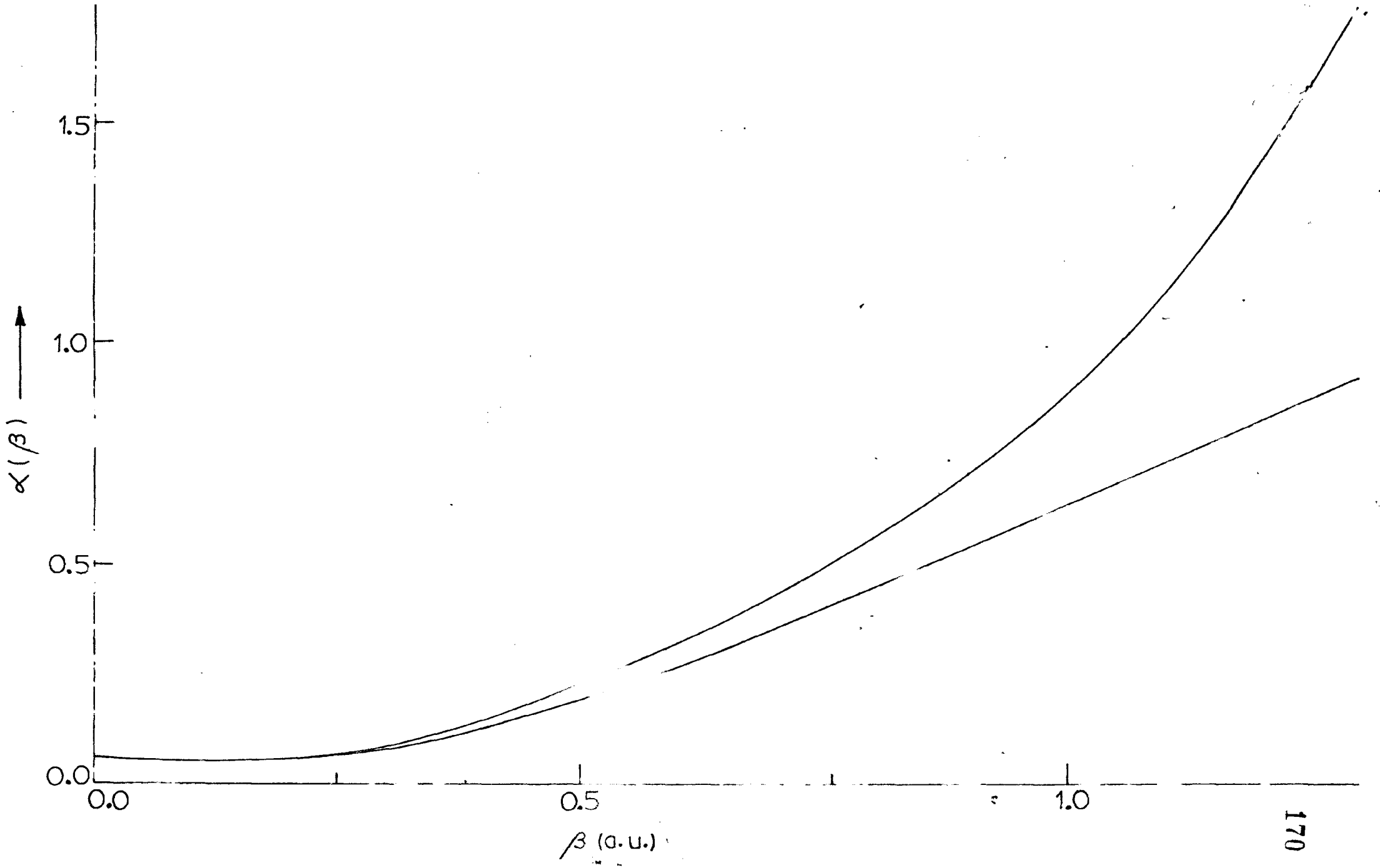

FIG.25

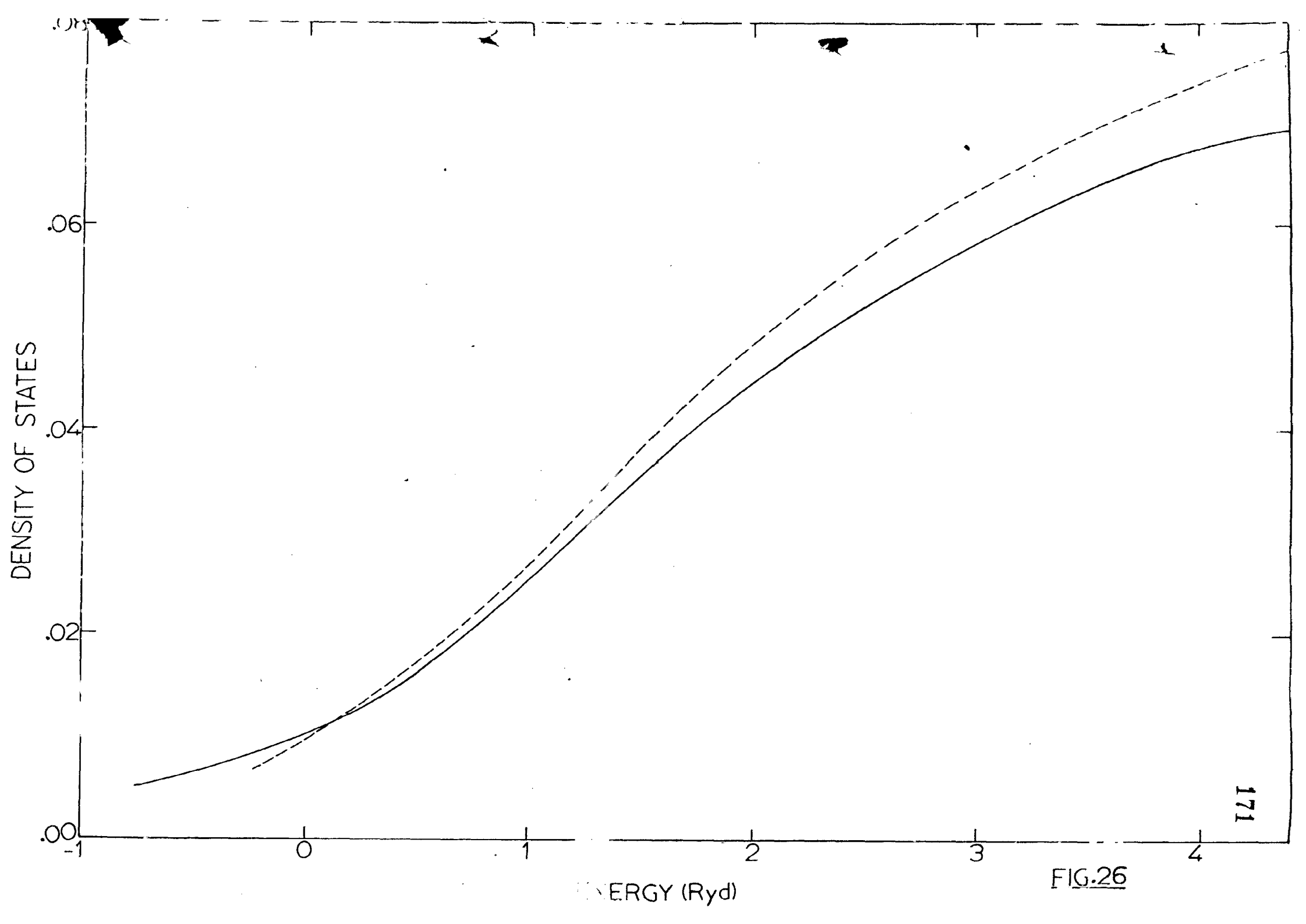

FIG.26

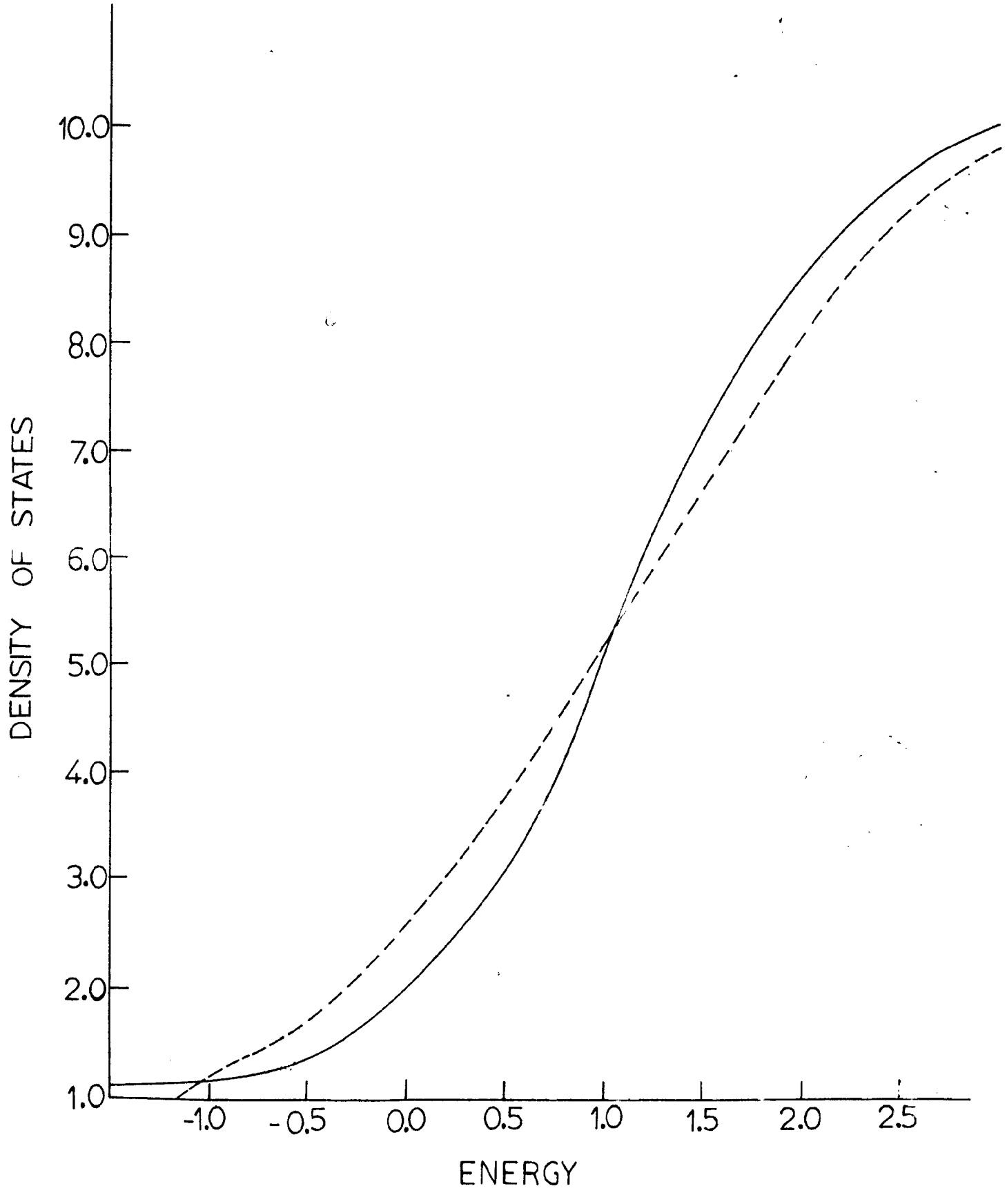
DENSITY OF STATES
10.0
9.0
8.0
7.0
6.0
5.0
4.0
3.0
2.0
1.0
-1.0
-0.5
0.0
0.5
1.0
1.5
2.0
2.5
ENERGY

FIG.27